수의학 박사학위 논문

The Role of Ninjurin1 on Pulmonary Fibrosis

폐섬유화증 발생 과정에서 Ninjurin1의 역할에 대한 연구

2019년 8월

서울대학교 대학원
수의학과 수의생명과학 전공

최 승 호

A Dissertation for the Degree of Doctor of Philosophy

The Role of Ninjurin1 on Pulmonary Fibrosis

August 2019

Seungho Choi

Supervisor: Prof. Yeo Sung Yoon, D.V.M., Ph.D.

Department of Veterinary Medicine
Veterinary Biomedical Sciences

The Graduate School of Seoul National University

The Role of Ninjurin1 on Pulmonary Fibrosis

지도교수 윤 여 성

이 논문을 수의학박사 학위논문으로 제출함
2019년 5월

서울대학교 대학원
수의학과 수의생명과학전공

최 승 호

최승호의 수의학박사 학위논문을 인준함
2019년 7월

위 원 장 성 제 경 (인)
부위원장 윤 여 성 (인)
위 원 황 인 구 (인)
위 원 오 승 현 (인)
위 원 이 순 신 (인)

ABSTRACT

The Role of Ninjurin1 on Pulmonary Fibrosis

By
Seungho Choi

Graduate School of Seoul National University

Supervisor: Prof. Yeo Sung Yoon, D.V.M., Ph.D.

Idiopathic pulmonary fibrosis (IPF) is a chronic interstitial lung disease, which is the most commonly diagnosed type of pulmonary fibrosis (PF) with unknown origin. Since the clinical symptoms of IPF are not specific and the cause is not well-defined, it is difficult to diagnose IPF and develop effective treatment. In the pathogenesis of IPF, macrophages are the major inflammatory cells involved in the induction of pulmonary inflammation and fibrosis, by producing various pro-inflammatory and pro-fibrotic mediators. Macrophages are the major source of IL-1β and TNFα, which are the major cytokines involved in induction of chronic inflammation. In addition, TGF-β1, a pro-fibrogenic mediator which plays a crucial role in activating fibroblasts, is also produced mainly by macrophages.

The transmembrane nerve injury-induced protein 1 (Ninjurin1 or Ninj1) is involved in progressing inflammatory diseases such as multiple sclerosis and

autoimmune encephalopathy. Ninj1 is expressed in most of tissues. It was reported that Ninj1 is expressed in immune cells, such as monocytes, macrophages, and microglia, and promotes their motility. In addition, Ninj1 is involved in promoting inflammatory response in macrophages, leading to induction of multiple sclerosis and systemic inflammation. Since Ninj1 plays crucial role in developing inflammatory diseases, the goal of this study was to investigate a novel function of Ninj1 in pulmonary fibrosis, a chronic inflammatory disease.

It was found that the expression of Ninj1 in a patient cohort is upregulated in lung specimens of IPF patients. In addition, Ninj1 expression level was also elevated in the lungs during development of PF by intratracheal injection of bleomycin (BLM) in mice. Following BLM injection, the expression of Ninj1 was elevated in macrophages and alveolar epithelial cells in the lung tissue. Moreover, when a mouse macrophage cell line, Raw264.7, and a mouse alveolar epithelial cell line, MLE-12, are exposed to BLM, their Ninj1 expression also increased. Therefore, it was hypothesized that Ninj1 would play a role in developing PF.

In order to examine if Ninj1 is involved in developing PF, WT and Ninj1 KO mice were treated with BLM and the degree of PF was compared. The histological analysis showed that BLM-injected Ninj1 KO mice exhibited a mild fibrotic and inflammation phenotype, as compared to WT mice. In addition, the accumulation of fibroblasts and myofibroblasts were significantly

lower in BLM-treated Ninj1 KO mice than in BLM-treated WT mice.

In order to investigate the differences in the pathogenesis of PF between WT and Ninj1 KO mice, the population of inflammatory cells was examined in the lungs after BLM injection. Unexpectedly, there was no significant difference in recruitment of inflammatory cells such as lymphocytes and macrophages. However, the expression of pro-inflammatory and pro-fibrotic cytokines, IL-1β, TNFα and TGF-β1, was diminished in BLM-treated Ninj1 KO mice. These results suggest that Ninj1 deficiency resulted in reduced inflammatory response to BLM.

Since there are three major cell types involved in the pathogenesis of PF, such as fibroblasts, macrophages and alveolar epithelial cells (AECs), it was first examined if Ninj1 deficiency alters fibrotic response to TGF-β1 in primary fibroblasts isolated from the lungs of WT and Ninj1 KO mice. However, there was no significant difference in TGF-β1 signaling and production of ECM components between WT and Ninj1 KO fibroblasts. Next, I investigated the effects of Ninj1 deficiency on inflammatory response to BLM in macrophages. The results showed no significant difference in NF-κB signaling, which is a main inflammatory signaling pathway involved in production of pro-inflammatory cytokines. Finally, WT and Ninj1 KO MLE-12 cells were treated with BLM, and the expression of chemokines was assessed. The results demonstrated no significant difference in the expression of pro-inflammatory and pro-fibrotic mediators, such as CXCL1, CXCL12, and TGF-β1 between

WT and Ninj1 KO MLE-12 cells. Taking together, Ninj1 deficiency did not affect fibroblast activation and inflammatory response of macrophages and AECs.

Since Ninj1 is a cell-to-cell adhesion molecule and interaction between epithelial cells, it was further investigated whether differential expression of Ninj1 affects the interaction between AECs and macrophages, leading to induction of inflammatory response in macrophages. First, I examined if Ninj1 is involved in adhesion of macrophages and AECs. However, Ninj1 deficiency did not affect binding affinity between macrophages and AECs. Next, the involvement of Ninj1 in activating macrophages by contact with AECs was investigated. When WT macrophages were co-cultured with WT AECs, the inflammatory response of WT macrophages were dramatically increased. In addition, when WT macrophages were co-cultured with BLM-treated WT AECs, activation of macrophages was promoted. On the other hand, as Ninj1 expression was suppressed either in AECs or macrophages, stimulation of macrophages by interacting with AECs was diminished when they were co-cultured. These results suggest that Ninj1 on AECs would have been involved in activation of macrophages.

Therefore, it was examined if Ninj1 would directly activate macrophages. Recombinant mouse $Ninj1^{1-50}$ ($rmNinj1^{1-50}$) was generated and treated to WT and Ninj1 KO macrophages. Treatment of $rmNinj1^{1-50}$ on WT macrophages triggered an inflammatory response, leading to increased expression of pro-

inflammatory cytokines. On the other hand, Treatment of rmNinj1$^{1-50}$ did not stimulate Ninj1 KO macrophages. These results suggest that exogenous Ninj1 would activate inflammatory response in macrophages by interacting with surface Ninj1 on macrophages.

Taking together, there was no marked difference in fibrotic response between WT and Ninj1 KO fibroblasts and in inflammatory response by BLM between WT and Ninj1 KO macrophages or AECs. However, the results suggest that Ninj1 may contribute to activation of macrophages by enhancing interaction with AECs having elevated Ninj1 expression due to injury-inducing stimuli. Consequently, Ninj1 contributes to the development of pulmonary fibrosis by enhancing inflammatory response of macrophages.

Keywords: Ninj1; macrophage; BLM; inflammation; IPF

Student number: 2014-30543

LIST OF ABBREVIATION

α-SMA	Alpha-smooth muscle actin
AEC	Alveolar epithelial cell
BAL	Bronchoalveolar lavage
BALF	Bronchoalveolar lavage fluid
BLM	Bleomycin
CAS9	CRISPR-associated protein 9
CD11b	Cluster of differentiation molecule 11b
CD19	Cluster of differentiation molecule 19
CD3	Cluster of differentiation molecule 3
CD45	Cluster of differentiation molecule 45
cDNA	Complementary deoxyribonucleic Acid
CM	Conditioned media
Col1a1	Collagen type I alpha-1
CRISPR	Clustered Regularly Interspaced Short Palindromic Repeats
CXCL1	Chemokine (C-X-C motif) ligand 1
CXCL12	Chemokine (C-X-C motif) ligand 12
DAMP	Damage-associated molecular patterns

ECM	Extracellular matrix
EGF	Epithelial growth factor
EGFR	Epithelial growth factor receptor
ELISA	Enzyme-linked immunosorbent assay
FACS	Fluorescence-activated cell sorting
FITC	Fluorescein isothiocyanate
GAPDH	Glyceraldehyde-3-phosphate dehydrogenase
IF	Immunofluorescence
IFNγ	Interferon gamma
IHC	Immunohistochemistry
IL-1β	Interleukin-1beta
IL-4	Interleukin-4
IL-10	Interleukin-10
IL-12	Interleukin-12
IL-13	Interleukin-13
iNOS	Inducible nitric oxide synthase
IPF	Idiopathic pulmonary fibrosis
KO	Knockout
mRNA	Messenger ribonucleic acid

MTS	Masson's Trichrome staining
MUC5B	Mucin 5B
NF-κB	Nuclear factor kappa light chain enhancer of activated B cells
Ninjurin	Nerve injury-induced protein
Ninj1	Nerve injury-induced protein 1
Ninj2	Nerve injury-induced protein 2
PAMP	Pathogen-associated molecular patterns
PAS	Periodic acid schiff
PBS	Phosphate-buffered saline
PBS-T	PBS+0.1% Tween 20
PCR	Polymerase chain reaction
PDGF	Platelet-derived growth factor
PE	Phycoerythrin
PF	Pulmonary fibrosis
qPCR	Semi-quantitative PCR
rmNinj1$^{1-50}$	Recombinant mouse Ninj1 (1-50 amino acids)
RNA	Ribonucleic acid
RT-PCR	Reverse transcription PCR

SEM	Standard error of means
SMAD2/3	SMAD Family Member 2/3
SMAD3	SMAD Family Member 3
TGF-α	Transforming growth factor-alpha
TGF-β1	Transforming growth factor-β1
TLR	Toll-like receptor
TNFα	Tumor necrosis factor alpha
VEGF	Vascular endothelial growth factor
WT	Wild type

TABLE OF CONTENTS

LIST OF FIGURES

LIST OF TABLES

INTRODUCTION

Fibrosis is a disease that is resulted from dysregulated wound healing process and chronic inflammation. Generally, wound healing process is subdivided into three phases; inflammation, proliferation and remodeling phases (Gonzalez et al., 2016; Gurtner et al., 2008). In inflammation phase, when tissues are damaged, inflammatory response is stimulated by damage-associated molecular patterns (DAMP) or pathogen-associated molecular patterns (PAMP), which are referred to as molecules that are released from damaged cells undergoing apoptosis or necrosis, or from pathogens, respectively (Huebener and Schwabe, 2013; Zhang et al., 2010). Inflammatory cells are then recruited into injury site and various cytokines and growth factors are released by the inflammatory cells, such as interleukin-1 (IL-1), interleukin-6 (IL-6), tumor necrosis factor alpha (TNFα), transforming growth factor-beta (TGF-β), platelet-derived growth factor (PDGF) and epidermal growth factor (EGF) (Barrientos et al., 2008; Gonzalez et al., 2016). The growth factors initiate proliferation phase, in which angiogenesis, fibroplasia and reepithelialization occur, leading to tissue remodeling at the final phase (Gonzalez et al., 2016). However, when the tissue is exposed to severe and repetitive injury, the wound healing process is uncontrolled and chronic inflammation is induced, resulting in development of fibrosis by producing excessive extracellular matrix (ECM) forming scar tissue (Wynn, 2008; Wynn and Ramalingam, 2012).

Fibrosis is characterized by excessive accumulation of ECM including collagens in various organs. The most lethal fibrotic diseases include liver cirrhosis, pulmonary fibrosis (PF), kidney and heart fibrosis, which lead to organ failure (Bataller and Brenner, 2005; Wynn, 2008; Ziegler and Kehrer, 1990). The previous reports demonstrated that while several fibrotic diseases, including liver cirrhosis, kidney and heart fibrosis are reversible (Eddy, 2005; Jung and Yim, 2017; Kong et al., 2014), PF is irreversible (Wynn, 2011). Idiopathic pulmonary fibrosis (IPF) is a chronic interstitial lung disease, which is the most commonly diagnosed type of PF with unknown origin, characterized by irreversible and fatal progressive lung scarring and pulmonary dysfunction (Selman and Pardo, 2006; Zeki et al., 2010). Like fibrosis in other organs, IPF is caused by a dysregulated wound healing process initiated by injury to the alveolar epithelial cells (AECs), leading to a chronic inflammation (King et al., 2011; Selman et al., 2001). The general clinical symptoms of pulmonary fibrosis includes short breath, dry cough, fatigue and weight loss (Bacci et al., 2018). Since the symptoms are not very specific to IPF, it is difficult to diagnose IPF and the current diagnostic makers for IPF are not reliable (Wuyts et al., 2013). In addition, the prognosis of IPF is extremely poor, with mean survival estimated to be 2 to 4 years after diagnosis (Raghu et al., 2011; Strock et al., 2017). However, even though previous studies have revealed several factors involved in the pathogenesis of IPF, the etiology is still poorly understood. In addition, there is no adequate treatment developed for complete cure for IPF

but just drugs to delay the disease progression or to relieve symptoms (Hewitt and Maher, 2019; Kolilekas et al., 2019). Therefore, it is urgent to understand exact pathogenesis of IPF and develop appropriate therapeutic strategies for IPF patients.

In the pathogenesis of IPF, macrophages are the major inflammatory cells involved in the induction of pulmonary inflammation and fibrosis by producing various pro-inflammatory and pro-fibrotic mediators (Borthwick et al., 2016; Bringardner et al., 2008; Wynn, 2008; Wynn and Vannella, 2016). The major cytokines, which cause chronic inflammation and prolonged wound healing process, are interleukin-1beta (IL-1β) and TNFα (Barrientos et al., 2008). It was reported that the expression level of IL-1β was higher in bronchoalveolar lavage fluid (BALF) of IPF patients than normal individuals (Lasithiotaki et al., 2016; Wilson et al., 2010). In addition, the expression of TNFα was also increased in the lungs of IPF patients (Hasegawa et al., 1997; Nash et al., 1993; Piguet et al., 1993). One of the major fibrogenic mediators, TGF-β1 has been implicated on development of IPF (Fernandez and Eickelberg, 2012; Tatler and Jenkins, 2012). Previous reports demonstrated that macrophages are the major source of TGF-β1 (Murray et al., 2011; Wynn and Barron, 2010). The significance of macrophages is thoroughly discussed in a recent review, detailing the contribution of macrophages to lung diseases, and their importance as immune effector cells within the lung in patients with IPF (Reynolds, 2005). In addition, the interaction between alveolar macrophages

and AECs is an important factor in pulmonary inflammation and fibrosis, and contact-dependent effects of alveolar macrophages and AECs are required (Fujii et al., 2002; Manzer et al., 2008; Tao and Kobzik, 2002; Young et al., 2016).

Macrophages play a central role in wound healing process whose aberration leads to fibrosis. Depletion of macrophages leads to attenuation of wound repair by impaired proliferative stage during would healing process (Ferrante and Leibovich, 2012). Tissue regeneration is initiated by macrophages producing various growth factors including TGF-β1 (Barrientos et al., 2008; Gonzalez et al., 2016). However, when the inflammation becomes chronic due to repetitive injuries, macrophages aberrantly produce excessive TGF-β1 and fibroblasts persistently activated, leading to uncontrolled production of ECM components and finally development of fibrosis (Fernandez and Eickelberg, 2012; Murray et al., 2011). Another aspect about macrophage that has been implicated in fibrogenesis is macrophage polarization. Polarization of macrophages is classified into two distinct populations, “classically” or “alternatively” activated macrophages referred to as M1 or M2 macrophages, respectively (Martinez and Gordon, 2014). M1 macrophages are induced by various factors such as DAMP, PAMP and interferon gamma (IFNγ), and they produce pro-inflammatory cytokines including IL-1β, interleukin-12 (IL-12) and TNFα (Ferrante and Leibovich, 2012; Martinez and Gordon, 2014). On the other hand, M2 polarization is induced by interleukin-4 (IL-4) and interleukin-13 (IL-13)

and M2 macrophages produce anti-inflammatory and pro-fibrotic mediators such as interleukin-10 (IL-10), TGF-β1 and vascular endothelial growth factor (VEGF) (Ferrante and Leibovich, 2012; Martinez et al., 2009). According to the previous reports, even though M1 and M2 macrophages exhibit different phenotypes, both phenotypes contribute to development of fibrosis by mediating fibroblast activation (Braga et al., 2015; Cao et al., 2014; Misharin et al., 2017).

Nerve injury-induced proteins (Ninjurin) consist of 2 transmembrane domains, an intracellular region, and extracellular region at the N- and C-termini (Araki and Milbrandt, 1996, 2000). Ninjurin family includes Ninjurin1 (Ninj1) and Ninjurin2 (Ninj2), which are 55% identical in their mRNA sequences (Araki and Milbrandt, 1996, 2000). The previous reports demonstrated that tissue distribution of Ninj1 and Ninj2 alters. While Ninj1 is expressed ubiquitously in all tissue types including lung and predominantly in epithelial cells, the expression of Ninj2 is limited to bone marrow, peripheral leukocyte, lung and lymph node in adults (Araki and Milbrandt, 2000; Araki et al., 1997). However, even though many research groups have demonstrated that Ninjurin proteins would be involved in various inflammatory and vascular diseases, the mechanism and function of Ninjurin proteins are still unclear (Lee et al., 2010).

Ninj1 was first found in Schwann cells and its expression is induced,

following an injury to the nerve (Araki and Milbrandt, 1996). In the previous report, 12 amino acid residues (from Pro26 to Asn37) positioned in the extracellular region of N-terminus, were identified as a homophilic domain having binding affinity in a trans-interaction, which is not conserved in Ninj2 (Araki and Milbrandt, 2000; Araki et al., 1997). Ninj1 is involved in migration of immune cells such as monocytes and macrophages in experimental model of autoimmune encephalopathy (Ahn et al., 2014a) as well as in multiple sclerotic lesions of human brain (Ifergan et al., 2011). Recent reports indicate that Ninj1-expressing leukocytes adhere to the endothelial cells and/or other leukocytes via homophilic or heterophilic binding, and enter the site of inflammation or targeted tissues (Lee et al., 2010). In addition, Ninj1 is involved in not only migration of immune cells but also inflammatory response in macrophages. Ninj1 is involved in promoting pro-inflammatory response in multiple sclerosis and systemic inflammation (Ahn et al., 2009; Jennewein et al., 2015; Tajouri et al., 2007). In addition, blocking Ninj1 causes Toll-like receptor (TLR)-mediated inflammatory response and reduces inflammation in organs (Jennewein et al., 2015).

In this study, since Ninj1 plays a crucial role in various inflammatory diseases, I hypothesized that Ninj1 could be involved also in developing pulmonary fibrosis, which is a chronic inflammatory disease. It was demonstrated that Ninj1 deficiency ameliorated the bleomycin (BLM)-induced pulmonary fibrosis, which is the most commonly used pulmonary fibrosis

model (Moeller et al., 2008). In addition, the results show that Ninj1 enhances interaction between macrophages and AECs, leading to promotion of macrophage activation.

MATERIALS AND METHODS

Animal care and experiments

All animal experiments were approved by the Institutional Animal Care and Use Committee at the National Cancer Center and carried out in accordance with the relevant guidelines and regulations. Ninj1 KO mice were provided by GT Oh (Ahn et al., 2014a; Yin et al., 2014). C57BL/6J WT and Ninj1 KO mice were maintained under 12 h light/dark cycles at 22℃ and 60% humidity, and provided with food and water *ad libitum*. Eight-wk-old WT and Ninj1 KO mice were used in this study. To induce pulmonary fibrosis, 1 mg/kg of BLM (Carbosynth, Compton, UK) or PBS was intratracheally injected, and necropsy was performed at 1, 3, 5, 7, 14 and 21 days after injection. Before excision of lungs, cell-free bronchoalveolar lavage fluid (BALF) and BAL cells were collected as described in the previous report (Jiang et al., 2010). After each mouse was euthanized by CO_2, the lung and trachea were surgically exposed. Six hundred μl of PBS was injected and aspirated through trachea. This step was proceeded total 3 times. Total volume of BALF collected was about 1.5 ml. BALF was centrifuged at 1,500 rpm for 3 min. The cell pellet was resuspended in 1 ml of PBS and subjected to inflammatory cell analysis. The supernatant, which is cell-free BALF, was stored at -20℃ for further experiments. The cell-free BALF was subjected to ELISA to evaluate the amount of IL-1β and TGF-β1. Cell-free BALF was also used to stimulate primary fibroblast. The lungs

collected at day 21 were fixed in 10% neutral formalin, and a paraffin block was generated. On days 1, 3, 5, 7, and 14, the right lungs were frozen in liquid nitrogen for RNA and protein analysis, whereas the left lungs were fixed in 10% neutral formalin for histological analysis. To measure levels of IL-1β and TGF-β1, enzyme-linked immunosorbent assay (ELISA kits; mouse IL-1β, KOMA Biotech, Seoul, Korea; mouse TGF-β1, AbFrontier, Seoul, Korea) was conducted using frozen lung tissue and cell-free BALF collected at day 7, following manufacturer's instruction.

Antibodies

The primary antibodies used for western blotting were rabbit anti-p-p65 (Cell Signaling Technology, MA, USA, cat. no. 3033), rabbit anti-p65, (Cell Signaling Technology, cat. no. 8242), mouse anti-α-tubulin (Sigma-Aldrich, MO, USA, cat. no. cp06), rabbit anti-p-SMAD3 (Cell Signaling Technology, cat. no. 9520), mouse anti-GAPDH (Merck Millipore, Darmstadt, Germany, CB1001), and rabbit anti-Ninj1 (Abclone, Seoul, Korea, customized). All primary antibodies for western blotting were diluted to 1:1,000 except for anti-Ninj1 antibody, 1:3,000. The primary antibodies for immunohistochemistry (IHC) were rabbit anti-Ninj1 (Abclone, 1:2,000), rat anti-ER-TR7 (Santa Cruz, CA, USA, cat. no. sc-73355, 1:200), and mouse anti-α-SMA (Sigma-Aldrich, cat. no. A2547, 1:1,000). The primary antibodies for immunofluorescence assay were rabbit anti-SMAD2/3 (Cell Signaling Technology, #3102, 1:500), rabbit anti-Ninj1 (Abclone, 1:1,000), FITC rat anti-F4/80 (eBioscience, CA, USA, cat.

no. 11-4801, 1:500) and mouse anti-α-SMA (Sigma-Aldrich, 1:1,000). For fluorescence-activated cell sorting (FACS) analysis, rabbit anti-Ninj1 (Abclone, 1:200), Alexa Fluor 647 anti-CD45 antibody (BD Bioscience, CA, USA, 103124, 1:200), PE rat anti-mouse CD11b antibody (BD Bioscience, cat. no. 553311, 1:200), FITC rat anti-mouse CD3 antibody (BD Pharminogen, CA, USA, cat. no. 555274, 1:200) and FITC rat anti-mouse CD19 (BD Pharminogen, cat. no. 553785, 1:200) were applied.

Extraction of microarray gene expression dataset

The dataset, GSE53845, was extracted to identify 8 normal and 29 IPF lung specimens. The data were analyzed as previously described (Leng et al., 2013). Briefly, in order to analyzed the differential expression of Ninj1 between normal and IPF patients, the expression data extracted were analyzed by using GEO2R analysis tool based on 'limma' R packages (Barrett and Edgar, 2006; Ritchie et al., 2015) (http://www.ncbi.nlm.nih.gov/projects/geo/). The significance of differential expression of Ninj1 between normal and IPF patients was determined by Welch's t-test.

Preparation of BALF and BAL cells

Before excision of lungs, cell-free bronchoalveolar lavage fluid (BALF) and bronchoalveolar lavage (BAL) cells were collected as described in the previous report (Jiang et al., 2010). Briefly, after each mouse was euthanized by CO_2, the lung and trachea were surgically exposed. Six hundred μl of PBS was

injected and aspirated through trachea. This step was proceeded total 3 times. Total volume of BALF collected was about 1.5 ml. BALF was centrifuged at 1,500 rpm for 3 min. The cell pellet was resuspended in 1 ml of PBS and subjected to inflammatory cell analysis. The supernatant, which is cell-free BALF, was stored at -20℃. BALF was subjected to ELISA to evaluate the amount of IL-1β and TGF-β1. Cell-free BALF was also used to stimulate primary fibroblast.

Inflammatory cell analysis

In order to assess the inflammatory cell population in brochoalveolar lavage (BAL) cells, 100 μL of the BAL cell suspension was fixed on slides using the Shandon Cytospin 4 Cytocentrifuge (Thermo Scientific, MA, USA). The cells were stained with Diff-Quick staining kit (Sysmex, Kobe, Japan) and a differential cell count was performed under light microscope. The remaining BAL cells were double-stained with fluorescent anti-CD45 and anti-CD11b antibodies. FACS analysis was performed using BD FACSCalibur (BD Bioscience).

Using lung tissue, the lungs were minced until the fragment size is smaller than 2mm. The lung fragments were digested by incubating them with Type IV Collagenase at 37℃ for 1 hr. The digested cells were centrifuged and the pallet was washed with PBS 3 times. The lung cells were stained with fluorescent anti-CD45, anti-CD3, anti-CD19 and anti-F4/80 antibodies and FACS analysis

was performed using BD FACSCalibur (BD Bioscience).

Primary cell isolation

Lung primary fibroblasts were isolated from lungs of WT and Ninj1 KO mice. The whole lungs were aseptically excised and placed on petri dish. The lungs were minced until the size of lung fragments is less than 2 mm. The lung fragments were placed in tissue culture dish in DMEM supplemented with 15% FBS and streptomycin (100 μg/ml)/penicillin (100 units/ml) and incubated in a humidified CO_2 incubator without changing media until crawling fibroblasts from tissue fragments were observed. The media was replaced with the fresh media and incubated until no tissue fragments was observed. The primary fibroblasts were subcultured and incubated in a humidified CO_2 incubator for additional 7 days. The culture media was changed every 2~3 day.

Peritoneal macrophages were isolated from WT or Ninj1 KO mice as described in the previous report (Zhang et al., 2008). The abdominal skin of the mouse was removed to expose peritoneal wall. To collect peritoneal cells, 5 ml of PBS was injected through peritoneal wall, using 10-ml syringe with 20 G needle, and aspirated PBS from peritoneum. This step was repeated twice. Peritoneal cells were centrifuged for 10 min at 400 x g. The cells were resuspended in DMEM supplemented with 10% FBS and streptomycin (100 μg/ml)/penicillin (100 units/ml), and seeded on culture plates. The cells were incubated in a humidified CO_2 incubator for 1 hr and washed with PBS 3 times

in order to remove nonadherent cells. The adherent cells are over 90% macrophages.

Recombinant mouse Ninj1$^{1-50}$

Recombinant protein was generated as described in the previous report (Woo et al., 2017). Briefly, the gene encoding mouse Ninj1 (1-50 a.a.) was amplified from mouse cDNA and inserted into pET32a vector (Stratagene, CA, USA). pET32a vectors containing the gene encoding mouse Ninj1 (1-50 a.a.) were transformed into BL-21(DE3) *Escherichia coli* cells and the BL21 cells were incubated in LB medium for 12 hrs. The protein expression was induced by adding IPTG to a final concentration of 0.1 mM and incubating for additional 6 hrs. The BL21 cells were lysed by probe sonication and the cell debris was removed by centrifugation. The lysate was incubated with Ni-NTA agarose (Qiagen, Hilden, Germany) overnight by gentle inverting. The lysate with Ni-NTA agarose was loaded onto the column and washed with PBS containing 25 mM imidazole (Sigma-Aldrich) five times. The recombinant mouse Ninj1 (rmNinj1$^{1-50}$) was eluted with PBS containing 250 mM imidazole and dialyzed with PBS overnight at 4°C. Endotoxin was removed by using The primers used to amplify the gene that encodes Ninj1 (1-50 a.a.) are described in Table 1.

Table 1. Primers for the gene encoding Ninj1 (1-50 a.a.)

No.	Genes	Direction	Primers (5’ -> 3’)
1	mouse Ninj1	Forward	GAG TAT GAG CTC AAC GGC GA
		Reverse	TGA CCA GGA AGA TGA GCA GC

Cell culture and treatment

All cell lines and primary cells were cultured at 37℃ in the humidified chamber with 5% CO_2. Raw264.7 was purchased from Korean Cell Line Bank (KCLB, Seoul, Korea). Raw264.7 and peritoneal macrophages were cultured in 10% FBS-supplemented DMEM (WelGene, Daegu, Korea) with streptomycin (100 μg/ml)/penicillin (100 units/ml). Raw264.7 cells and peritoneal macrophages were exposed to BLM (50 μg/ml) or recombinant mouse Ninj1 (rmNinj1, 0, 10 or 50 μg/ml) for 6 hrs or various time periods as indicated in figures. The cells were harvested for western blot and RT-PCR. MLE-12, a pneumocyte cell line, was purchased from ATCC (Manassas, VA, USA). MLE-12 was cultured in 2% FBS-supplemented DMEM (WelGene) with streptomycin (100 μg/ml)/penicillin (100 units/ml). MLE-12 cells were transfected with scramble or siNinj1 using TransIT-X2 System (Mirus Bio LLC., WI, USA), following manufacturer's protocol and incubated for 48 hrs. Then, MLE-12 cells were treated with BLM (0, 10 or 50 μg/ml) or rmNinj1$^{1\text{-}50}$ (0, 10 or 50 μg/ml) for 24 hrs, and western blot and RT-PCR were performed.

Generation of Ninj1 KO cell lines using CRISPR Cas9

CRISPR Cas9 All-in-one lentiviral expression vectors targeting Ninj1 were purchased from transOMIC Technologies inc. (Huntsville, AL, USA). MLE-12 and Raw264.7 cells were transfected with the CRISPR Cas9 expression vector using TransIT®-2020 Transfection Reagent (Mirus Bio LLC.) and the cells were incubated in a cell culture chamber for 48 hrs. The transfected cells were

sorted by tRFP, using SONY cell sorter SH800Z (SONY, Tokyo, Japan). The sorted cells were plated on 96-well plate for single cell colony selection. Ninj1 expression was evaluated by performing western blot analysis. Ninj1-expressing cells were referred to as WT and Cas9-drived Ninj1-deficient cells were referred to as Ninj1 KO.

Co-culture of MLE-12 and Raw264.7

WT or Ninj1 KO MLE-12 cells with or without BLM (50 μg/ml) treatment for 12 hrs and CFSE-stained WT or Ninj1 KO Raw264.7 cells were co-cultured for 30 min, and the number of Raw264.7 cells bound to MLE-12 cells was assessed using the BD FACSCalibur (BD Bioscience). For RNA and protein analysis, after co-culture of WT or Ninj1 KO MLE-12 and CFSE-stained WT or Ninj1 KO Raw264.7 for 6 hrs, Raw264.7 cells were sorted using the SONY cell sorter SH800Z (SONY, Tokyo, Japan), and RNA and protein were isolated from the sorted Raw264.7 cells. To collect conditioned media (CM), the media was changed to serum-free medium after 6 hrs of co-culture and CM was collected 12 hrs after media change.

Stimulation of fibroblasts by TGF-β1, BALF and CM

Primary fibroblasts were isolated from WT or Ninj1 KO mice. In order to evaluate activation of fibroblasts, activation and localization of SMAD2/3, migration, production of collagens and expression of α-SMA were assessed. To examine activation and localization of SMAD2/3, recombinant mouse TGF-β1

(20 ng/ml), BALF (1:4 diluted in serum-free DMEM) or CM from co-culture of MLE-12 and Raw264.7 cells or rmNinj1-treated Raw264.7 cells were introduced after 24 hrs of starvation. The fibroblasts were incubated for 30 min or 1 hr in a humidified CO_2 incubator and harvested for western blotting and immunofluorescence assay. To assess migration of fibroblasts, the transwell migration assay was performed as described in the previous report (Jang et al., 2016). Briefly, cell-free BALF collected from the BLM-treated WT and Ninj1 KO mice (day 7), or the CM from co-cultures of MLE-12 and Raw264.7 cells or rmNinj1-treated Raw264.7 cells was used as chemoattractant. The primary fibroblasts were seeded in the upper chamber of the transwell inserts and diluted BALF (1:4 dilutions in serum-free medium) or CM was placed in the lower chamber. The fibroblasts were incubated in a humidified CO_2 incubator for 6 hrs, and the number of migrated fibroblasts was counted under light microscope. To measure collagens secreted by primary fibroblasts, the fibroblasts were incubated with diluted BALF or CM for 12 hrs. The media was collected and subjected to hydroxyproline assay. To examine expression of α-SMA, the fibroblasts were incubated with diluted BALF or CM for 12 hrs and collected for RNA isolation and immunofluorescence assay. RNA was isolated and cDNA was synthesized, followed by real-time PCR.

Histological evaluation of pulmonary fibrosis

To observe histological changes after BLM treatment, 5 μm-thick lungs tissue sections were stained with hematoxylin and eosin. Masson's Trichrome

Staining (MTS) was also performed to evaluate the severity of pulmonary fibrosis, according to modified Ashcroft scale described in the previous report (Hübner et al., 2008). Periodic acid schiff (PAS) staining was performed to evaluate inflammatory status in the fibrotic lungs, using 5 μm-thick lung tissue sections. Histology of lung tissue was observed under light microscope.

Immunohistochemistry

Immunohistochemistry (IHC) was performed according to the protocol in the previous report (Jang et al., 2016). In brief, the 5 μm-thick sections of paraffin-embedded lung tissue were deparaffinized and rehydrated. The endogenous peroxidase was blocked with 3% H_2O_2 for 30 min at room temperature and washed 3 times with distilled water. Antigen retrieval was then performed by heating the sections in boiling 10 mM citrate supplemented with 0.1% Tween 20 and 0.5% EDTA in microwave oven for 6 min and washed the sections 3 times with PBS-T (0.05% Tween 20). In order to block endogenous mouse Ig, the sections were incubated in MOM™ Mouse Ig Blocking Reagent (Vector Laboratories, CA, USA) for 1 hr at room temperature. The sections were then blocked by using Antibody Diluent Reagent Solution (Invitrogen, CA, USA) for 30 min. The sections were incubated with primary antibodies overnight at 4℃ and washed with PBS+0.1% Tween 20 (PBS-T) 3 times, followed by secondary antibody conjugation for 1 hr. The sections were washed with PBS-T 3 times and incubated with streptavidin-HRP solution for 15 min at room temperature. After washing with PBS-T 3 times, detection was

performed using 3,3-diaminobenzidine (DAB) substrate solution (Dako, Carpinteria, CA, USA). The sections were washed in distilled water, counterstained with hematoxylin, dehydrated and mounted. The primary antibodies for IHC were anti-Ninjurin1 (Abclone, 1:2000), anti-ER-TR7 (Santa Cruz, CA, USA, sc-73355, 1:200), and anti-α-SMA (Sigma-Aldrich, A2547, 1:1000).

Immunofluorescence assay

Immunofluorescence assay was performed according to the protocol in the previous report (Jang et al., 2016). In brief, the 5 μm-thick sections of paraffin-embedded lung tissue were deparaffinized and rehydrated. Antigen retrieval was then performed by heating the sections in boiling 10 mM citrate supplemented with 0.1% Tween 20 and 0.5% EDTA in microwave oven for 6 min and washed the sections 3 times with PBS-T (0.05% Tween 20). For cells, they were cultured on the cover slides in 12-well plates. The cells were fixed in an acetone-methanol (1:1) mixture for 30 min at -20℃. The tissue sections and cells were blocked with Antibody Diluent Reagent Solution (Invitrogen) for 1 hr. The samples were incubated with primary antibodies overnight at 4 ℃ and secondary antibodies for 2 hrs at room temperature. After mounting the slides with VectaShield Mounting Medium with DAPI (Vector Laboratories), the slides were sealed with nail polish and stored at -20℃ until observation using a confocal microscope (Nikon Instruments Inc., New York, USA).

Hydroxyproline assay

The amount of collagens accumulated in the lungs or secreted from primary fibroblasts were measured using the Hydroxyproline Colorimetric Assay Kit (BioVision, CA, USA), following the manufacturer's instruction. Briefly, the whole lung specimens were homogenized in 100 μl distilled water per 10 mg lung tissue. One hundred μl of hydrochloric acid (~12 N) was added to 100 μl of each lung homogenate. For conditioned media, 100 μl of each sample was taken and 100 μl of HCl was added to each sample. The samples were hydrolyzed at 120℃ for 3 hrs. Samples were vortexed and centrifuged at 10,000 x g for 3 min. Fifty μl of each hydrolyzed sample was transferred to 96-well plate and dried in a 60℃ oven. For standard curve preparation, 0.1, 0.2, 0.4, 0.6, 0.8 and 1 μg of hydroxyproline standards were prepared in 96-well plate. One hundred μl of DMAB was added to each sample and incubated at 60℃ for 90 min, following incubation with 100 μl of Chloramine T reagent at room temperature for 5 min. The absorbance was measured at 560 nm in microplate reader. The amount of hydroxyproline was calculated and expressed in μg/mg lung tissue.

mRNA expression analysis

RNA was isolated from cells and lung specimens using TriZol (Invitrogen, CA, USA) following the manufacturer's instruction. Briefly, 1 ml of TriZol was added to each sample and mixed by pipetting. Two hundred μl of chloroform was added to each sample and vortexed. Samples were centrifuged at 12,000 x

g for 15 min and 400 μl of supernatant was collected into new tubes. Six hundred μl of isopropanol was added to each sample and mixed by inverting. Samples were centrifuged at 10,000 x g for 10 min and the supernatant was removed. Pellet was washed with 1 ml of 75% EtOH by vortexing and centrifuged at 7,500 x g for 5 min. The supernatant was discarded and the pellet was air-dried until the pellet started turning transparent. DEPC-treated distilled water was added to dissolve RNA. 2 μg of RNA was used to synthesize cDNA using PrimeScript RT reagent Kit (Takara, Shiga, Japan) as described in the manufacturer's instruction. Briefly, each RNA sample was mixed with dNTP and oligo dT included in the kit and incubated at 65℃ for 5 min. The mixture of reverse transcriptase, reaction buffer and RNase inhibitor was added to each sample and incubated at 42℃ for 60 min, followed by incubation at 95℃ for 5 min. Reverse-transcription PCR (RT-PCR) and semi-quantitative real-time PCR were performed, using the primers listed in Table 1. The RT-PCR products were detected through agarose gel electrophoresis. semi-quantitative real-time PCR was proceeded, following the method in the previous report (Livak and Schmittgen, 2001). Briefly, Semi-quantitative real-time PCR was performed using Stratagene Mx3000P QPCR system (Agilent Technologies, CA, USA). PCR conditions were one cycle of 10 min at 95℃, 40 cycles of 30 sec at 95℃, 30 sec at 60℃ and 30 sec at 72℃. The mRNA expression of each sample was calculated by $2^{-\Delta\Delta Ct}$ method (Livak and Schmittgen, 2001). Each sample was analyzed in triplicate.

Table 2. Primers for RT- and semi-quantitative real-time PCR

No.	Genes	Direction	Primers (5' -> 3')
1	mouse Ninj1	Forward	GAG TAT GAG CTC AAC GGC GA
		Reverse	TGA CCA GGA AGA TGA GCA GC
2	mouse IL-1β	Forward	GCC TTG GGC CTC AAA GGA AAG AAT C
		Reverse	GGA AGA CAC AGA TTC CAT GGT GAA G
3	mouse iNOS	Forward	GTG GTG ACA AGC ACA TTT GG
		Reverse	GGC TGG ACT TTT CAC TCT GC
4	mouse TNFα	Forward	ATA GCT CCC AGA AAA GCA AGC
		Reverse	CAC CCC GAA GTT CAG TAG ACA
5	mouse TGF-β1	Forward	CTT CAG CTC CAC AGA GAA GA
		Reverse	CAC GAT CAT GTT GGA CAA CTG
6	mouse col1a1	Forward	GAC CTC AAG ATG TGC CAC TC
		Reverse	CAA GGG TGC TGT AGG TGA AG
7	mouse CXCL1	Forward	GAG CTG CGC TGT CAG TGC CT
		Reverse	TGC CAT CAG AGC AGT CTG TC
8	mouse CXCL12	Forward	CAC TTT CAC TCT CGG TCC AC
		Reverse	GCT CCT CCT GTA AGT TCC TC
9	mouse α-SMA	Forward	GAA GAG CTA CGA ACT GCC TG
		Reverse	CAG ACA GAG TAC TTG CGT TC
10	mouse MUC5B	Forward	CAG CAA ACG TCG TCA ACT GG
		Reverse	TTG GGT TGG CAG AGT GTT GT
11	mouse β-actin	Forward	TGG AAT CCT GTG GCA TCC ATG AAA C
		Reverse	TAA AAC GCA GCT CAG TAA CAG TCC G

Western blot analysis

Western blot was performed as described in the previous report (Jang et al., 2016). Briefly, cells or tissue specimens were lysed using lysis buffer containing 20 mM Tris-HCl (pH 7.6), 1 mM EDTA, 140 mM NaCl, 1% NP-40, 1 mM sodium fluoride, and 1 mM sodium vanadate. The concentration of protein was determined by using a bicinchoninic acid protein assay kit (Pierce, IL, USA). Protein samples were prepared by supplementing with sodium dodecyl sulfate (SDS)-sample buffer and boiling for 5 min at 95 ℃. SDS-polyacrylamide gel electrophoresis (PAGE) was then performed to separate the protein by size. The proteins were transferred to polyvinyldene fluoride membrane (PALL Life Science, NY, USA). The proteins on the membrane were blocked in 5% skim milk and washed with TBS-T (0.1% Tween 20). The primary antibodies were conjugated overnight at 4℃, followed by conjugation with secondary antibodies for 1 hr at room temperature. Detection was performed by using Absignal (Abclone, Seoul, Korea). All western blot results were semi-quantified by using Image J program.

Statistical analysis

SPSS23.0 was used for all statistical analyses. Welch's t-test was used to compare gene expression level between lungs from healthy and IPF patients. All experimental data were evaluated by Student's t-test. All numerical data were expressed as mean ± SEM values of triplicate experiments. The significance level was limited to 5% (p<0.05).

RESULTS

1. The expression of Ninj1 is elevated in the fibrotic lungs

1.1. Establishment of BLM-induced pulmonary fibrosis

As previously mentioned, BLM is the most commonly used agent to induce pulmonary fibrosis in animal model (Moeller et al., 2008). BLM (1 mg/kg) was injected through trachea of mice and lungs were collected as scheduled in Fig. 1. Paraffin-embedded lung tissue sections, collected at day 21 after BLM injection, were subjected to Masson's Trichrome Staining (MTS) in order to detect collagens and determine fibrosis score. Observation on MTS revealed that collagens were accumulated in the lung tissue collected at day 21 after a single injection of BLM (Fig. 2A, B). Hydroxyproline assay showed that the amount of collagens accumulated in the lungs significantly increased (Fig. 3A). In addition, the expression of *col1a1* mRNA was elevated by BLM injection in a time-dependent manner (Fig. 3B). These results indicate that intratracheal injection of BLM induced pulmonary fibrosis within 21 days.

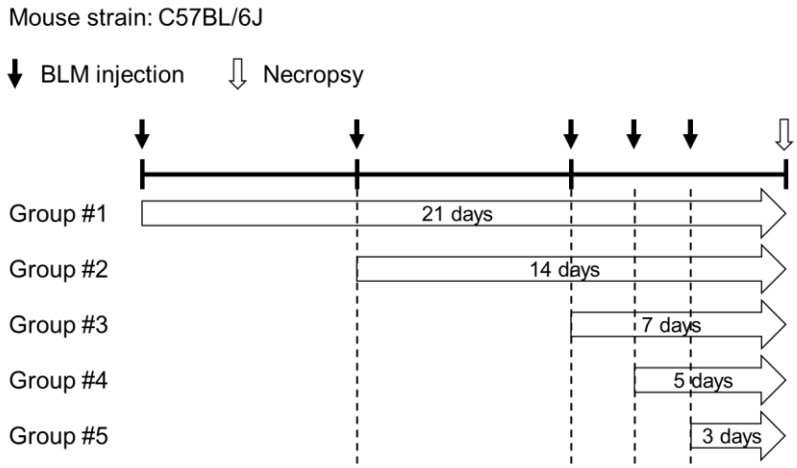

Figure 1. ***In vivo*** **experimental schedule for bleomycin (BLM) injection using C57BL/6J mice.**

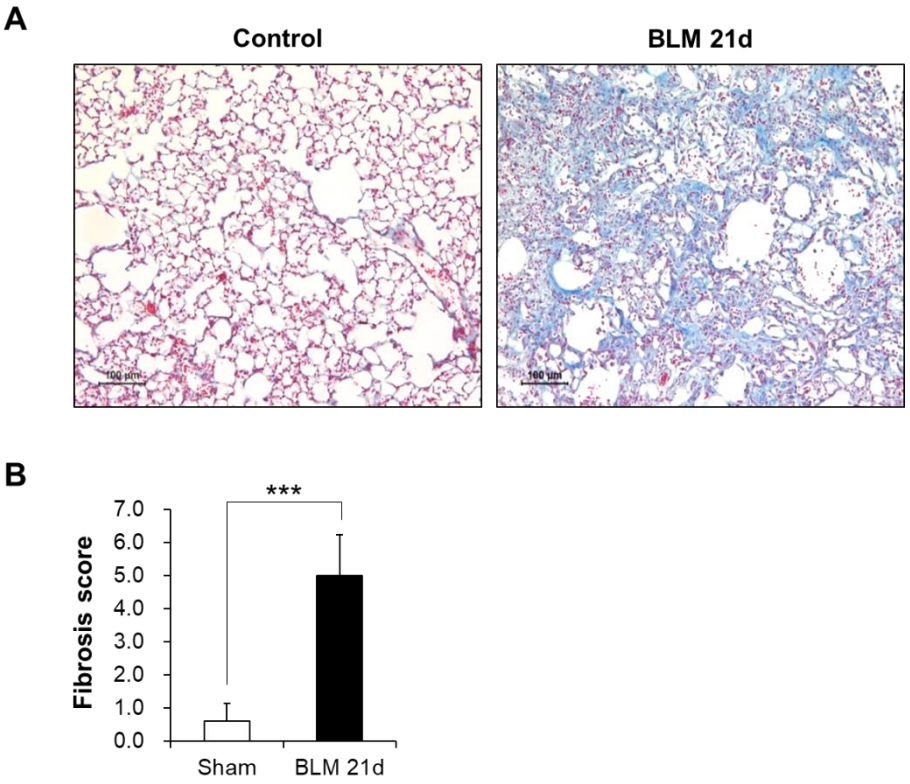

Figure 2. Induction of pulmonary fibrosis by intratracheal injection of BLM.

BLM (1 mg/kg) was intratracheally injected and lungs were collected at day 21 after BLM injection. Histological analysis was performed by MTS. (A) Representative images of MTS in paraffin-embedded lung sections from sham control and BLM-injected mice (n=5, scale bar=100 μm). (B) Degree of fibrosis scored by modified Ashcroft scale. Data are presented as means ± SEM. ***p<0.001.

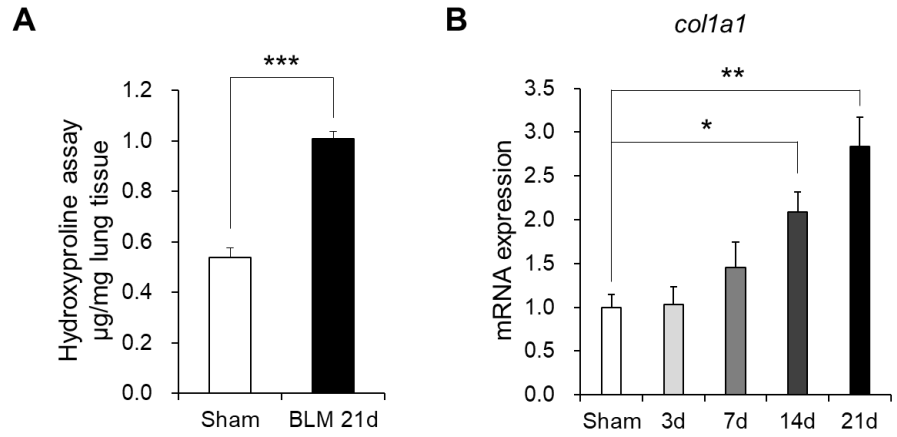

Figure 3. Accumulation of collagens in the lungs of BLM-treated mice.

BLM (1 mg/kg) was intratracheally injected and lungs were collected at indicated time points after BLM injection. Hydroxyproline assay and Semi-quantitative real-time PCR were performed to assess the expression of collagens. (A) Hydroxyproline assay to measure collagen contents in the lung tissue collected at day 21 after BLM injection. (B) Semi-quantitative real-time PCR to assess the expression of *col1a1* in the lungs collected at the indicated time points. Data are presented as means ± SEM. *p<0.05; **p<0.01; ***p<0.001.

1.2. Expression of Ninj1 is increased during developing pulmonary fibrosis

In order to determine if Ninj1 plays a role in the development of pulmonary fibrosis, the expression of Ninj1 was first examined in the lung specimens from normal people (n=8) and IPF patients (n=29). In GSE53845, Ninj1 gene expression level was upregulated in fibrotic lungs (Fig. 4). Ninj1 expression level was also investigated in BLM-induced pulmonary fibrosis model. Lungs were collected at day 3, 7, 14 and 21 after BLM injection for mRNA and protein expression analysis. Interestingly, as pulmonary fibrosis was induced, the expression levels of Ninj1 mRNA (Fig. 5A) and protein (Fig. 5B) were markedly elevated after BLM injection. These results suggest that increased Ninj1 plays a role in developing pulmonary fibrosis.

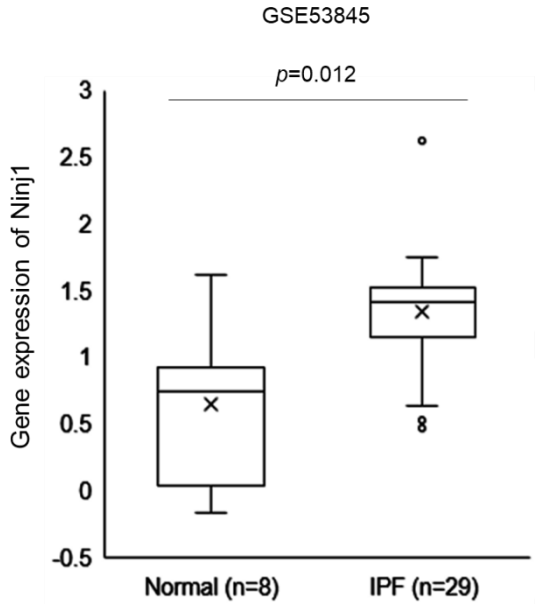

Figure 4. Ninj1 expression in the lungs of normal and IPF patients.

Box plot for the expression of Ninj1 in the lung specimens of normal (n=8) and IPF patients (n=29) based on microarray gene expression dataset, GSE53845.

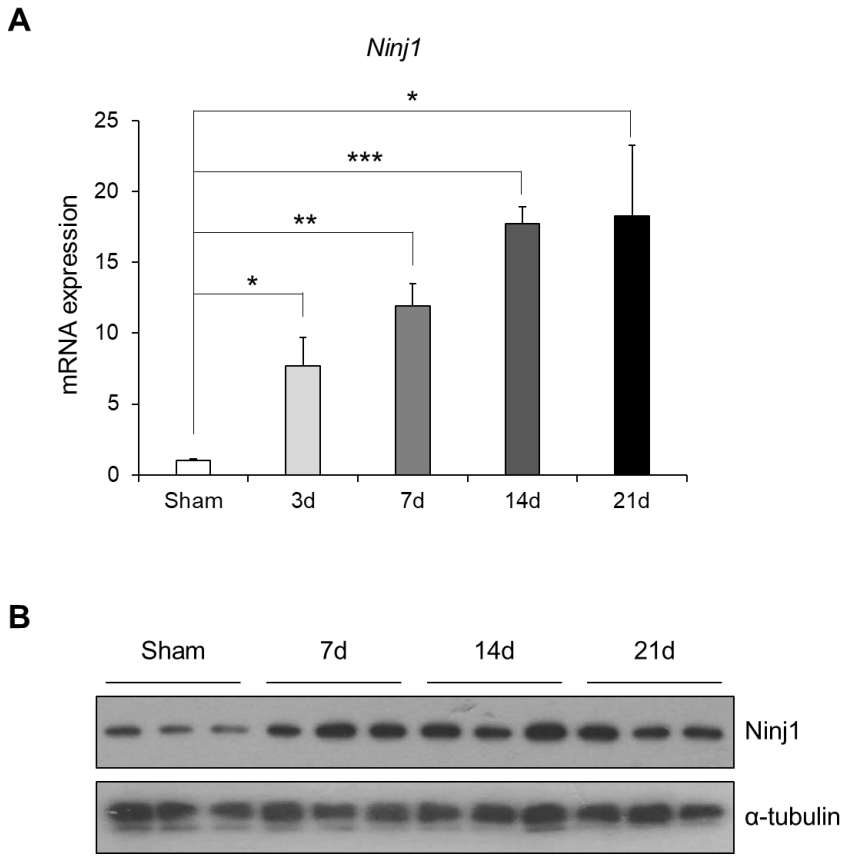

Figure 5. Ninj1 expression in the fibrotic lungs.

BLM (1 mg/kg) was intratracheally injected and lungs were collected at indicated time points after BLM injection. Semi-quantitative real-time PCR and western blot were performed to assess the gene expression of *Ninj1*. (A) Semi-quantitative real-time PCR to assess mRNA expression level of *Ninj1*, using lung specimen of sham control and BLM-treated mice (n=3). (B) Western blot analysis to assess the expression of Ninj1 protein, using lung specimen of sham control and BLM-treated mice (n=3). Data are expressed as means ± SEM. *p<0.05; **p<0.01; ***p<0.001.

1.3. Ninj1 expression is increased in macrophages and alveolar epithelial cells

Since Ninj1 is expressed in inflammatory cells such as macrophages (Ifergan et al., 2011; Jennewein et al., 2015), it was examined if elevation of Ninj1 expression in BLM-treated lungs was due to infiltration of Ninj1-expressing macrophages or increased Ninj1 expression in other cell types. Immunofluorescence (IF) revealed that the number of Ninj1-expressing F4/80-positive macrophages increased at day 7 after BLM treatment (Fig. 6, arrows). Interestingly, the expression of Ninj1 increased also in F4/80-negative cells, such as AECs (Fig. 6, arrow heads). These results showed that when pulmonary fibrosis is induced by BLM, Ninj1 expressing-macrophages are infiltrated and the expression of Ninj1 is elevated in AECs, suggesting that Ninj1 plays a role in the development of pulmonary fibrosis.

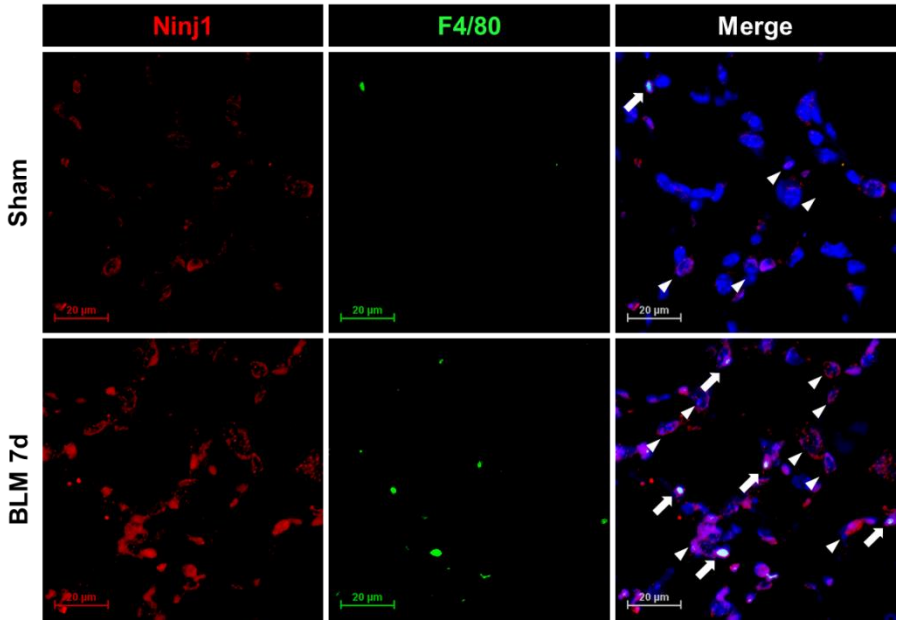

Figure 6. Ninj1 epxression in various cell types in the fibrotic lung tissue. Representative images of immunofluorescence assay for Ninj1 using paraffin block sections of lungs collected at day 7 after saline or BLM injection. Arrows, macrophages; arrow heads, alveolar epithelial cells.

2. Ninj1 deficiency results in decreased severity of pulmonary fibrosis

2.1. KO mice exhibit a mild fibrosis phenotype after administration of BLM

As described in the previous results, BLM treatment led to elevation of Ninj1 expression by infiltrated macrophages and AECs. Therefore, hypothesizing that Ninj1 contributes to the development of pulmonary fibrosis, the development of pulmonary fibrosis was compared between WT and Ninj1 KO mice, in which exon 1 of Ninj1 was deleted (Fig. 7A). BLM (1 mg/kg) was intratracheally injected into WT and Ninj1 KO mice and lungs were collected at days 3, 5, 7, 14 and 21 after injection (Fig. 7B). The severity of pulmonary fibrosis was assessed by performing MTS and scoring according to modified Ashcroft scoring system. As shown in Fig. 8A, collagens were accumulated in the lungs of both WT and Ninj1 KO mice. However, collagen accumulation was significantly diminished in the lungs of Ninj1 KO mice, compared to WT mice (Fig. 8A). In addition, the degree of fibrosis was also lower in Ninj1 KO mice than WT mice (Fig. 8B). These results indicate that the severity of pulmonary fibrosis was lower when Ninj1 was deficient.

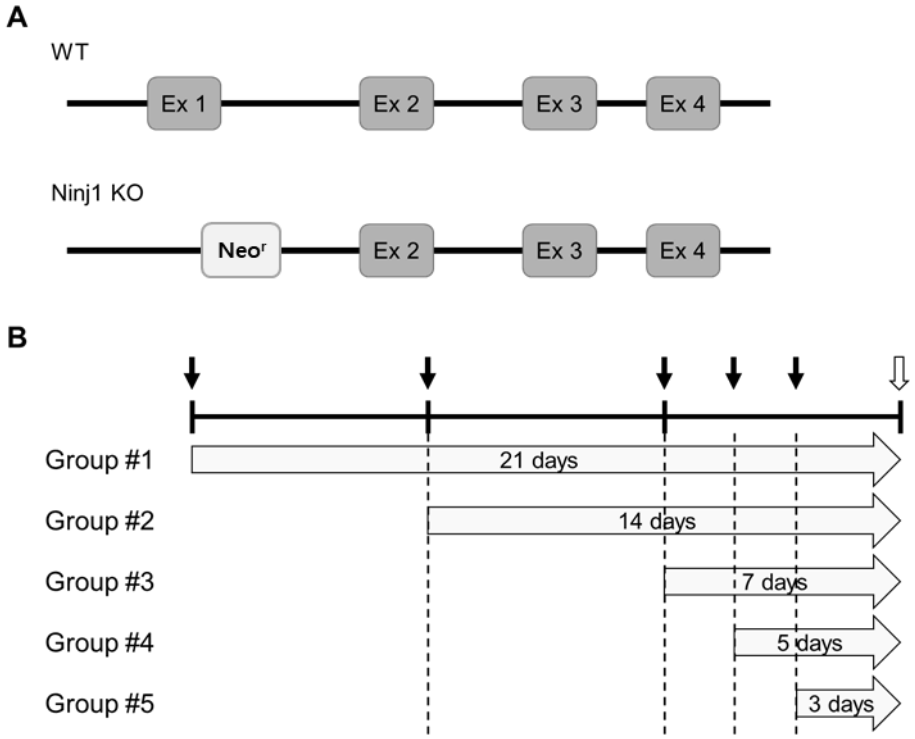

Figure 7. Schematic representation of Ninj1 gene of WT and Ninj1 KO mice and BLM injection schedule.

(A) Gene structure of Ninj1 in WT and Ninj1 KO mice. (B) Experimental schedule for BLM injection and necropsy.

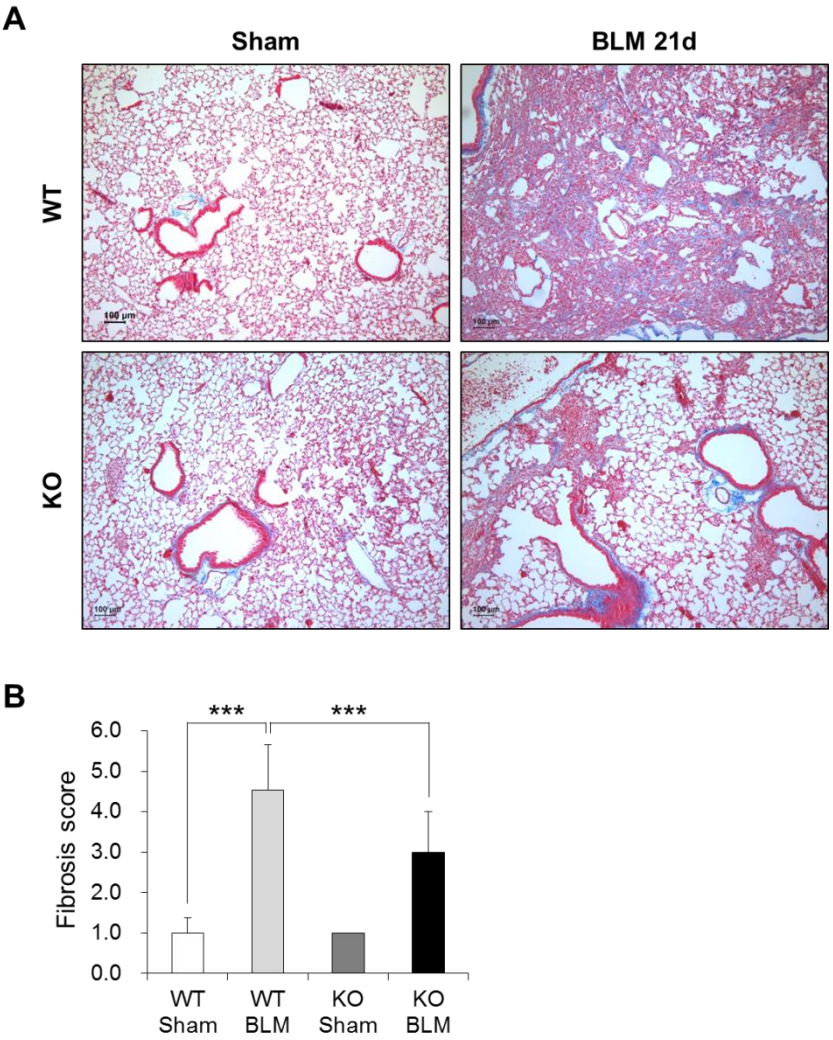

Figure 8. BLM-induced pulomary fibrosis in WT and Ninj1 KO mice.

BLM was intratracheally injected in WT and Ninj1 KO mice and histological analysis for pulmonary fibrosis was assess by MTS. (A) Representative images of MTS (n=13). Scale bar=100 μm. (B) Degree of fibrosis was scored according to modified Ashcroft scoring system (n=13). Data are expressed as means ± SEM. ***p<0.001.

2.2. Production of collagens is diminished in the lungs of Ninj1 KO mice

In order to quantify collagens accumulated in the lungs, hydroxyproline assay was performed using lung tissue collected from WT and Ninj1 KO mice at indicated time points after BLM injection. Hydroxyproline assay showed collagen accumulation was significantly diminished in the lungs of Ninj1 KO mice at day 21, compared to WT mice (Fig. 9A). Semi-quantitative real-time PCR also demonstrated that mRNA expression of *col1a1* was about 2.3 and 2.8 times higher in WT lungs than Ninj1 KO lungs at day 14 and 21, respectively (Fig. 9B). These results suggest that the expression of collagens was reduced in Ninj1 KO mice due to inactivation of fibroblasts.

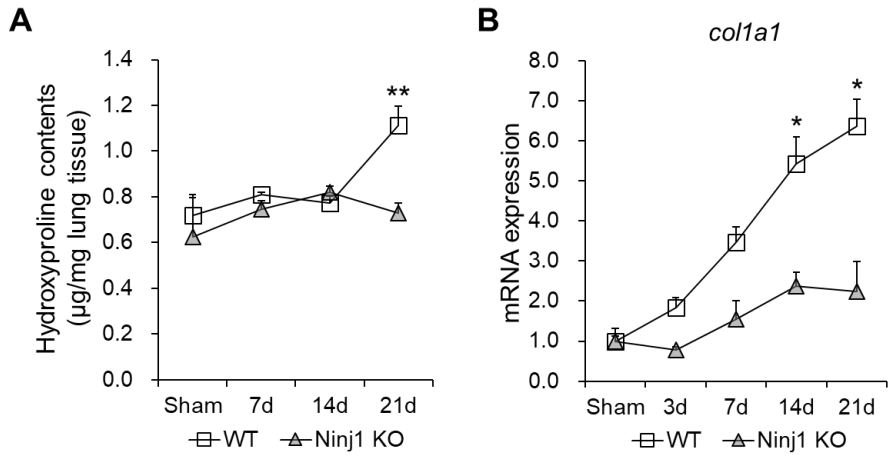

Figure 9. Production of collagens in BLM-treated WT and Ninj1 KO mice. Lungs were collected from WT and Ninj1 KO mice at indicated time points after BLM injection for hydroxyproline assay and RNA analysis. (A) Hydroxyprolines assay to determine collagen contents accumulated in the lungs. (B) Semi-quantitative real-time PCR to assess the mRNA expression of *col1a1* in the lungs (n=3). Data are expressed as means ± SEM of triplicates. *p<0.05, **p<0.01.

2.3. Accumulation of fibroblasts and myofibroblasts is reduced in BLM-treated Ninj1 KO mice, compared to BLM-treated WT mice

One of the major aspects in the pathogenesis of pulmonary fibrosis is the activation of lung fibroblasts which results in transformation into myofibroblasts (Wilson and Wynn, 2009). Lung sections were subjected immunohistochemistry (IHC) using antibodies against ER-TR7 as a fibroblast marker and α-SMA as a myofibroblast marker. As shown in Fig. 10A, the number of ER-TR7-positive cells was dramatically lower in the lungs of Ninj1 KO mice than WT mice. In addition, the number of α-SMA-positive cells was also significantly lower in in the lungs of Ninj1 KO mice than WT mice. According to semi-quantitative real-time PCR results, while mRNA expression *of α-SMA* in the lungs of WT mice gradually but significantly increased, Ninj1 KO mice exhibited only a slight increase in *α-SMA* expression (Fig. 10B). These results indicate that while fibroblasts were markedly activated in the lungs of WT mice, they were only mildly activated in the lungs of Ninj1 KO mice.

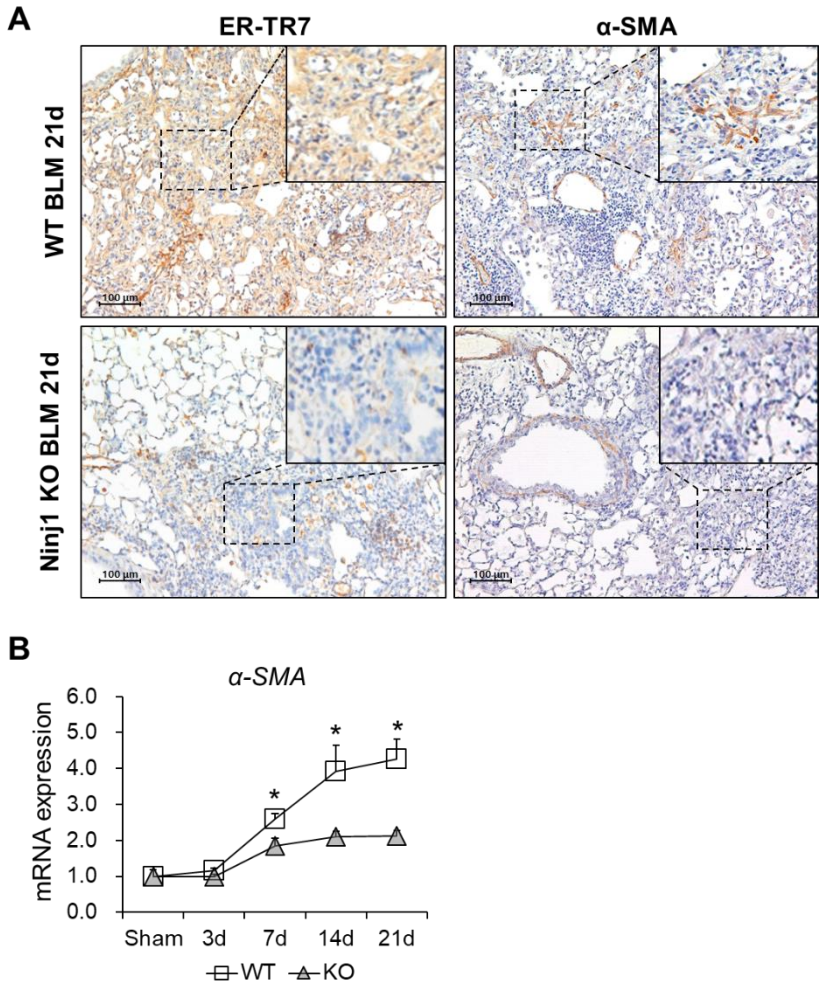

Figure 10. Accumulation and activation of fibroblasts in BLM-treated WT and Ninj1 KO mice.

Lungs were collected from WT and Ninj1 KO mice at indicated time points after BLM injection for IHC and RNA analysis. (A) Representative images of IHC for ER-TR7 (fibroblast marker) and α-SMA (myofibroblast marker), using the lung tissue sections (scale bar=100 μm, n=5). (B) Semi-quantitative real-time PCR to assess the mRNA expression of *α-SMA* in the lungs collected at

the indicated time points. (n=3). Data are expressed as means ± SEM of triplicates. *p<0.05.

2.4. Mucin production is alleviated in BLM-treated Ninj1 KO mice

It was reported that the expression of MUC5B, tracheobronchial mucin, is markedly higher in IPF patients than healthy individuals (Seibold et al., 2011). PAS staining showed that secretion of mucin was less in the bronchus of Ninj1 KO mice than in WT mice (Fig. 11A) and mRNA expression of *MUC5B*, tracheobronchial mucin, was also significantly lower in Ninj1 KO mice than in WT mice (Fig. 11B), indicating that the degree of inflammatory status was lower in the lungs of Ninj1 KO mice than WT mice.

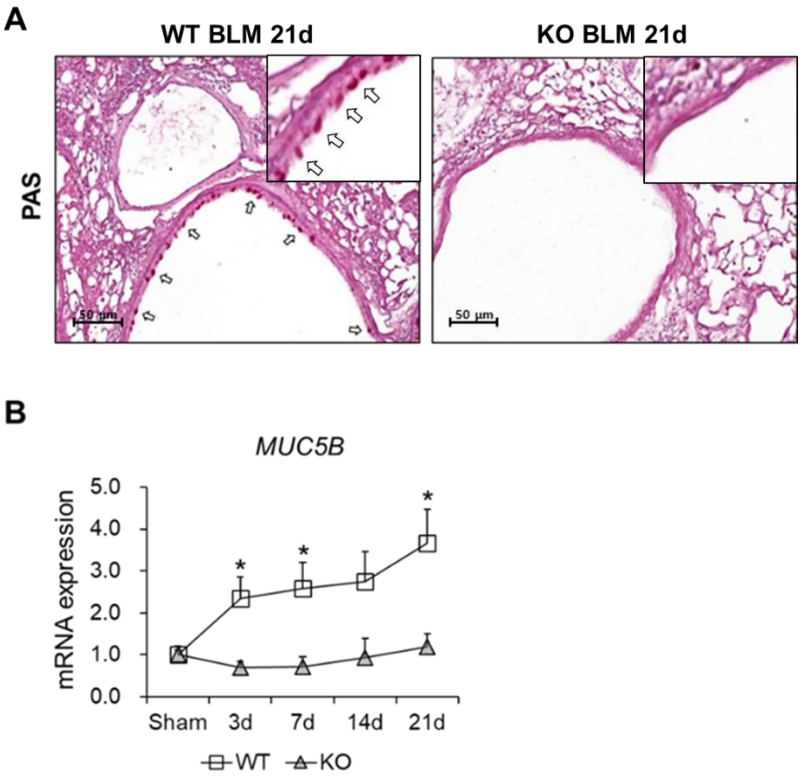

Figure 11. Mucin production in the lungs in BLM-treated WT and Ninj1 KO mice.

Lungs were collected from WT and Ninj1 KO mice at indicated time points after BLM injection for periodic acid schiff (PAS) staining and RNA analysis. (A) Representative images of PAS staining in the lung sections (scale bar=50 μm, n=5). (B) Semi-quantitative real-time PCR to assess the mRNA expression of *MUC5B* in the lungs collected at the indicated time points. (n=3). Data are expressed as means ± SEM of triplicates. **p*<0.05.

2.5. The population of inflammatory cells does not alter between BLM-treated WT and Ninj1 KO mice

During development of pulmonary fibrosis, inflammatory cells are recruited to injury site and produce various pro-inflammatory and pro-fibrotic mediators (Wilson and Wynn, 2009; Wynn and Ramalingam, 2012). Therefore, it was further examined if the fibrotic differences between WT and Ninj1 KO mice would have been resulted from differences in the recruitment of inflammatory cells. It was observed that the number of total BAL cells increased in both WT and Ninj1 KO mice as BLM was injected (Fig. 12A). In addition, as observed in Diff-Quick staining in BAL cells, there was no significant difference in the number of total BAL cells between WT and Ninj1 KO mice (Fig. 12B, C). In addition, CD11b-positive macrophage population in BALF was not significantly different between the BLM-treated WT and Ninj1 KO mice (Fig. 13A, B). These results indicated that even though there is a difference in fibrotic phenotype between BLM-treated WT and Ninj1 KO mice, the inflammatory cell population is not significantly different between them.

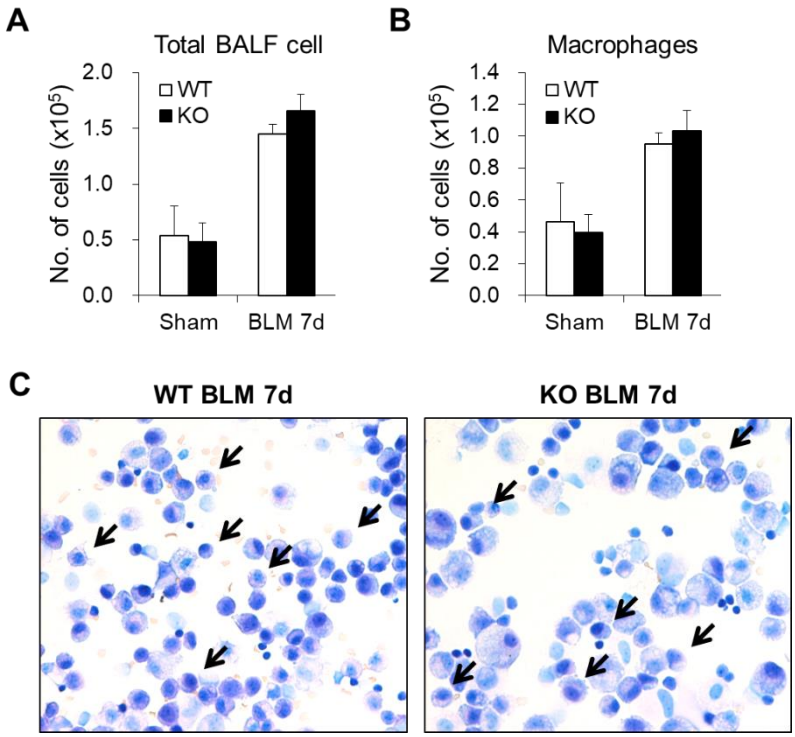

Figure 12. Recruitment of inflammatory cells in BLM-treated WT and Ninj1 KO mice.

BLM was intratracheally injected to WT and Ninj1 KO mice, and BAL cells were collected at day 3 and 7 after injection. The BAL cells were subjected to Diff-Quick staining and FACS analysis. The number of total BAL cells (A) and macrophages (B) among the BAL cells from control and BLM-treated WT and Ninj1 KO mice (n=5). (C) Representative images of BAL cells with Diff-Quick staining (n=5). Data are expressed as means ± SEM.

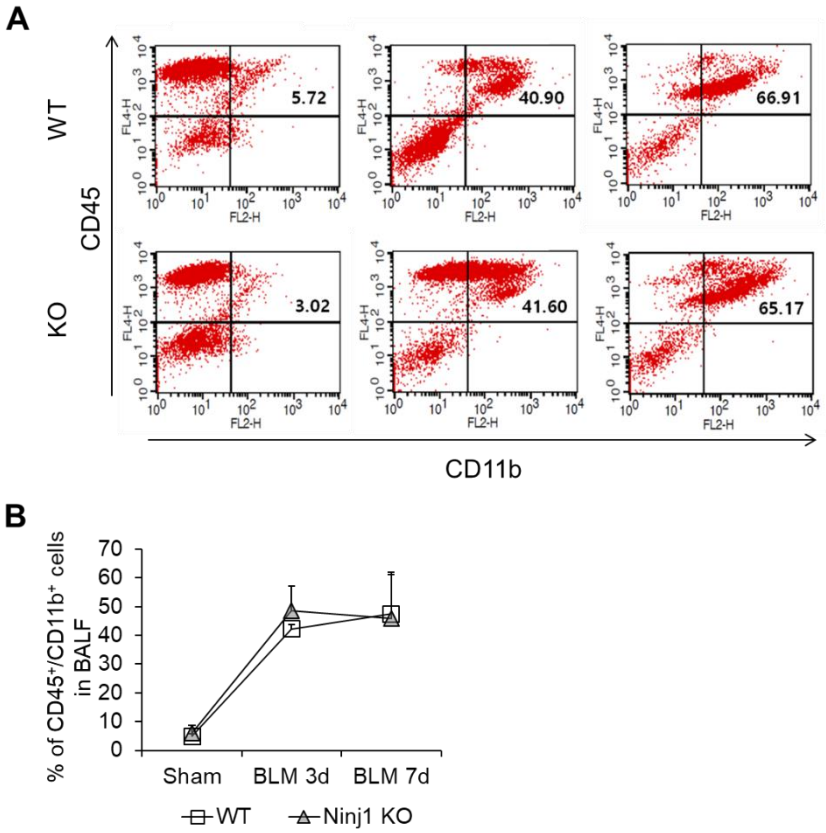

Figure 13. Macrophage population in BLM-treated WT and Ninj1 KO mice.

BLM was intratracheally injected to WT and Ninj1 KO mice, and BAL cells were collected at day 3 and 7 after injection. The BAL cells were subjected to Diff-Quick staining and FACS analysis. Representative images (A) and semi-quantification (B) of flow cytometry for $CD45^+/CD11b^+$ macrophages (n=4). Data are expressed as means ± SEM.

2.6. The expression of pro-inflammatory and pro-fibrotic cytokines is diminished in BLM-treated Ninj1 KO mice

In the pathogenesis of pulmonary fibrosis, expression of pro-inflammatory and pro-fibrotic mediators such as IL-1β, TNFα and TGF-β1 play a crucial role (Lebrun et al., 2017; Wilson and Wynn, 2009). As compared to control mice, while the mRNA expression of pro-inflammatory mediators (IL-1β, TNFα and iNOS) and pro-fibrotic cytokine (TGF-β1) was significantly elevated in the lungs of BLM-injected WT mice, the expression of these mediators in the lungs of Ninj1 KO mice was slightly induced but significantly less than WT mice (Fig. 14 and 15). In detail, according to the results of semi-quantitative real-time PCR, the average mRNA expression of *IL-1β* in WT lungs reached highest level at day 3, *TNFα* and *iNOS* at day 14, and *TGF- β1* at day 14 and 21 (Fig. 15).

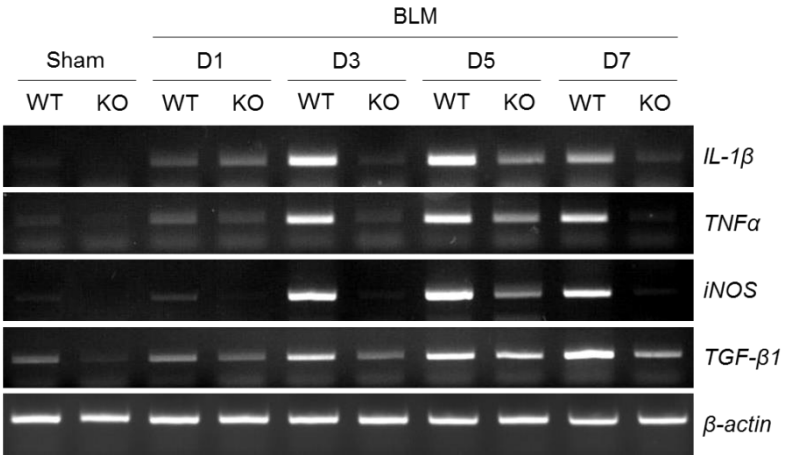

Figure 14. Assessment of cytokine expression in the lungs of BLM-treated WT and Ninj1 KO mice by RT-PCR.

Lungs were collected from WT and Ninj1 KO mice at indicated time points after BLM injection. The expression of pro-inflammatory and pro-fibrotic cytokines was analyzed. Representative images of RT-PCR to assess the expression of pro-inflammatory and pro-fibrotic cytokines in the lungs of sham and BLM-treated WT and Ninj1 KO mice (n=5).

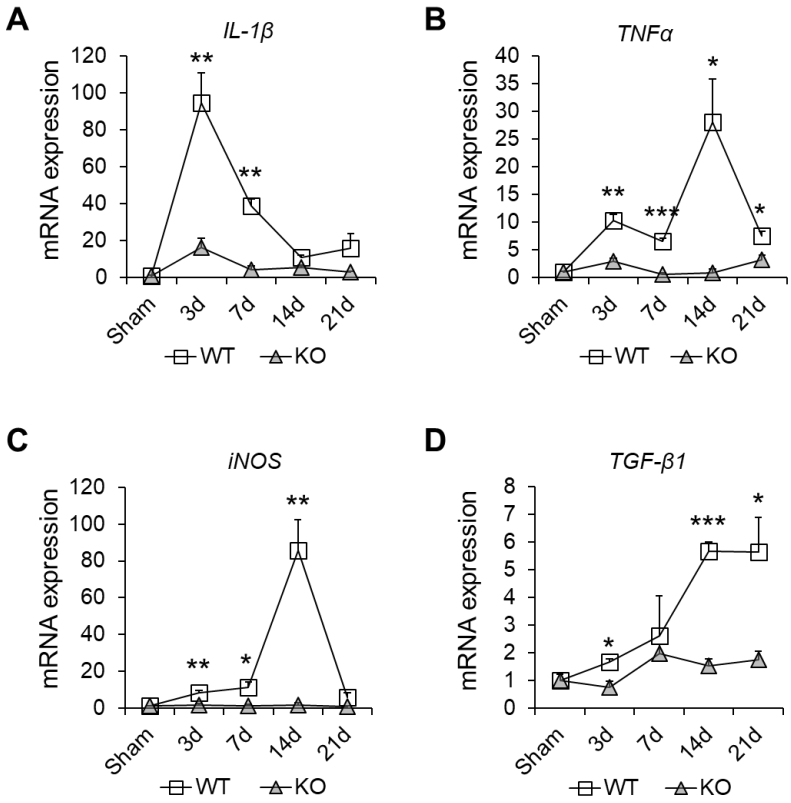

Figure 15. Assessment of cytokine expression in the lungs of BLM-treated WT and Ninj1 KO mice by semi-quantitative real-time PCR.

Lungs were collected from WT and Ninj1 KO mice at indicated time points after BLM injection. Semi-quantitative real-time PCR to assess the expression of pro-inflammatory and pro-fibrotic cytokines, IL-1β (A), TNFα (B), iNOS (C) and TGF-β1 (D), in the lungs of sham and BLM-treated WT and Ninj1 KO mice (n=3). Data are expressed as means ± SEM of triplicates. *p<0.05, **p<0.01, ***p<0.001.

2.7. Secretion of pro-inflammatory and pro-fibrotic cytokines is diminished in bronchoalveolar lavage fluid (BALF) of BLM-treated Ninj1 KO mice

In order to investigate if the mRNA expression of pro-inflammatory and pro-fibrotic cytokines in the lung tissue is correlated with secretion of those cytokines, the amount of those cytokines were measured by ELISA using bronchoalveolar lavage fluid (BALF) of BLM-treated WT and Ninj1 KO mice (WT BALF and Ninj1 KO BALF, respectively). ELISA revealed that the level of secreted IL-1β and TGF-β1 in KO BALF was significantly lower than in WT BALF (Fig. 16A, B). These results suggest that decreased level of secreted IL-1β and TGF-β1 would have resulted in amelioration of fibroblast activation.

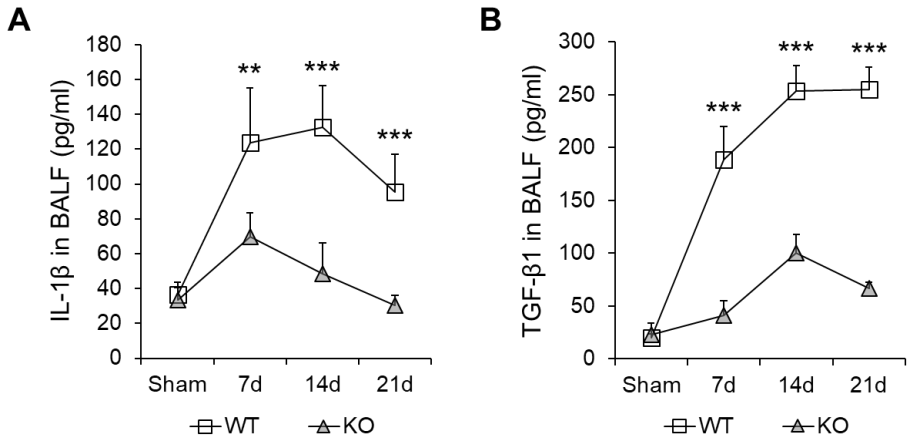

Figure 16. Secretion of pro-inflammatory and pro-fibrotic cytokines in BALF.

Bronchoalveolar lavage fluid (BALF) was collected from BLM-treated WT and Ninj1 KO mice at indicated time points after BLM injection and ELISA for IL-1β and TGF-β1 was performed. (A) ELISA for IL-1β secretion in BALF (n=5). (B) ELISA for TGF-β1 secretion in BALF (n=5). Data are expressed as means ± SEM of triplicates. ** $p<0.01$; *** $p<0.001$.

2.8. Expression of pro-inflammatory and pro-fibrotic mediators are decreased in lungs of BLM-treated Ninj1 KO mice, compared to BLM-treated WT mice

Since TGF-β1 signaling plays a central role in fibrogenesis via activation of fibroblasts (Biernacka et al., 2011), it was examined if BALF from WT or Ninj1 KO mice would activate fibroblasts through TGF-β1 signaling. Western blot analysis indicated that while BALF of BLM-treated WT mice induced phosphorylation of SMAD3, BALF of BLM-treated Ninj1 KO mice did not induce SMAD3 phosphorylation (Fig. 17A, B). The treatment of BALF from WT mice induced nuclear localization of SMAD3 in the primary fibroblasts, but BALF from the Ninj1 KO mice did not induce (Fig. 17C). These results indicate that since BALF from BLM-treated WT mice activated TGF-β1 signaling while BALF from BLM-treated Ninj1 KO mice did not, the expression of TGF-β1 was greater in the lungs of BLM-treated WT mice.

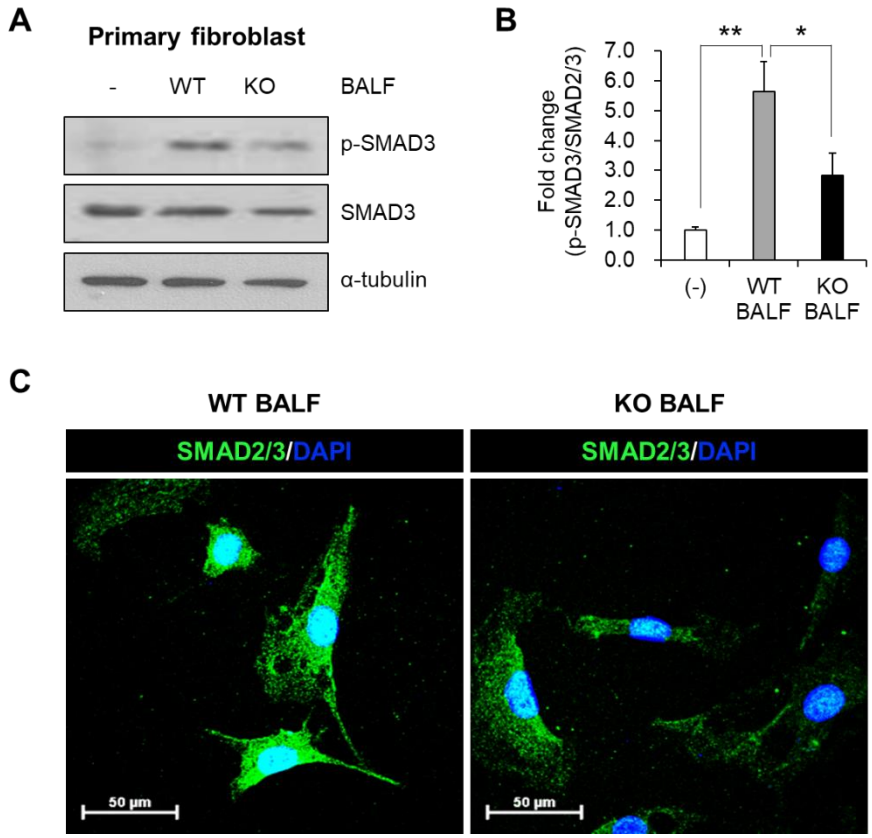

Figure 17. Effect of BALF on TGF-β signaling in primary fibroblasts.

BALF was collected from BLM-treated WT (WT BALF) and Ninj1 KO mice (KO BALF) at day 7 after BLM injection. Primary fibroblasts were treated with BALF and western blot and IF were performed to examine activation of SMAD3. Representative images (A) and semi-quantification (B) of western blot. (C) Representative images of IF for SMAD2/3 (scale bar=50 μm). Data are expressed as means ± SEM of triplicates. *p<0.05; **p<0.01.

2.9. BALF from BLM-treated Ninj1 KO mice does not show pro-fibrotic effect on primary fibroblasts

Activation of fibroblasts is characterized by differentiation into myofibroblasts, increased motility, proliferation and production of collagens. As shown in Fig. 18, while WT BALF treatment induced the expression of α-SMA, Ninj1 KO BALF did not induced. WT BALF also induced migration of fibroblasts but Ninj1 KO BALF did not (Fig. 19A, B). In addition, proliferation of fibroblasts was increased by WT BALF but not by Ninj1 KO BALF (Fig. 20A). Finally, hydroxyproline assay demonstrated that production of collagens was lower in fibroblasts treated with Ninj1 KO BALF than WT mice (Fig. 20B). These results suggest that attenuation of pulmonary fibrosis in Ninj1 KO mice would have been due to changes in the pro-inflammatory and pro-fibrotic mediators, and Ninj1 could be one of the key molecules involved in production of the mediators.

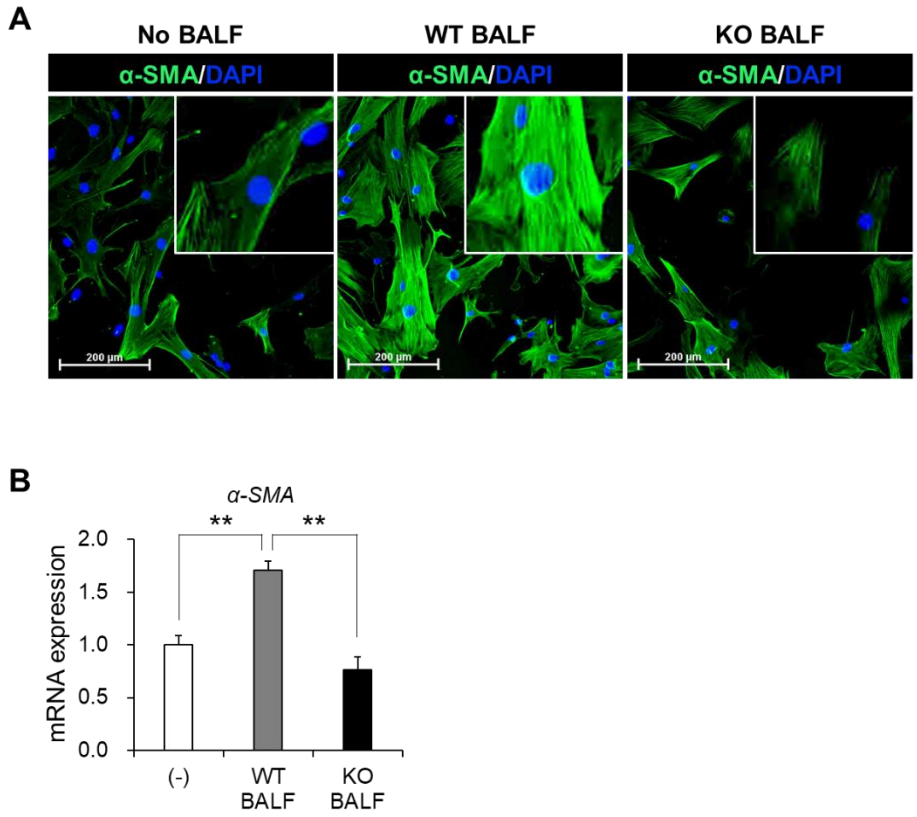

Figure 18. Effects of BALF on differentiation of fibroblasts into myofibroblasts.

BALF was collected from BLM-treated WT (WT BAFL) and Ninj1 KO mice (KO BALF) at day 21 after BLM injection. Immunofluorescence assay and Semi-quantitative real-time PCR were performed after primary fibroblasts were treated with BALF. (A) Representative images of IF for α-SMA. (B) Semi-quantitative real-time PCR to assess the mRNA expression of *α-SMA*. Data are expressed as means ± SEM of triplicates. ***p*<0.01.

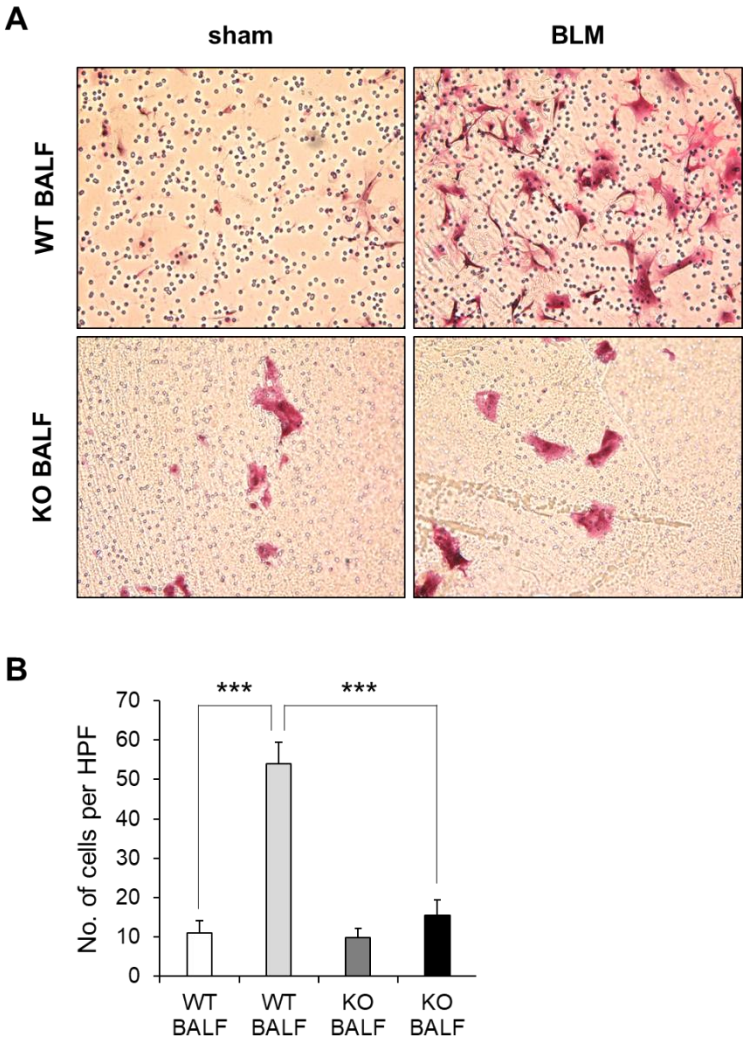

Figure 19. Effects of BALF on migration of primary fibroblasts.

Transwell migration assay was performed to assess the difference in mitility of fibroblasts treated with WT or Ninj1 KO BALF. (A) Representative images of transwell migration assay. (B) The number of migrated cells per high power field (HPF) (n=3). Data are expressed as means ± SEM of triplicates. ***p<0.001.

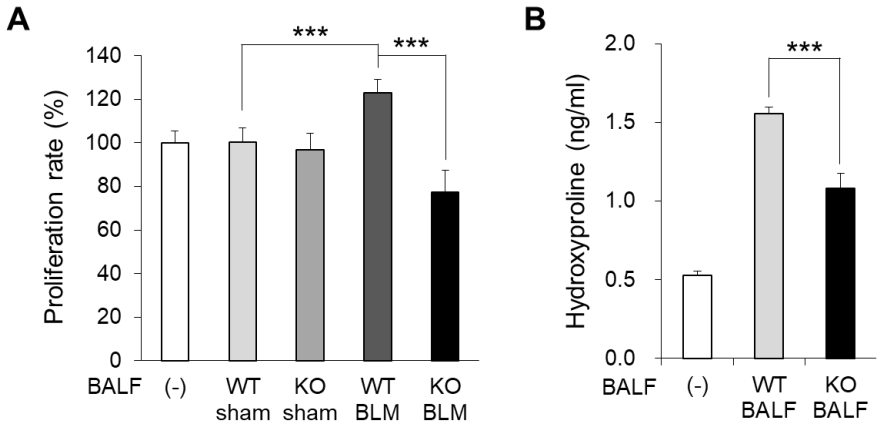

Figure 20. Effects of BALF on proliferation and collagen production of primary fibroblasts.

MTT assay and hydroxyproline assay were performed after primary fibroblasts were treated with BALF. (A) MTT assay to assess proliferation rate. (B) Hydroxyproline assay to examine production of collagens (n=3). Data are expressed as means ± SEM of triplicates. ***p<0.001.

3. Ninj1 deficiency does not affect fibroblast activation and inflammatory response in macrophages and alveolar epithelial cells

3.1. Ninj1 deficiency does not affect activation of fibroblasts.

Since fibroblasts are the main player that produce ECM components, it was examined if Ninj1 deficiency alters fibroblast activation by TGF-β1. Phosphorylation of SMAD3 (p-SMAD3), a downstream signaling molecule of TGF-β1 signaling pathway, was assessed by western blot. The expression of p-SMAD3 was elevated by TGF-β1 treatment in both WT and Ninj1 KO fibroblasts and it was slightly higher in Ninj1 KO fibroblasts (Fig. 21A). However, the mRNA expression of *col1a1* in Ninj1 KO fibroblasts, was not higher than in WT fibroblasts (Fig. 21B). These results indicate that there is no significant difference in pro-fibrotic activity between WT and Ninj1 KO fibroblasts.

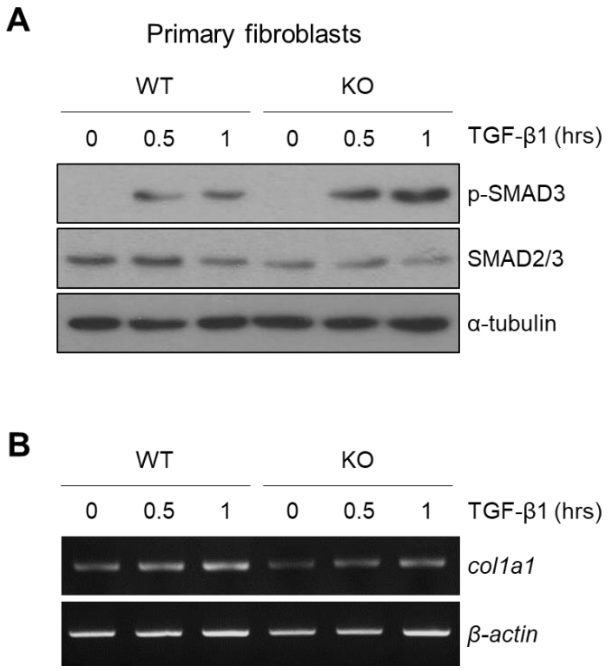

Figure 21. Activation of WT and Ninj1 KO fibroblasts by TGF-β1 treatment.

Primary fibroblasts were isolated from WT and Ninj1 KO mice and they were treated with TGF-β1 (20 ng/ml). Phosphorylation of SMAD was assessed by western blot and the expression of *col1a1* was determined by RT-PCR. (A) Representative images of western blot. (B) Representative images of RT-PCR for *col1a1*.

3.2. The expression of Ninj1 in macrophages is elevated by BLM treatment

As shown in Fig. 5 and 6, injecting BLM resulted in the elevation of Ninj1 expression in the lungs of treated mice. Macrophage is a key inflammatory cell type in the pathogenesis of fibrosis (Borthwick et al., 2016; Bringardner et al., 2008; Wynn, 2008). Therefore, the expression of Ninj1 was examined in macrophages as treated with inflammatory stimuli, namely BLM. It was found that the expression of Ninj1 protein in Raw264.7 cells was up-regulated by BLM exposure in a dose-dependent manner (Fig. 22A, B). FACS analysis also indicated that the expression of surface Ninj1 was increased by BLM treatment (Fig. 22C). These results suggest that increased expression of Ninj1 may contribute to inflammatory response in macrophage.

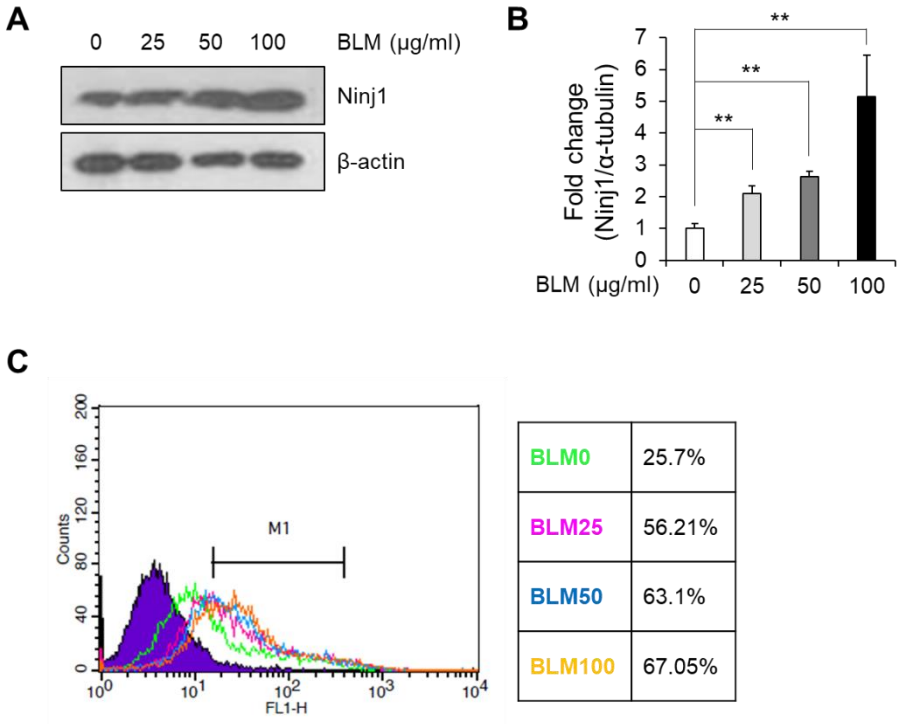

Figure 22. The expression of Ninj1 in BLM-treated Raw264.7 cells

Raw264.7 cells were treated with BLM with indicated doses and the expression of NInj1 was assessed by western blot and FACS analysis. Representative images of western blot to determine Ninj1 expression (A) and semi-quantification (B). (C) FACS analysis to examine the expression of cell surface Ninj1. Data are expressed as means ± SEM of triplicates. $^{**}p<0.01$.

3.3. Ninj1 deficiency does not alter NF-κB signaling in macrophages by BLM treatment

Since the expression of Ninj1 was elevated in BLM-treated macrophages, it was then examined if Ninj1 deficiency alters the expression of pro-inflammatory and pro-fibrotic cytokines in macrophages. The number of alveolar macrophages in BALF from untreated mice was only about $0.4x10^5$ cells per mouse (Fig. 12B), which was too small number to perform further experiments such as western blotting and RT- or semi-quantitative real-time PCR (Zhang et al., 2000). Previously, peritoneal macrophages are used to study lung fibrosis and inflammation instead of alveolar macrophages (Tao et al., 2014; Zhang et al., 2000). Therefore, peritoneal macrophages were used to assess the effects of Ninj1 deficiency on the inflammatory response. Peritoneal macrophages were isolated from WT and Ninj1 KO mice and they were treated with BLM. The expression of cytokines (*IL-1β* and *TNFα*) was all elevated by BLM treatment in both WT and Ninj1 KO peritoneal macrophages. However, there was no significant difference in the expression of those cytokines between WT and Ninj1 KO peritoneal macrophages (Fig. 23A, B). Ninj1-deficient Raw264.7 cell line (Ninj1 KO Raw264.7) was generated by using CRIPR Cas9 technique. Consistent with the results for peritoneal macrophages, Ninj1 deficiency in Raw264.7 cells did not alter the expression of *IL-1β* and *TNFα*, either (Fig. 24A, B). The expression of TGF-β1 was not increased by BLM treatment in both peritoneal macrophages and Raw264.7 cells, regardless of Ninj1 expression. (Fig. 23C, 24C). These results suggest that Ninj1 deficiency

did not affect the response of macrophages to extracellular stimuli.

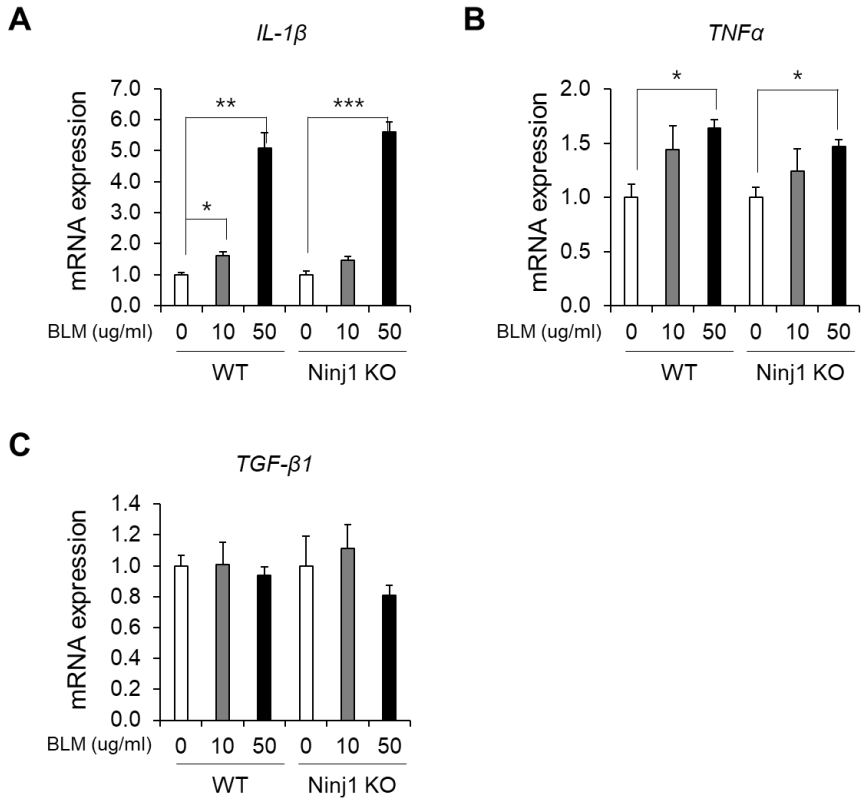

Figure 23. The expression of pro-inflammatory and pro-fibrotic mediators in BLM-treated peritoneal macrophages.

WT and Ninj1 KO peritoneal macrophages were isolated and treated with BLM. The expression of cytokines was assessed by semi-quantitative real-time PCR. mRNA expression of IL-1β (A), TNFα (B) and TGF-β1 (C). Data are expressed as means ± SEM of triplicates. *p<0.05; **p<0.01; ***p<0.001.

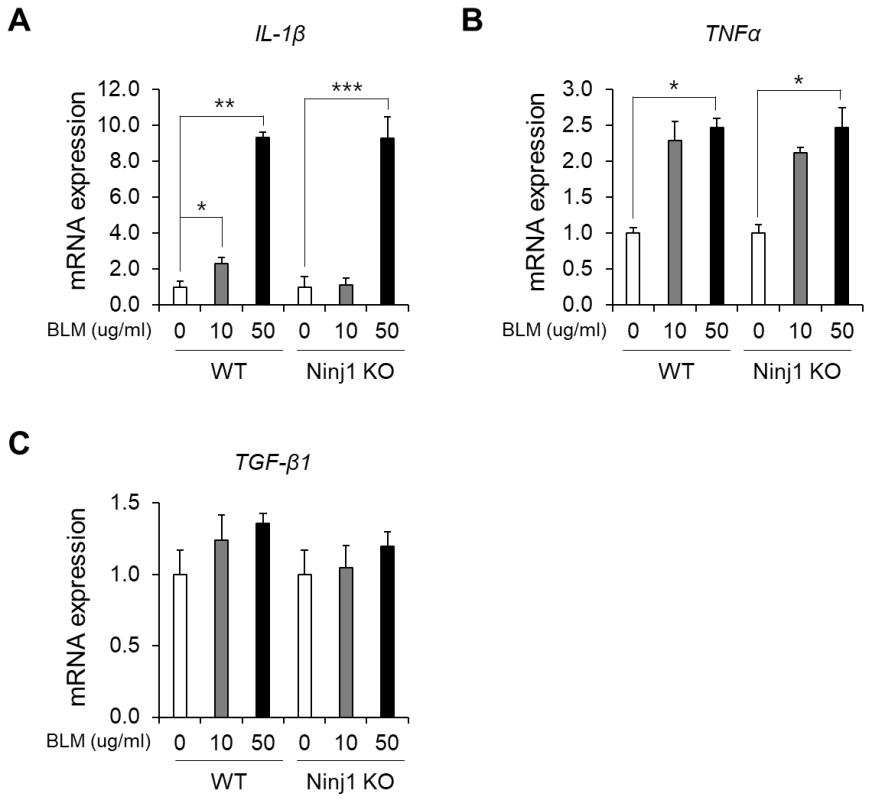

Figure 24. The expression of pro-inflammatory and pro-fibrotic mediators in BLM-treated Raw264.7 cells.

Ninj1-deficient Raw264.7 cells (Ninj1 KO Raw264.7) were generated by using CRISPR Cas 9 technique. WT and Ninj1 KO Raw264.7 cells were treated with BLM and the expression of cytokines was assessed by semi-quantitative real-time PCR. mRNA expression of *IL-1β* (A), *TNFα* (B) and *TGF-β1* (C). Data are expressed as means ± SEM of triplicates. *p<0.05; **p<0.01; ***p<0.001..

3.4. The expression of Ninj1 in AECs is elevated by BLM treatment

The expression of Ninj1 was examined in AECs, which play an important role in developing pulmonary fibrosis (Selman and Pardo, 2006; Zoz et al., 2011). Interestingly, the mRNA expression level of Ninj1 in MLE-12 cells, a type II pneumocyte cell line, was elevated (Fig. 25A, B). In addition, FACS analysis revealed that surface Ninj1 expression was also increased in BLM-treated MLE-12 cells (Fig. 25C). These results suggest that Ninj1 may play a pro-fibrotic role in AECs during fibrogenesis.

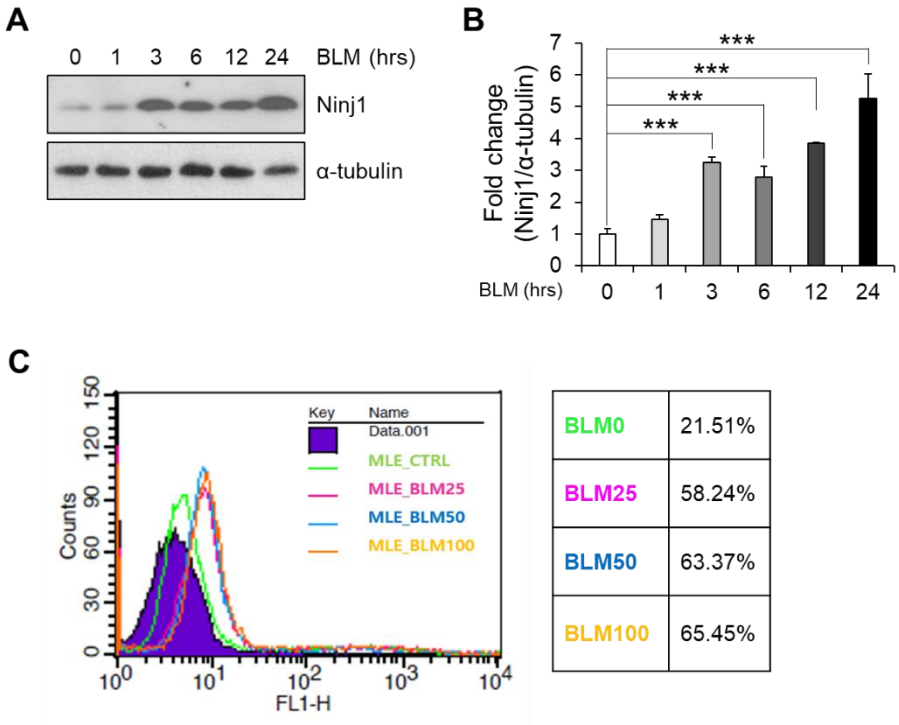

Figure 25. The expression of Ninj1 in BLM-treated MLE-12 cells

MLE-12 cells were treated with BLM with indicated doses and the expression of NInj1 was assessed by western blot and FACS analysis. Representative images (A) and semi-quantification (B) of western blot to determine Ninj1 expression. (C) FACS analysis to examine the expression of cell surface Ninj1. Data are expressed as means ± SEM of triplicates. ***p<0.001.

3.5. Altered expression of Ninj1 does not affect BLM-induced response in AECs

The previous studies reported that AECs play a crucial role in recruitment of macrophages in lung inflammatory diseases by producing pro-inflammatory mediators (de Boer et al., 2000; Manicone, 2009). Therefore, it was examined if the expression of pro-inflammatory mediators was reduced in Ninj1-deficient AECs. Ninj1 KO MLE-12 cells were generated by using CRISPR Cas9 technique. WT and Ninj1 KO MLE-12 cells were treated with BLM and mRNA analysis was performed. Semi-quantitative real-time PCR showed the expression of pro-inflammatory mediators, *CXCL1* and *CXCL12*, was significantly increased in both WT and Ninj1 KO MLE-12 cells. However, there was no marked difference in their expression between WT and Ninj1 KO MLE-12 cells (Fig. 26A, B). The expression of *TGF-β1* was not increased by BLM treatment in both WT and Ninj1 KO MLE-12 cells (Fig. 26C). Consistent with these results, when the conditioned media (CM) from WT or Ninj1 KO MLE-12 cells, with or without BLM, was introduced to WT and Ninj1 KO Raw264.7 cells, activation of p65 remained unaltered (Fig. 27A, B). These results indicated that Ninj1 deficiency did not affect the response of AECs to extracellular stimuli.

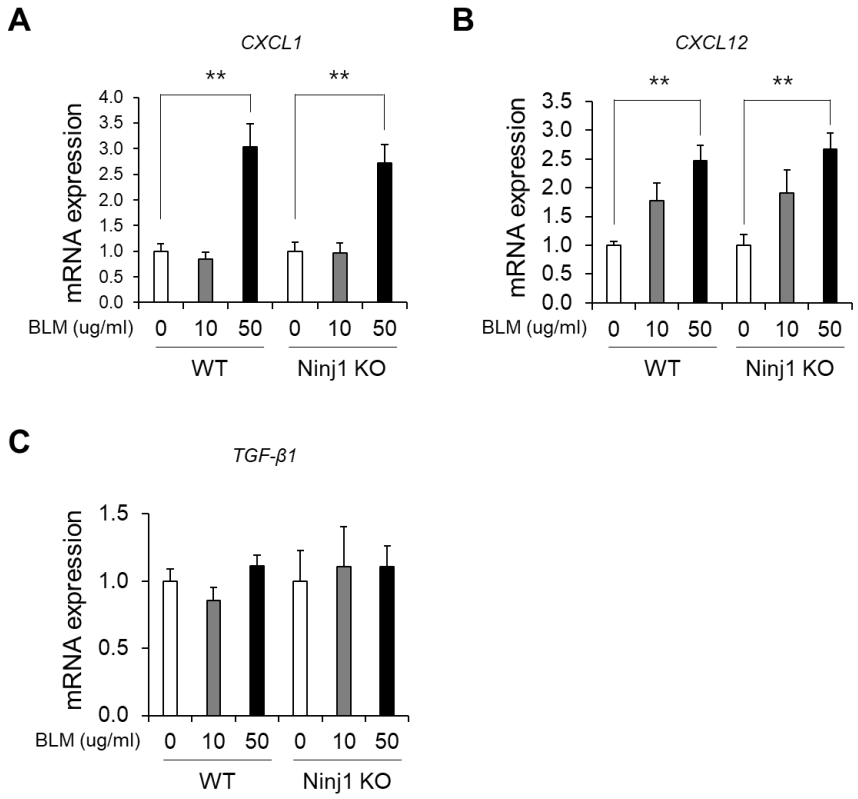

Figure 26. The expression of pro-inflammatory and pro-fibrotic mediators in BLM-treated MLE-12 cells.

WT and Ninj1 KO MLE-12 cells were treated with BLM and mRNA analysis was performed to assess the expression of pro-inflammatory mediators in MLE-12 cells. Semi-quantitative real-time PCR for the expression of *CXCL1* (A), *CXCL12* (B) and *TGF-β1* (C). Data are expressed as means ± SEM of triplicates. $^{**}p<0.01$.

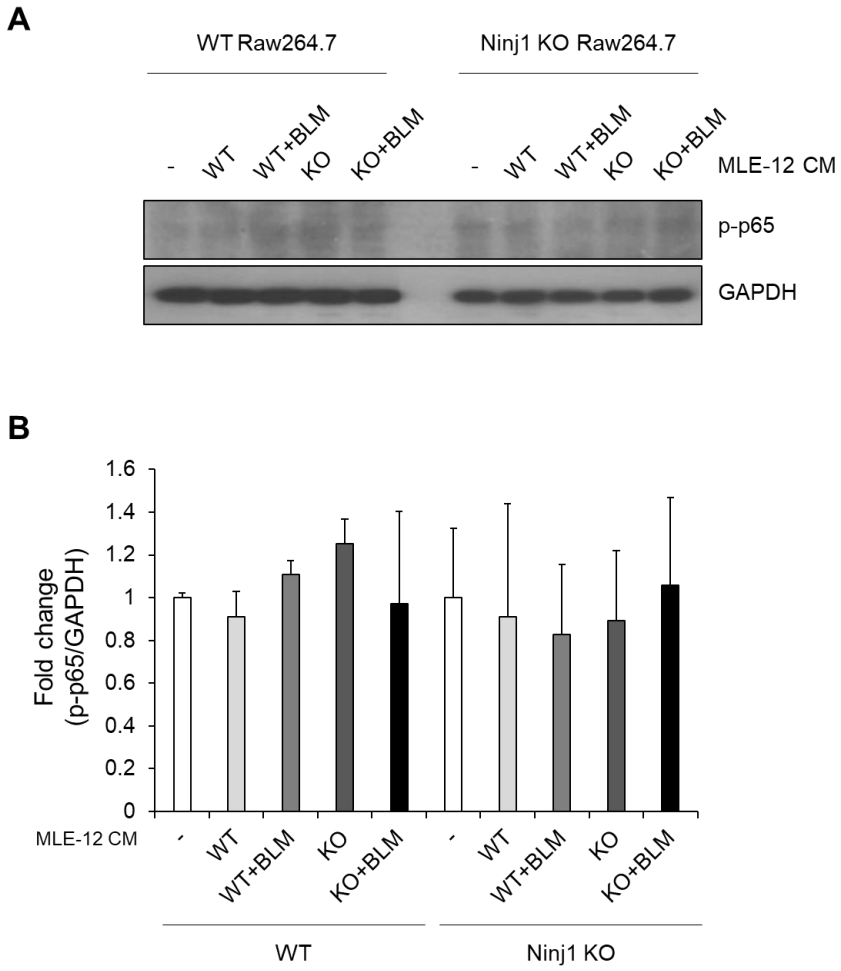

Figure 27. Effect of CM from BLM-treated MLE-12 cells on activation of Raw264.7 cells.

WT and Ninj1 KO MLE-12 cells were treated with BLM, followed by CM collection. CM was introduced to WT or Ninj1 KO Raw 264.7 cells and western blot was performed to examine activation of p65. Representative images (A) and semi-quantification (B) of western blot. Data are expressed as means ± SEM of triplicates. $^{**}p<0.01$.

4. Ninj1 promotes macrophage-to-alveolar epithelial cell interaction, leading to contact-dependent activation of inflammatory response in macrophages

4.1. Ninj1 Deficiency does not affect cell-to-cell adhesion between macrophages and AECs

As previously mentioned, the interaction between macrophages and alveolar epithelial cells is an essential process in pulmonary inflammatory diseases (Fujii et al., 2002; Manzer et al., 2008; Tao and Kobzik, 2002). In addition, Ninj1 has homophilic binding properties in cell-to-cell adhesion (Lee et al., 2010). Therefore, it was examined if Ninj1 was involved in cell-to-cell adhesion between AECs and macrophages. WT or Ninj1 KO Raw264.7 cells were co-cultured with WT or Ninj1 KO MLE-12 cells and the number of Raw264.7 cells was analyzed by FACS. Ninj1 deficiency in either or both of Raw264.7 and MLE-12 cells did not affect binding affinity between those two cell types (Fig. 28). Next, since BLM treatment induced elevated Ninj1 expression in MLE-12 cells, the number of Raw264.7 cells bound to WT or Ninj1 KO MLE-12 cells with or without BLM treatment was assessed. Raw264.7 cells bound to WT MLE-12 cells were increased after exposure to BLM (Fig. 29). However, the number of Raw264.7 cells bound to Ninj1 KO MLE-12 cells was also increased due to BLM exposure (Fig. 29). These results suggested that Ninj1 may not be necessary for adhesion of two cell lines.

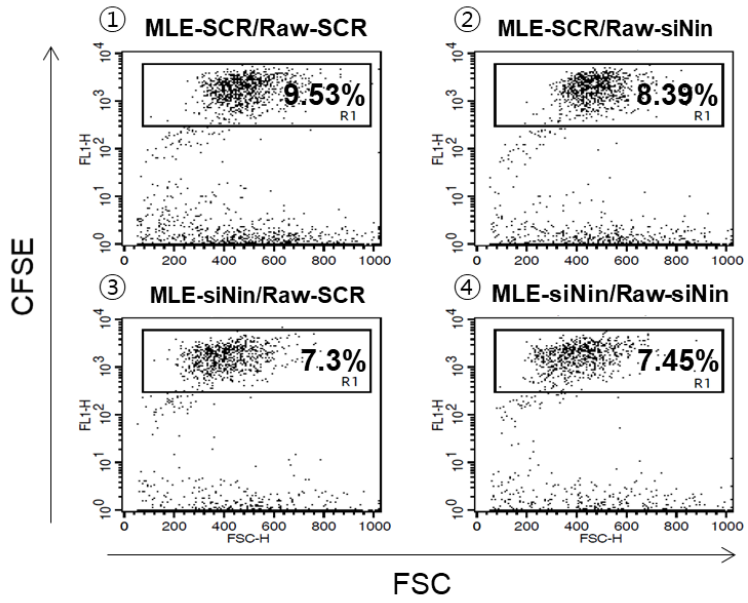

Figure 28. Effect of Ninj1 deficiency on adhesion between Raw264.7 and MLE-12 cells.

WT or Ninj1 KO MLE-12 cells and CFSE-stained WT or Ninj1 KO Raw264.7 cells were co-cultured and the number of Raw264.7 cells bound to MLE-12 cells was assessed by FACS analysis. Representative images of flow cytometry analysis to assess the number of Raw264.7 cells bound to MLE-12 cells.

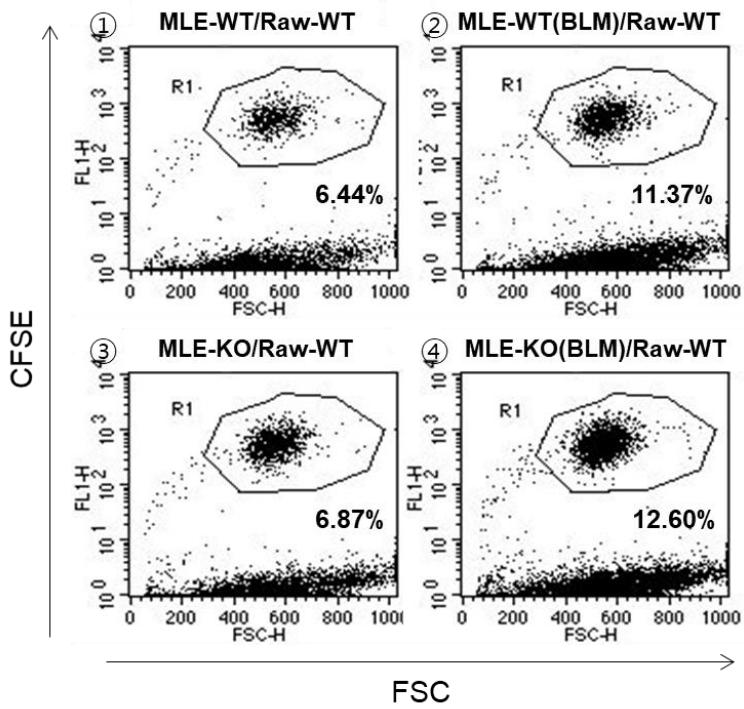

Figure 29. Effect of Ninj1 deficiency on adhesion between Raw264.7 and BLM-treated MLE-12 cells.

WT or Ninj1 KO MLE-12 cells were treated with vehicle or BLM and co-culture with CFSE-stained WT Raw264.7 cells. The number of Raw264.7 cells bound to MLE-12 cells was assessed by FACS analysis. Representative images of flow cytometry analysis to assess the number of Raw264.7 cells bound to MLE-12 cells.

4.2. Ninj1 is involved in induction of pro-inflammatory and pro-fibrotic cytokines in co-culture of macrophages and AECs

WT or Ninj1 KO MLE-12 and WT or Ninj1 KO Raw264.7 cells were co-cultured for 6 hrs and total RNA was isolated from the co-culture. mRNA analysis was performed by RT-PCR. When WT Raw264.7 and WT or Ninj1 KO MLE-12 cells were co-cultured, the expression of cytokines, *IL-1β* and *TGF-β1* was elevated (Fig. 30). However, when Ninj1 was deficient in Raw264.7 cells, the expression of the cytokines did not increase (Fig. 30). These results suggest that Ninj1 would be involved in interaction between AECs and macrophages.

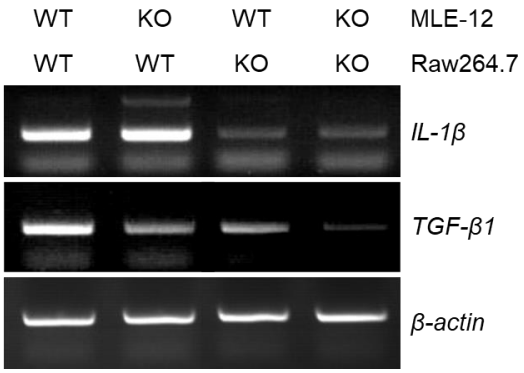

Figure 30. The expression of cytokines in co-culture of Raw264.7 and MLE-12 cells.

Raw264.7 and MLE-12 cells were co-cultured and the expression of pro-inflammatory and pro-fibrotic cytokines was assessed by RT-PCR. Representative images of RT-PCR for *IL-1β* and *TGF-β1*.

4.3. Ninj1 is involved in production of TGF-β1 in co-culture of AECs and macrophages

Conditioned media (CM) was collected from co-culture of MLE(WT)-Raw(WT), MLE(WT)-Raw(KO), MLE(KO)-Raw(WT) and MLE(KO)-Raw(KO). Primary fibroblasts were treated with CMs and activation of TGF-β1 signaling was assessed. As shown in Fig. 31, when primary fibroblasts were treated with MLE(WT)-Raw(WT) CM or MLE(WT)-Raw(KO) CM, phosphorylation of SMAD3 was induced, and SMAD3 was translocated into the nucleus (Fig. 32). However, MLE(KO)-Raw(WT) CM or MLE(KO)-Raw(KO) CM did not induce phosphorylation of SMAD3 (Fig. 31) and nuclear localization of SMAD2/3 (Fig. 32). These results suggest that when Ninj1 is deficient in AECs, the production of TGF-β1 is diminished.

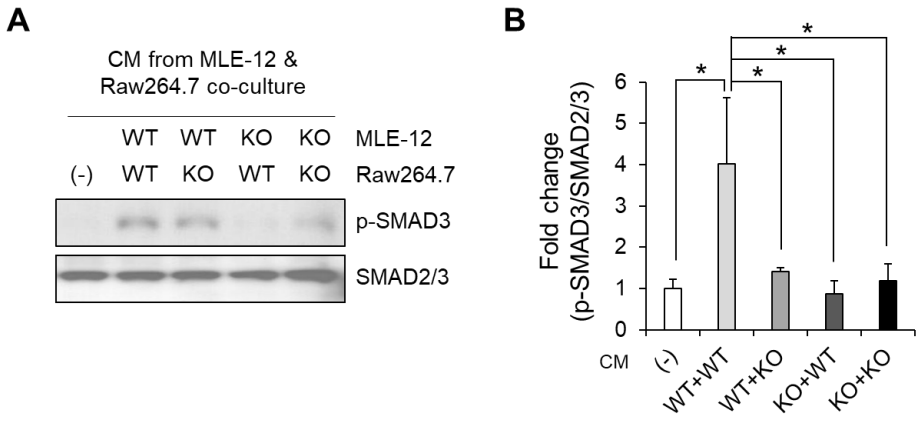

Figure 31. Effect of CM from co-culture of MLE-12 and Raw264.7 cells on TGF-β1 signaling in fibroblasts.

Conditioned media (CM) was collected from co-culture of MLE(WT)-Raw(WT), MLE(WT)-Raw(KO), MLE(KO)-Raw(WT) and MLE(KO)-Raw(KO). Primary fibroblasts were treated with CMs and phosphorylation of SMAD3 was assessed by western blot. Representative images (A) and semi-quantification (B) of western blot. Data are expressed as means ± SEM of triplicates. *p<0.05.

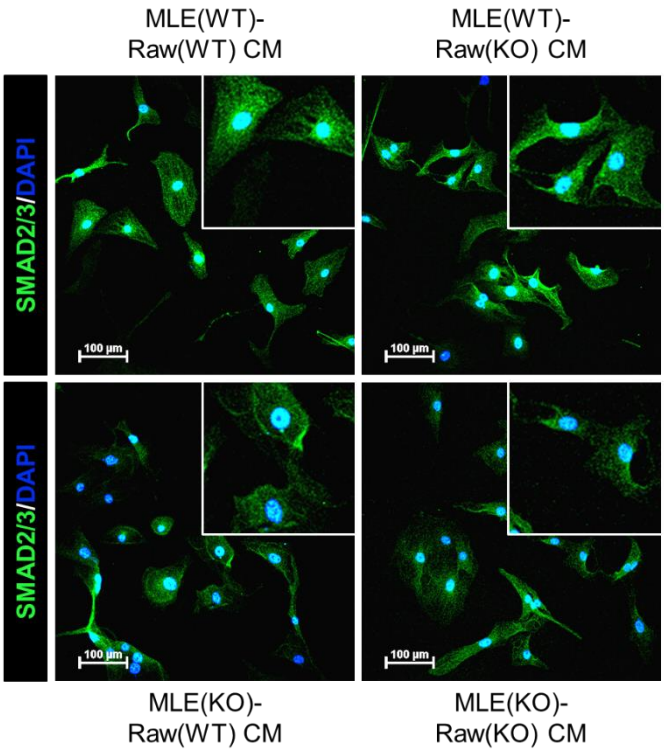

Figure 32. Effect of CM from co-culture of MLE-12 and Raw264.7 cells on nuclear localization of SMAD2/3 in fibroblasts.

Primary fibroblasts were treated with CMs and nuclear localization of SMAD2/3 was assessed by IF. Representative images of IF to assess nuclear localization of SMAD2/3.

4.4. Activation of fibroblast is diminished when treated with CM from co-culture of Ninj1-deficient ACEs and macrophages

The primary fibroblasts were treated with CM. The mRNA of *α-SMA* in fibroblasts was significantly lower when treated with CM from MLE(WT)-Raw(KO), MLE(KO)-Raw(WT) or MLE(KO)-Raw(KO) (Fig. 33A, B). IF assay also demonstrated decreased expression of α-SMA in fibroblasts treated with CM from MLE(WT)-Raw(KO), MLE(KO)-Raw(WT) or MLE(KO)-Raw(KO) (Fig. 33C). In addition, it was observed that migration of fibroblasts was markedly decreased when Ninj1 was deficient in either of MLE-12 or Raw264.7 cells (Fig. 34A, B). The hydroxyproline assay showed that production of collagens in fibroblasts was also reduced by the same CM (Fig. 35). Taking together, these results suggest that when Ninj1 is deficient in either of AECs and macrophages, the production of pro-fibrotic mediators, such as TGF-β1, is diminished, resulting in decreased activation of fibroblasts.

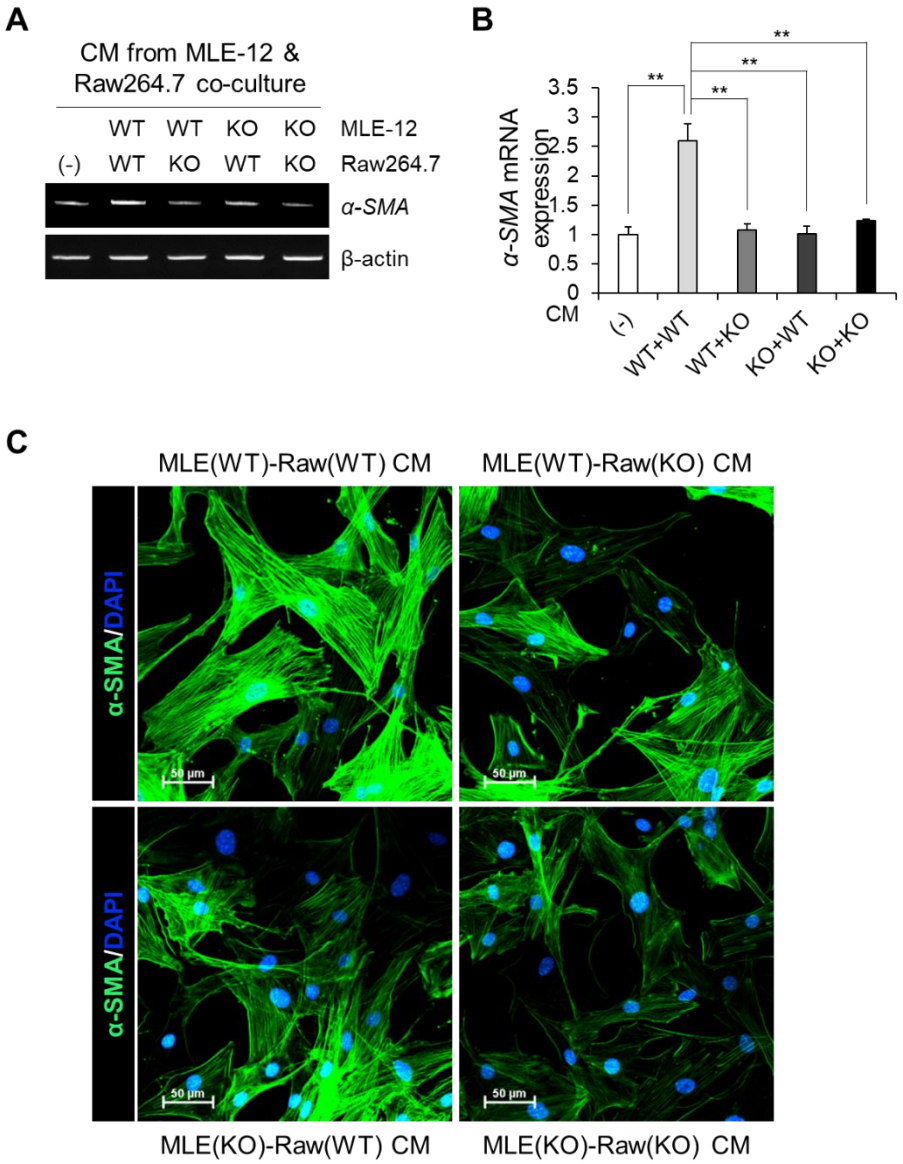

Figure 33. Effect of CM from co-culture of MLE-12 and Raw264.7 cells on activation of primary fibroblasts.

Fibroblasts were treated with CMs and differentiation of fibroblasts was assessed by performing RT- and semi-quantitative real-time PCR, and IF for α-SMA. Representative images of RT-PCR (A) and semi-quantitative real-time

PCR (B) for *α-SMA*. (C) Representative images of IF to assess α-SMA expression. Data are expressed as means ± SEM of triplicates. $^{**}p<0.01$.

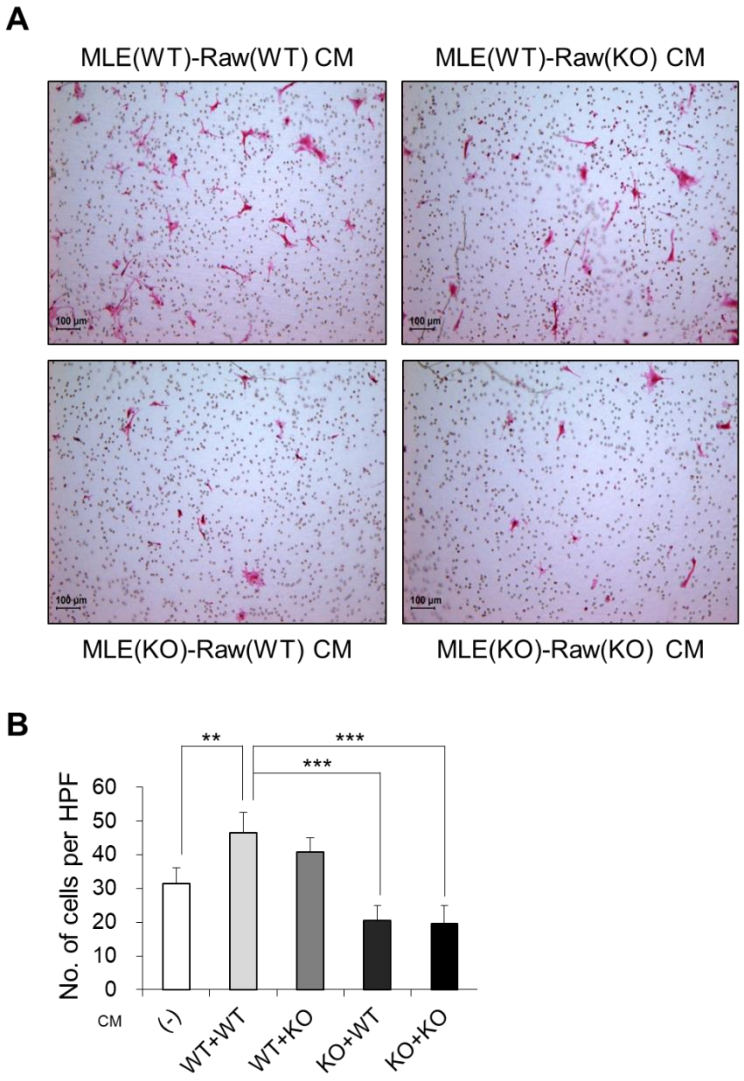

Figure 34. Effect of CM from co-culture of MLE-12 and Raw264.7 cells on migration of primary fibroblasts.

Fibroblasts were treated with CMs and activation of fibroblasts was assessed by performing transwell migration assay and hydroxyproline assay. (A) Representative images (A) and the number of migrated cells per HPF (n=3) (B) of transwell migration assay. Data are expressed as means ± SEM. ** p<0.01.

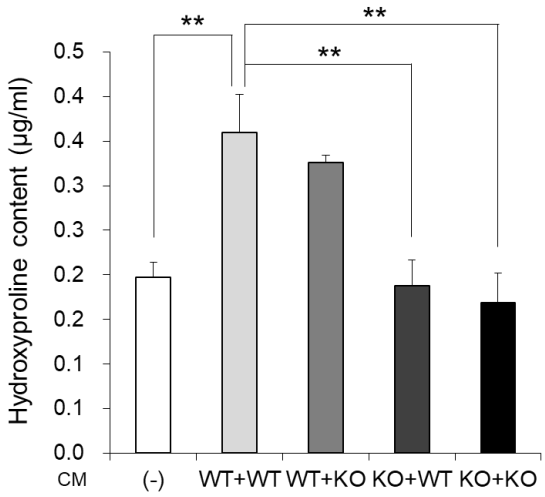

Figure 35. Effect of CM from co-culture of MLE-12 and Raw264.7 cells on production of collagens in primary fibroblasts.

Fibroblasts were treated with CMs and activation of fibroblasts was assessed by performing transwell migration assay and hydroxyproline assay (n=3). Data are expressed as means ± SEM. $^{**}p<0.01$; $^{***}p<0.001$.

4.5. Ninj1 plays a crucial role in stimulating macrophages by mediating interaction with AECs

In order to determine if co-culture of AECs and macrophages induces activation of macrophages, WT or Ninj1 KO MLE-12 and W or Ninj1 KO Raw264.7 cells were co-cultured for 6 hrs and Raw264.7 cells were sorted for further examination. Sorted WT or Ninj1 KO Raw264.7 cells were subjected to western blot and RT-PCR. As shown in Fig. 36A, when co-cultured with WT MLE-12, inflammatory signaling NF-κB was activated in WT Raw264.7 cells. Unexpectedly, when co-cultured with Ninj1 KO MLE-12, NF-KB was also activated in WT Raw264.7 cells (Fig. 36A). In addition, even though Ninj1 is deficient in Raw264.7 cells, NF-κB was activated by co-culture with WT or Ninj1 KO MLE-12 cells (Fig. 36A). When Ninj1 was deficient in either of cell lines, phosphorylation of Erk1/2 is diminished (Fig. 36A). Moreover, when Ninj1 was deficient in either of cell lines, the expression of pro-inflammatory and pro-fibrotic cytokines was reduced in Raw264.7 cells (Fig. 36B). These results suggest that Ninj1 would be involved in interaction between macrophages and AECs, resulting in activation of macrophages.

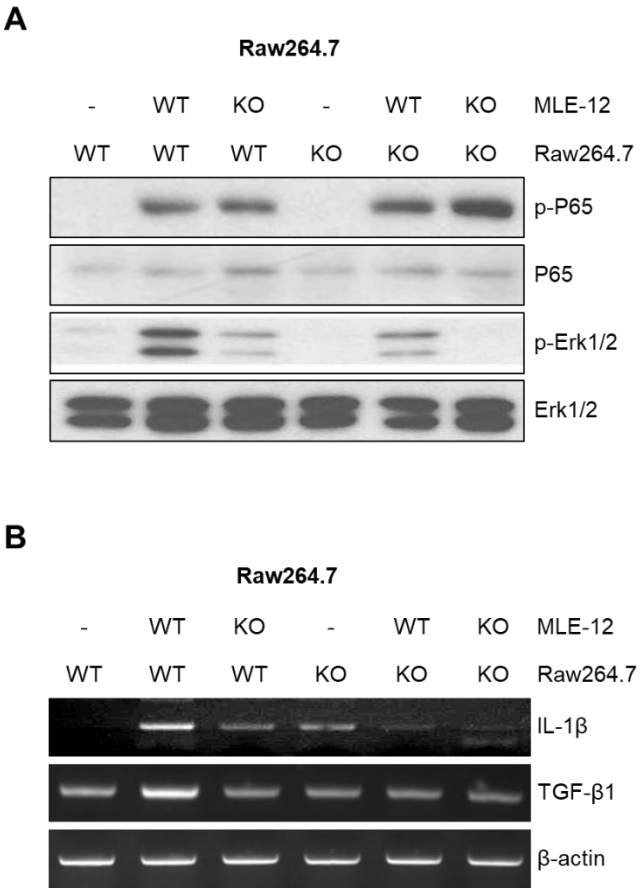

Figure 36. Inflammatory response in Raw264.7 cells after co-culture with MLE-12 cells.

WT or Ninj1 KO Raw264.7 cells were co-dultured with WT or Ninj1 KO MLE-12 cells and sorted by FACS. Sorted Raw264.7 cells were subjected to western blot and RT-PCR to assess the inflammatory response. (A) Representative images of western blot to examine phosphorylation of p65 and Erk1/2. (B) Representative images of western blot to examine the expression of *IL-1β* and *TGF-β1*.

4.6. Increased expression of Ninj1 by BLM treatment in AECs enhances activation of macrophages

As previously described, the expression of Ninj1 is elevated by BLM treatment in AECs, it was hypothesized that increased Ninj1 expression in BLM-treated AECs may enhance the interaction between AECs and macrophages, resulting in promotion of activation of macrophages. It was observed that Raw264.7 cells bound to WT MLE-12 cells exhibited activation of the inflammatory signaling protein, p65 (Fig. 37A, B). Moreover, in Raw264.7 cells bound to the BLM-treated WT MLE-12 cells, there was an increased activation of p65 (Fig. 37A, B). Even though p65 was activated when bound to Ninj1 KO MLE-12 cells, no further increase was observed in the activation when bound to BLM-treated Ninj1 KO MLE-12 cells (Fig. 37A, B). Consistent with these results, while the expression of *IL-1β*, *TNFα* and *TGF-β1* was enhanced when Raw264.7 cells were bound to BLM-treated WT MLE-12, the expression of those cytokines was diminished in the Raw 264.7 cells bound to BLM-treated Ninj1 KO MLE-12 (Fig. 38A, B, C). These results suggested that when macrophages are bound to AECs, they are activated and produce pro-fibrotic mediators, leading to activation of fibroblasts. However, the results also suggested that if Ninj1 is deficient either in macrophages or AECs, macrophages are not activated even though they are bound to AECs.

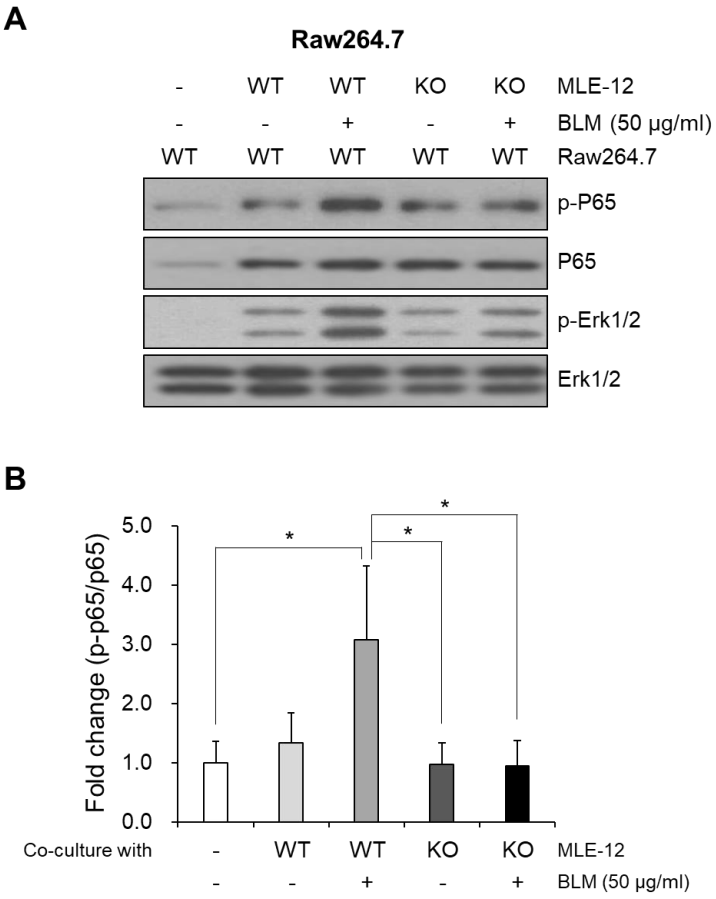

Figure 37. Inflammatory response in Raw264.7 cells after co-culture with MLE-12 cells with or without BLM treatment.

The sorted Raw264.7 cells were subjected to western blot in order to assess inflammatory signaling. Representative images (A) and semi-quantification (B) of western blot for p-p65. Data are expressed as means ± SEM of triplicates. *p<0.05.

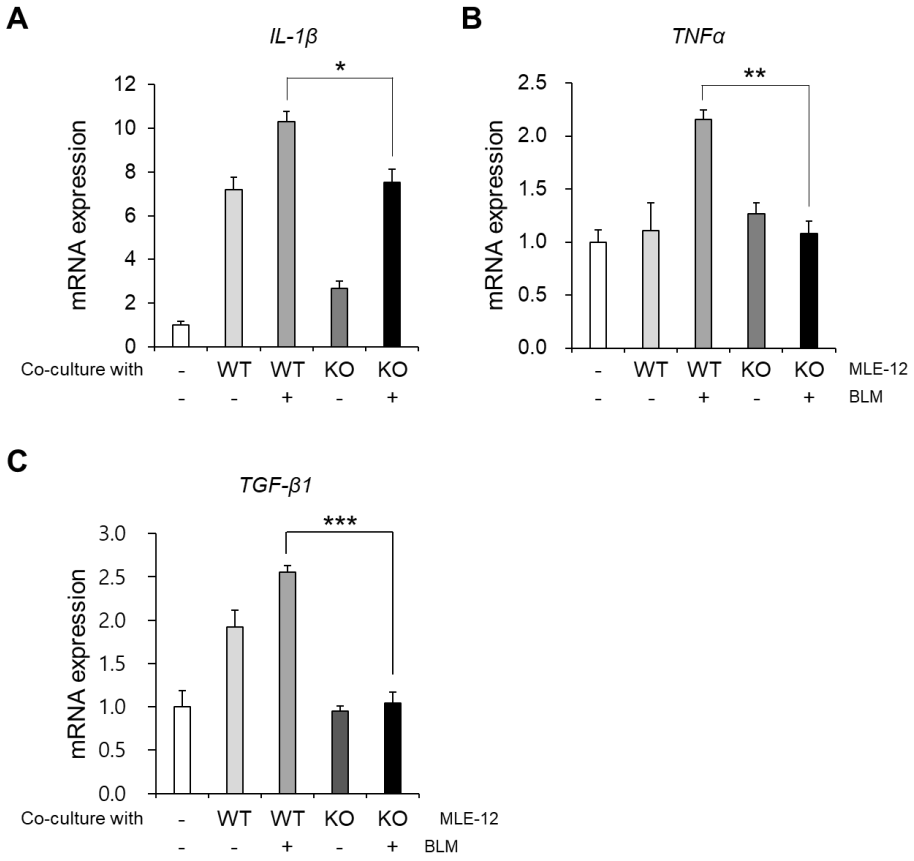

Figure 38. The expression of cytokines in Raw264.7 cells after co-culture with MLE-12 cells with or without BLM treatment.

The sorted WT Raw264.7 cells were subjected to semi-quantitative real-time PCR to determine the expression of cytokines. Semi-quantitative real-time PCR for *IL-1β* (A), *TNFα* (B) and *TGF-β1* (C). Data are expressed as means ± SEM of triplicates. **p*<0.05; ***p*<0.01; ****p*<0.001.

4.7. rmNinj1$^{1-50}$ enhances inflammatory response in macrophages

As interaction between MLE-12 and Raw264.7 cells induces the production of pro-fibrotic cytokines and Ninj1 deficiency attenuates the effect, it was hypothesized that Ninj1 directly activates macrophages. The recombinant mouse Ninj1 1-50 a.a. (rmNinj1$^{1-50}$), which covers the extracellular domain of Ninj1 where the homophilic binding domain is located (Araki et al., 1997), was generated, using E. coli. (BL21), and endotoxin was removed before use (Fig. 39). WT and Ninj1 KO peritoneal macrophages and Raw264.7 cells were treated with rmNinj1$^{1-50}$ and the inflammatory response was evaluated. The phosphorylation of NF-κB signaling protein p65 was significantly elevated in WT peritoneal macrophages (Fig. 40A, B) and WT Raw264.7 cells (Fig. 41A, B) when exposed to rmNinj1$^{1-50}$. On the other hand, the exposure of rmNinj1$^{1-50}$ to Ninj1 KO macrophages slightly induced phosphorylation of p65 at 1 hr but the effect was not preserved after 1 hr (Fig. 40, 41). In addition, the mRNA expression of *IL-1β* was induced in WT macrophages treated with rmNinj1$^{1-50}$ while its expression was not increased in Ninj1 KO macrophages (Fig. 42A, B and 43A, B). Incidentally, while the expression of *TGF-β1* in WT peritoneal macrophages was increased by rmNinj1$^{1-50}$ exposure (Fig. 42C), the expression of *TGF-β1* remained unchanged in WT Raw264.7 cells (Fig. 43C). These results suggested that Ninj1 would have directly activated macrophages possibly through Ninj1-Ninj1 homophilic binding, resulting in the production of pro-fibrotic mediators that activate fibroblasts.

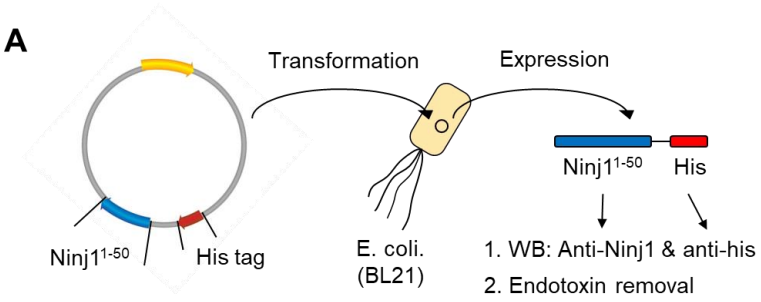

B

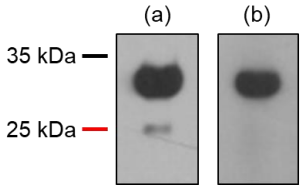

C

	ET Conc. (ng/ml)
Before ET removal	0.1252
After ET removal	0.0425

Figure 39. Generation of rmNinj1$^{1-50}$.

Recombinant mouse Ninj1 1-50 a.a. (rmNinj1$^{1-50}$) was generated by using E. coli. expression system. rmNinj1$^{1-50}$ was isolated from E. coli. and purified, followed by removal of endotoxin (ET). Western blot was performed to confirm isolation of rmNinj1$^{1-50}$ and endotoxin (ET) was removed. (A) Schematic representation of expreimental method for rmNinj1$^{1-50}$ generation. (B) Images of western blot for anti-Ninj1 (a) and anti-His (b). (C) Measurement of ET concentration (Conc.) before and after ET removal.

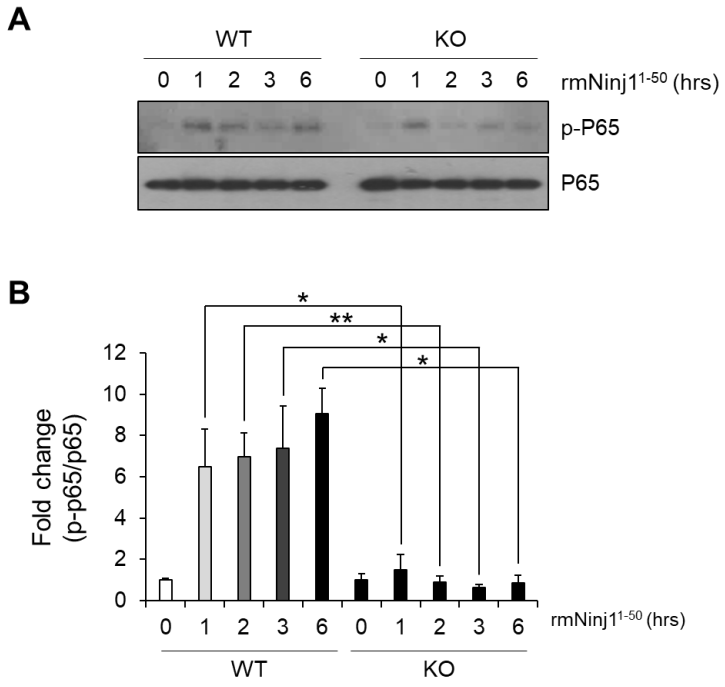

Figure 40. Effect of rmNinj1$^{1-50}$ on NF-κB signaling in in peritoneal macrophages.

WT or Ninj1 KO peritoneal macrophages were treated with rmNinj1$^{1-50}$ (50 μg/ml) and cells were collected at the indicated time points for protein isolation. Activation of p65 was assess by western blot. Representative images (A) and semi-quantification (B) of western blot. Data are expressed as means ± SEM of triplicates. *p<0.05; **p<0.01.

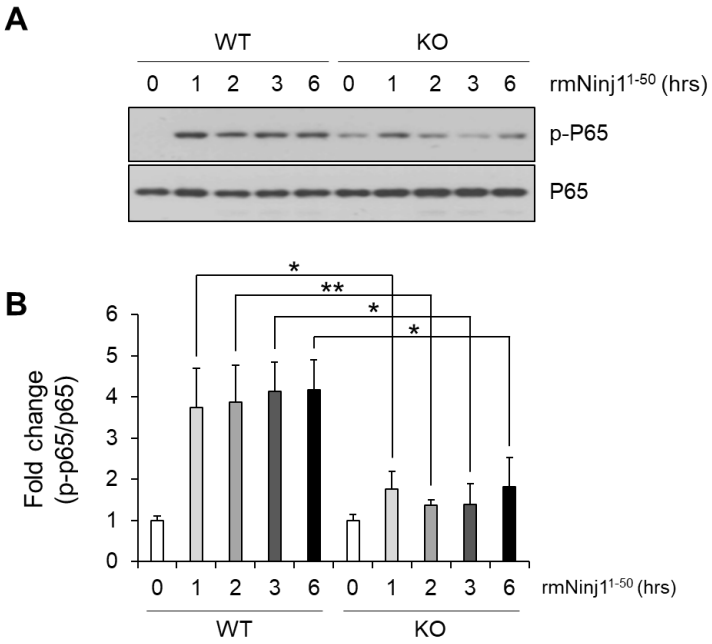

Figure 41. Effect of rmNinj1$^{1-50}$ on NF-κB signaling in Raw264.7 cells.

WT or Ninj1 KO Raw264.7 cells were treated with rmNinj1$^{1-50}$ (50 μg/ml) and cells were collected at the indicated time points for protein isolation. Activation of p65 was assess by western blot. Representative images (A) and semi-quantification (B) of western blot. Data are expressed as means ± SEM of triplicates. *p<0.05; **p<0.01.

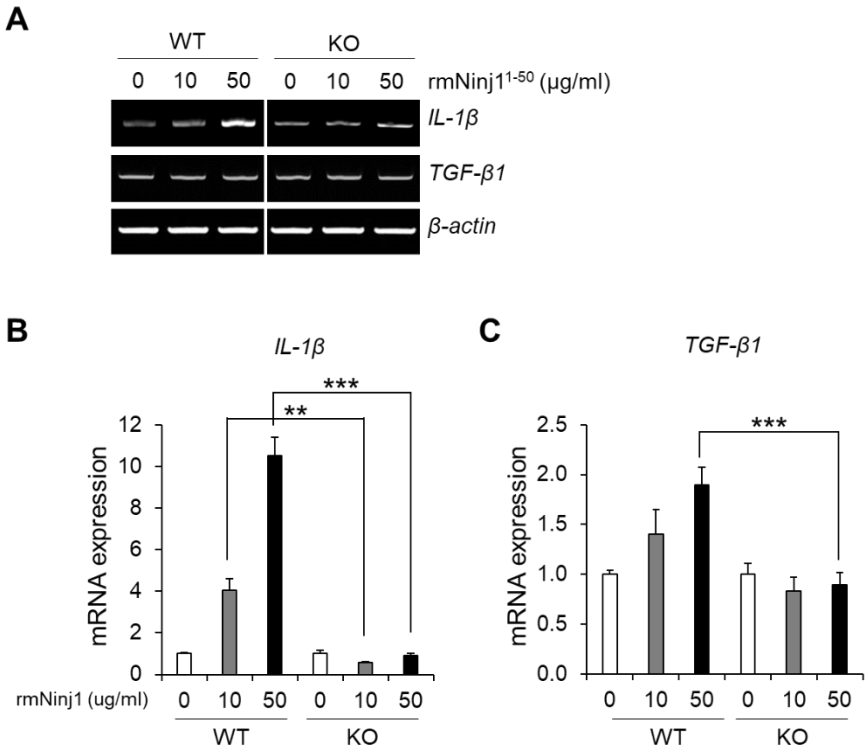

Figure 42. Effect of rmNinj1$^{1-50}$ on the expression of cytokines in peritoneal macrophages.

WT or Ninj1 KO peritoneal macrophages were treated with rmNinj1$^{1-50}$ and the expression of IL-1β and TGF-β1 was assessed by RT- and semi-quantitative real-time PCR. RT-PCR (A) and semi-quantitative real-time PCR for *IL-1β* (B) and *TGF-β1* (C). Data are expressed as means ± SEM of triplicates. ***p*<0.01; ****p*<0.001.

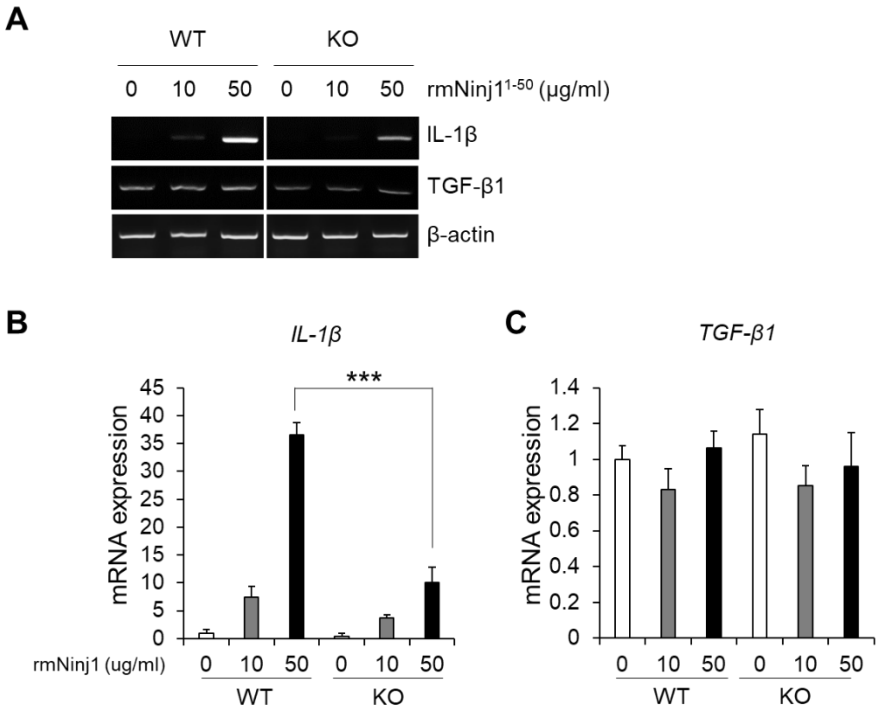

Figure 43. Effect of rmNinj1$^{1-50}$ on the expression of cytokines in Raw264.7 cells.

WT or Ninj1 KO Raw264.7 cells were treated with rmNinj1$^{1-50}$ and the expression of IL-1β and TGF-β1 was assessed by RT- and semi-quantitative real-time PCR. RT-PCR (A) and semi-quantitative real-time PCR for *IL-1β* (B) and *TGF-β1* (C). Data are expressed as means ± SEM of triplicates. ***p<0.001.

4.8. Production of pro-fibrotic mediators are elevated in rmNinj1$^{1-50}$-treated WT Raw264.7 cells but not in rmNinj1$^{1-50}$-treated Ninj1 KO Raw264.7 cells.

Conditioned media (CM) was collected from vehicle- or rmNinj1$^{1-50}$-treated WT or Ninj1 KO Raw264.7 cells. The primary fibroblasts were treated with CM and activation of TGF-β1 signaling was assessed. As shown in Fig. 28, when CM from WT or Ninj1 KO Raw264.7 cells was introduced to primary fibroblasts, phosphorylation of SMAD3 was mildly increased (Fig. 44A, B), and SMAD3 was rarely translocated into the nucleus (Fig. 45). However, when CM from rmNinj1$^{1-50}$-treated WT Raw264.7 cells was introduced, phosphorylation of SMAD3 was markedly increased (Fig. 44A, B) and nuclear localization of SMAD3 was induced (Fig. 45). On the other hand, when CM from rmNinj1$^{1-50}$-treated Ninj1 KO Raw264.7 cells was introduced, phosphorylation and nuclear localization of SMAD3 were slightly induced, compared to CM from rmNinj1$^{1-50}$-treated WT Raw264.7 cells (Fig. 44A, B, 45). As SMAD3 was activated in the fibroblasts treated with CM from rmNinj1$^{1-50}$-treated WT Raw264.7 cells, the protein and mRNA expression of α-SMA were significantly elevated in fibroblasts, indicating that the fibroblasts were differentiated into myofibroblasts (Fig. 46A, B). However, when they were treated with CM from rmNinj1$^{1-50}$-treated Ninj1 KO Raw264.7 cells, there was only slight but not significant increase in the expression of α-SMA (Fig. 46A, B). In addition, transwell migration assay demonstrated that while treatment of CM from rmNinj1$^{1-50}$-treated WT Raw264.7 cells promoted the

mobility of fibroblasts, CM from rmNinj1$^{1-50}$-treated Ninj1 KO Raw264.7 cells did not show the effect (Fig. 47A, B). These results indicate that the expression of pro-fibrotic mediators, which induce SMAD3 activation, was significantly elevated in rmNinj1$^{1-50}$-treated WT Raw264.7 cells but not in rmNinj1$^{1-50}$-treated Ninj1 KO Raw264.7 cells.

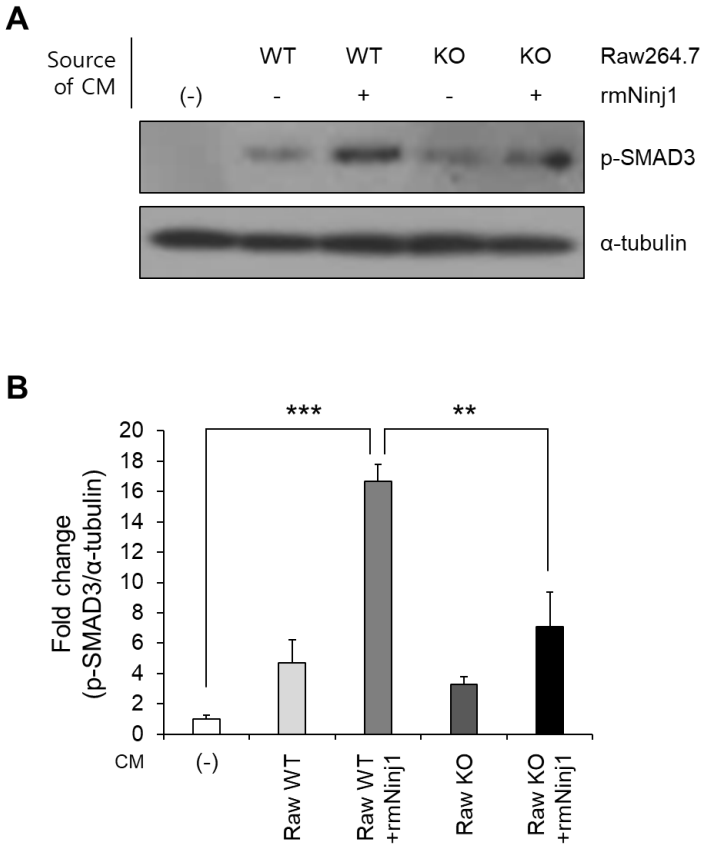

Figure 44. Activation of TGF-β1 signaling in primary fibroblasts treated with CM from rmNinj1$^{1-50}$-treated Raw264.7 cells.

WT or Ninj1 KO Raw264.7 cells were treated with vehicle or rmNinj1$^{1-50}$ (50 μg/ml) and CM was collected. Primary fibroblasts were then treated with CMs and phosphorylation of SMAD3 was assessed by western blot. (A) Representative images (A) and semi-quantification (B) of western blot. Data are expressed as means ± SEM of triplicates. $^{**}p<0.01$; $^{***}p<0.001$.

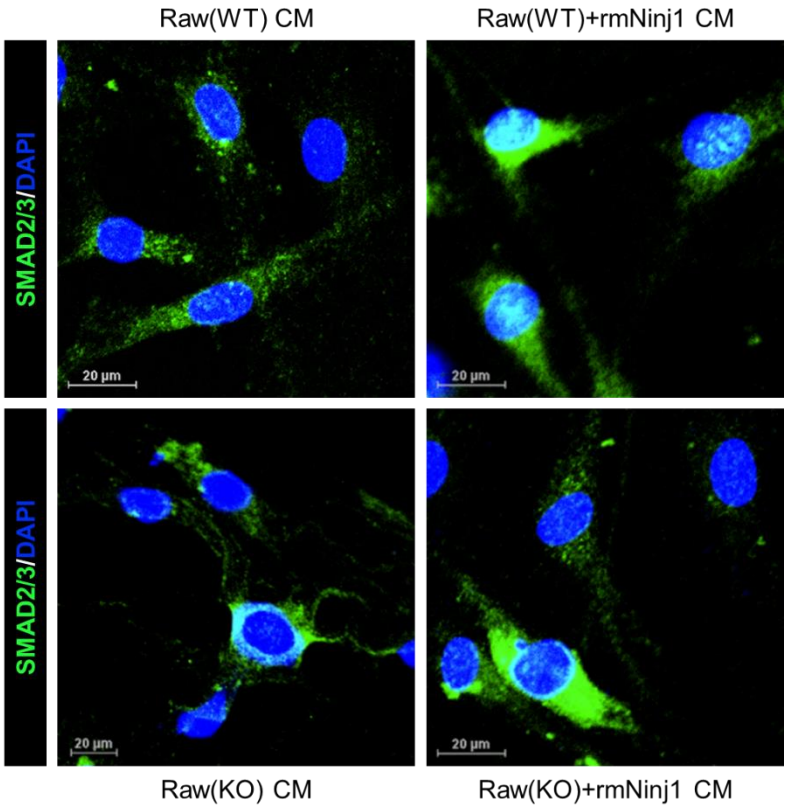

Figure 45. Nuclear localization of SMAD2/3 in primary fibroblasts treated with CM from rmNinj1$^{1-50}$-treated Raw264.7 cells.

Primary fibroblasts were then treated with CMs from rmNinj1$^{1-50}$-treated WT or Ninj1 KO Raw264.7 cells and nuclear localization of SMAD2/3 was assessed by IF. Representative images of IF for SMAD3 nuclear localization.

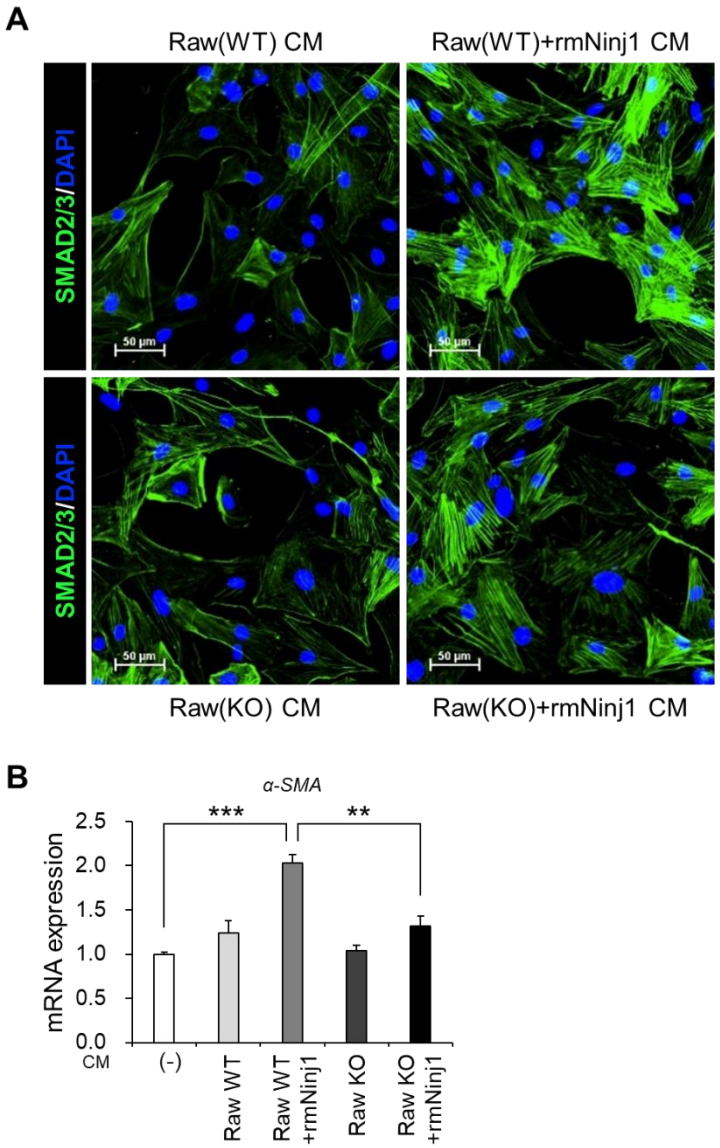

Figure 46. Activation of primary fibroblasts into myofibroblasts as treated with CM from rmNinj1$^{1-50}$-treated Raw264.7 cells.

Primary fibroblasts were treated with CMs from rmNinj1$^{1-50}$-treated WT or Ninj1 KO Raw264.7 cells. The expression of α-SMA was assessed by IF and semi-quantitative real-time PCR for α-SMA. (A) Representative images of IF

for α-SMA. (B) Semi-quantitative real-time PCR to examine the expression of α-SMA in CM-treated fibroblasts. Data are expressed as means ± SEM of triplicates. $^{**}p<0.01$; $^{***}p<0.001$.

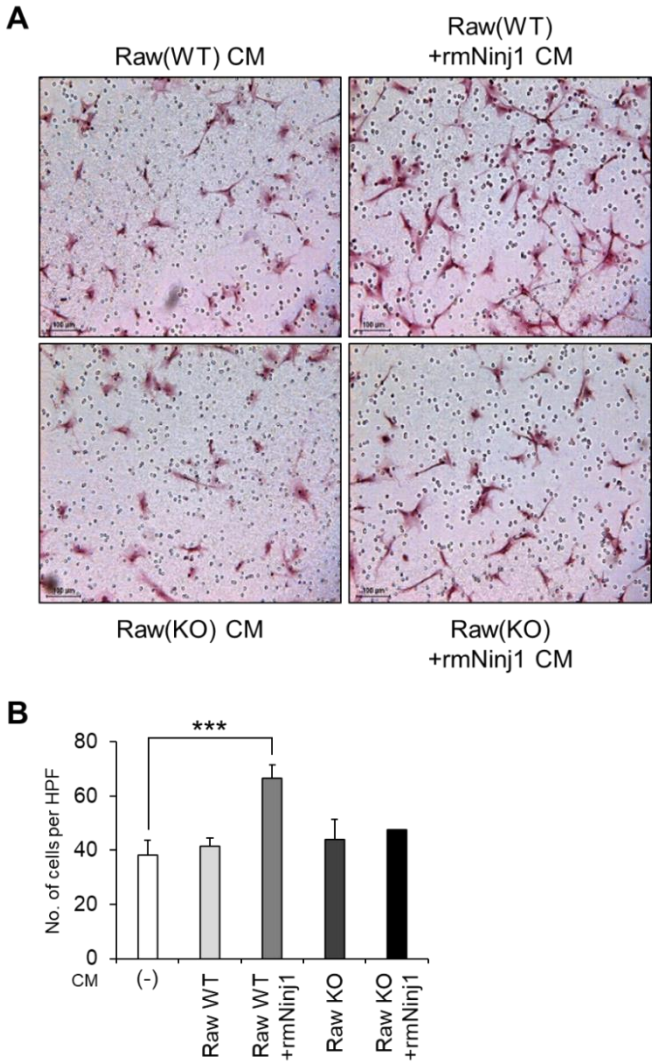

Figure 47. Migration of primary fibroblasts cultured in CM from rmNinj1$^{1\text{-}50}$-treated Raw264.7 cells.

Primary fibroblasts were subjected to transwell migration assay, using CM from rmNinj1$^{1\text{-}50}$-treated WT or Ninj1 KO Raw264.7 cells as a chemoattractant. Representative images (A) and the number of migrated cells per HPF (B) of transwell migration assay. Data are expressed as means ± SEM of triplicates. ***p<0.001.

DISCUSSION

IPF is a chronic inflammatory disease with uncontrolled production of ECM components, forming scar tissue in the lungs (Gifford et al., 2012). Recent studies have emphasized the role of Ninj1 in induction of inflammation (Ahn et al., 2014b; Ifergan et al., 2011; Jennewein et al., 2015; Lee et al., 2010). Here, I further demonstrated a novel role of Ninj1 during the development of pulmonary fibrosis. This study revealed the involvement of Ninj1 in stimulation of inflammatory response in macrophages by promoting contact-dependent interaction with AECs, thereby proving a contribution in developing pulmonary fibrosis.

In this study, it was first found that following BLM injection, the expression of Ninj1 was markedly elevated in the lungs of BLM-treated mice. In addition, the histology of the lungs from Ninj1 KO mice exhibited mild inflammatory and fibrotic phenotype, as compared to WT mice. When lung inflammation is induced, the expression of TGF-α, one of pro-inflammatory cytokines, is produced by marophages and induces hypersecretion of mucus by activating epithelial growth factor receptor (EGFR) (Barnes, 2004). While the number of mucin-producing goblet cells was increased in the lungs of BLM-treated WT mice, they were rarely detected in BLM-treated Ninj1 KO mice, suggesting that the inflammation status in Ninj KO mice was not as severe as WT mice. One aspect in the pathogenesis of pulmonary fibrosis is an increase in the infiltration

of immune cells including macrophages, thereby leading to chronic inflammation (Bringardner et al., 2008; Wilson and Wynn, 2009; Wynn and Ramalingam, 2012). Ninj1 has been reported to have a role in the migration of immune cells (Ifergan et al., 2011). Unexpectedly, the number of infiltrated inflammatory cells, including macrophages, in the lungs of BLM-treated Ninj1 KO mice was not significantly different from BLM-treated WT mice. Conversely, the expression of pro-inflammatory and pro-fibrotic mediators were diminished in the lungs of Ninj1 KO mice. These results suggested that Ninj1 plays a role in the induction of inflammatory response during the development of pulmonary fibrosis.

It was then investigated how Ninj1 deficiency reduced production of inflammatory cytokines. Recent reports indicated that macrophages are the major inflammatory cell type in the development of pulmonary fibrosis (King et al., 2011). When the lungs are injured, macrophages are activated and release pro-inflammatory cytokines (IL-1β and TNFα) as well as a pro-fibrotic mediator (TGF-β1) which directly activate the fibroblasts to release numerous ECM components (Wynn, 2011; Wynn and Barron, 2010; Wynn and Vannella, 2016). It was reported that Ninj1 is expressed mainly in macrophages and plays a crucial role in regulating the activity of macrophages (Lee et al., 2016). Since Ninj1 expression was elevated in macrophages by BLM as shown in the results, it was hypothesized that Ninj1 deficiency may reduce inflammatory response in macrophages. Unexpectedly, Ninj1 deficiency did not alter the inflammatory

response of macrophages to BLM, suggesting that even though BLM enhances Ninj1 expression, inflammatory response by BLM does not require Ninj1. The further study is necessary to investigate how BLM promoted Ninj1 expression.

Histological analysis and *in vitro* experiment revealed that Ninj1 expression was upregulated also in AECs by BLM treatment. It was reported that alveolar epithelial cells paly a pivotal role in the development of pulmonary inflammation and fibrosis (Selman and Pardo, 2006; Yang et al., 2013; Zoz et al., 2011). Alveolar epithelial cells release various pro-fibrotic chemokines and growth factors, including CXCL1, CXCL12 and TGF-β1, following lung injury (Camelo et al., 2014; Moore et al., 2005; Sharma et al., 2014). Therefore, it was examined if Ninj1 deficiency alters the expression of those mediators, following BLM-induced damage response in AECs. However, even though the expression of Ninj1 in AECs was elevated by BLM treatment, there was no significant difference in the expression of inflammation-stimulating factors between WT and Ninj1 KO AECs. CXCL1 and CXCL12 are involed in recruitment of inflammatory cells into injury site (Li and Ransohoff, 2009; Sawant et al., 2016). Especially, CXCL12 plays role in recruitment of monocytes/macrophages (Li and Ransohoff, 2009). These results suggest that since the expression of chemokines was not significant differet between WT and Ninj1 KO AECs in the response to BLM, there was no difference in inflammatory cell recruitment and population between BLM-treated WT and Ninj1 KO mice even though severity of pulmonary fibrosis was lower in Ninj1

KO mice.

I then hypothesized that Ninj1 would be involved in cell-to-cell contact interaction by homophilic binding. The previous reports indicated that contact-dependent interaction between AECs and macrophages is essential for initiation of inflammation in the pathogenesis of interstitial lung diseases (Fujii et al., 2002; Manzer et al., 2008; Tao and Kobzik, 2002). Ninj1 is a homomeric adhesion molecule, which leads to cell-to-cell adhesion (Ahn et al., 2009; Lee et al., 2010). However, the data demonstrated that there was no significant difference in adhesion of AECs and macrophages depending on Ninj1 expression. Interestingly, it was found that macrophages were activated as they were bound to AECs and they were activated more when bound to BLM-treated AECs, leading to a significant increase in production of pro-fibrotic mediators that activates fibroblasts. In addition, even though macrophages were bound to AECs, they are not activated when Ninj1 is depleted either in AECs and macrophages. In this study, it was confirmed that Ninj1-mediated interaction between AECs and macrophages enhanced activation of macrophages so that they produced pro-fibrotic mediators, which finally led to differentiation of fibroblasts into myofibroblast. Even though Ninj1 was not required for adhesion of AECs and macrophages as previously concluded, the inflammatory response of macrophages was enhanced as BLM-induced elevation of Ninj1 expression promoted a contact-dependent interaction with AECs. Therefore, it was hypothesized that Ninj1 may directly activate macrophages.

The rmNinj1 expressing 1-50 a.a. (rmNinj1$^{1-50}$), which includes homophilic binding domain (26-37 a.a.) (Lee et al., 2010), was generated. Since rmNinj1$^{1-50}$ was generated by using E. coli. system, endotoxin, which is known as lipopolysaccharide (LPS) that activates NF-κB signaling in macrophages (Janeway and Medzhitov, 2002), was removed. Inflammatory response of WT macrophages was induced when they were treated with rmNinj1$^{1-50}$, producing pro-fibrotic mediators, IL-1β and TGF-β1 (Artlett, 2012; Fernandez and Eickelberg, 2012). On the other hand, Ninj1 KO macrophages were not activated by rmNinj1$^{1-50}$. In the previous report, Ninj1 directly binds to LPS and mediates LPS-induced NF-κB signaling in macrophages (Shin et al., 2016). Even though endotoxin was removed when rmNinj1$^{1-50}$ was generated, remaining ET would activate NF-κB signaling. However, rmNinj1$^{1-50}$ generated in this study, does not include LPS-binding domain (81-100 a.a.) (Shin et al., 2016). Therefore, these results strongly suggest that Ninj1 has the ability to directly activate NF-κB signaling in macrophages. These results were confirmed by treating primary fibroblasts with CM from rmNinj1$^{1-50}$-treated WT or Ninj1 KO macrophages in order to assess the differences in activation of fibroblasts. As expected, CM from vehicle-treated WT or Ninj1 KO macrophages mildly activated fibroblasts and there was no significant difference in activation of fibroblasts between CMs from WT or Ninj1 KO macrophages. These results indicate that there is no significant difference in the basal expression of pro-fibrotic mediators between WT and Ninj1 KO

Raw264.7 cells. In contrast, while CM from rmNinj1$^{1-50}$-treated WT promote activation of fibroblast, CM from rmNinj1$^{1-50}$-treated Ninj1 KO Raw264.7 cells did not. As shown in the results, however, while IL-1β expression level was increased, TGF-β1 expression level did not increase in from rmNinj1$^{1-50}$-treated WT Raw264.7 cells. In addition, even though the expression of TGF-β1 was not up-regulated in macrophages by rmNinj1$^{1-50}$ treatment, their CM induced SMAD3 activation in fibroblasts. IL-1β signaling, which is one of the major inflammatory signaling pathways, is involved in gene expression of TGF-β1 which would transmit autocrine signal to activate fibroblast (Artlett, 2012). Taking these data together, since rmNinj1$^{1-50}$ includes N-terminal region where the homophilic binding domain is located (Ahn et al., 2014a; Araki et al., 1997), it may have directly activated macrophages by homophilic interaction with Ninj1 on macrophages. However, the molecular mechanism of how Ninj1 on AECs enhances the inflammatory response of macrophages needs further investigation. Moreover, since AEC-to-macrophage contact-dependent interaction and treatment of rmNinj1$^{1-50}$ induced production of IL-1β and TGF-β1 in macrophages, it is necessary to investigate if Ninj1 is involved in macrophages polarization that regulates wound healing and fibrosis (Ferrante and Leibovich, 2012; Martinez et al., 2009).

CONCLUSION

In this study, a novel function of Ninj1 has been investigated in pulmonary fibrosis. I found that the expression of Ninj1 in lungs of IPF patietns and BLM-treated mice was elevated, and AECs and macrophages expressed increased Ninj1 level. The elevated Ninj1 expression enhanced the activation of macrophages by promoting the interaction with AECs, leading to increase in pro-fibrotic mediators that activate fibroblasts. A recent report suggested that targeting macrophage-directed factors could be an effective therapeutic strategy for patients with IPF (Byrne et al., 2016). Therefore, this study also emphasizes on the importance of the function of macrophages in pulmonary fibrosis and the involvement of Ninj1 in macrophage activation. However, even though elevation of Ninj1 and its involvement in interaction between AECs and macrophages were demonstrated in this study, there are several limitations to be considered in the this study. First, it is still unknown how BLM promoted Ninj1 expression in AECs and macrophages. Second, it is necessary to investigate how Ninj1 promoted interaction between AECs and macrophages, leading to macrophage activation and how rmNinj1$^{1\text{-}50}$ contributed to activation of inflammatory response in macrophages. Taking all together, these findings indicate that Ninj1 could be a potential target to inhibit activation of macrophages for preventing future episodes of IPF incidence.

REFERENCES

Ahn, B.J., Le, H., Shin, M.W., Bae, S.J., Lee, E.J., Lee, S.Y., Yang, J.H., Wee, H.J., Cha, J.H., Seo, J.H.*, et al.* (2014a). Ninjurin1 enhances the basal motility and transendothelial migration of immune cells by inducing protrusive membrane dynamics. J Biol Chem *289*, 21926-21936.

Ahn, B.J., Le, H., Shin, M.W., Bae, S.J., Lee, E.J., Wee, H.J., Cha, J.H., Lee, H.J., Lee, H.S., Kim, J.H.*, et al.* (2014b). Ninjurin1 deficiency attenuates susceptibility of experimental autoimmune encephalomyelitis in mice. J Biol Chem *289*, 3328-3338.

Ahn, B.J., Lee, H.J., Shin, M.W., Choi, J.H., Jeong, J.W., and Kim, K.W. (2009). Ninjurin1 is expressed in myeloid cells and mediates endothelium adhesion in the brains of EAE rats. Biochem Biophys Res Commun *387*, 321-325.

Araki, T., and Milbrandt, J. (1996). Ninjurin, a novel adhesion molecule, is induced by nerve injury and promotes axonal growth. Neuron *17*, 353-361.

Araki, T., and Milbrandt, J. (2000). Ninjurin2, a novel homophilic adhesion molecule, is expressed in mature sensory and enteric neurons and promotes neurite outgrowth. J Neurosci *20*, 187-195.

Araki, T., Zimonjic, D.B., Popescu, N.C., and Milbrandt, J. (1997). Mechanism of homophilic binding mediated by ninjurin, a novel widely expressed adhesion molecule. J Biol Chem *272*, 21373-21380.

Artlett, C.M. (2012). The Role of the NLRP3 Inflammasome in Fibrosis. Open Rheumatol J *6*, 80-86.

Bacci, E.D., O'Quinn, S., Leidy, N.K., Murray, L., and Vernon, M. (2018).

Evaluation of a respiratory symptom diary for clinical studies of idiopathic pulmonary fibrosis. Respir Med *134*, 130-138.

Barnes, P.J. (2004). Alveolar macrophages as orchestrators of COPD. COPD *1*, 59-70.

Barrett, T., and Edgar, R. (2006). Gene expression omnibus: microarray data storage, submission, retrieval, and analysis. Methods Enzymol *411*, 352-369.

Barrientos, S., Stojadinovic, O., Golinko, M.S., Brem, H., and Tomic-Canic, M. (2008). Growth factors and cytokines in wound healing. Wound Repair Regen *16*, 585-601.

Bataller, R., and Brenner, D.A. (2005). Liver fibrosis. J Clin Invest *115*, 209-218.

Biernacka, A., Dobaczewski, M., and Frangogiannis, N.G. (2011). TGF-β signaling in fibrosis. Growth Factors *29*, 196-202.

Borthwick, L.A., Barron, L., Hart, K.M., Vannella, K.M., Thompson, R.W., Oland, S., Cheever, A., Sciurba, J., Ramalingam, T.R., Fisher, A.J.*, et al.* (2016). Macrophages are critical to the maintenance of IL-13-dependent lung inflammation and fibrosis. Mucosal Immunol *9*, 38-55.

Braga, T.T., Agudelo, J.S., and Camara, N.O. (2015). Macrophages During the Fibrotic Process: M2 as Friend and Foe. Front Immunol *6*, 602.

Bringardner, B.D., Baran, C.P., Eubank, T.D., and Marsh, C.B. (2008). The role of inflammation in the pathogenesis of idiopathic pulmonary fibrosis. Antioxid Redox Signal *10*, 287-301.

Byrne, A.J., Maher, T.M., and Lloyd, C.M. (2016). Pulmonary Macrophages: A New Therapeutic Pathway in Fibrosing Lung Disease? Trends Mol Med *22*, 303-316.

Camelo, A., Dunmore, R., Sleeman, M.A., and Clarke, D.L. (2014). The epithelium in idiopathic pulmonary fibrosis: breaking the barrier. Front Pharmacol *4*, 173.

Cao, Q., Wang, Y., and Harris, D.C. (2014). Macrophage heterogeneity, phenotypes, and roles in renal fibrosis. Kidney Int Suppl (2011) *4*, 16-19.

de Boer, W.I., Sont, J.K., van Schadewijk, A., Stolk, J., van Krieken, J.H., and Hiemstra, P.S. (2000). Monocyte chemoattractant protein 1, interleukin 8, and chronic airways inflammation in COPD. J Pathol *190*, 619-626.

Eddy, A.A. (2005). Can renal fibrosis be reversed? Pediatr Nephrol *20*, 1369-1375.

Fernandez, I.E., and Eickelberg, O. (2012). The impact of TGF-β on lung fibrosis: from targeting to biomarkers. Proc Am Thorac Soc *9*, 111-116.

Ferrante, C.J., and Leibovich, S.J. (2012). Regulation of Macrophage Polarization and Wound Healing. Adv Wound Care (New Rochelle) *1*, 10-16.

Fujii, T., Hayashi, S., Hogg, J.C., Mukae, H., Suwa, T., Goto, Y., Vincent, R., and van Eeden, S.F. (2002). Interaction of alveolar macrophages and airway epithelial cells following exposure to particulate matter produces mediators that stimulate the bone marrow. Am J Respir Cell Mol Biol *27*, 34-41.

Gifford, A.H., Matsuoka, M., Ghoda, L.Y., Homer, R.J., and Enelow, R.I. (2012). Chronic inflammation and lung fibrosis: pleotropic syndromes but

limited distinct phenotypes. Mucosal Immunol *5*, 480-484.

Gonzalez, A.C., Costa, T.F., Andrade, Z.A., and Medrado, A.R. (2016). Wound healing - A literature review. An Bras Dermatol *91*, 614-620.

Gurtner, G.C., Werner, S., Barrandon, Y., and Longaker, M.T. (2008). Wound repair and regeneration. Nature *453*, 314-321.

Hasegawa, M., Fujimoto, M., Kikuchi, K., and Takehara, K. (1997). Elevated serum tumor necrosis factor-alpha levels in patients with systemic sclerosis: association with pulmonary fibrosis. J Rheumatol *24*, 663-665.

Hewitt, R.J., and Maher, T.M. (2019). Idiopathic Pulmonary Fibrosis: New and Emerging Treatment Options. Drugs Aging *36*, 485-492.

Huebener, P., and Schwabe, R.F. (2013). Regulation of wound healing and organ fibrosis by toll-like receptors. Biochim Biophys Acta *1832*, 1005-1017.

Hübner, R.H., Gitter, W., El Mokhtari, N.E., Mathiak, M., Both, M., Bolte, H., Freitag-Wolf, S., and Bewig, B. (2008). Standardized quantification of pulmonary fibrosis in histological samples. Biotechniques *44*, 507-511, 514-507.

Ifergan, I., Kebir, H., Terouz, S., Alvarez, J.I., Lécuyer, M.A., Gendron, S., Bourbonnière, L., Dunay, I.R., Bouthillier, A., Moumdjian, R.*, et al.* (2011). Role of Ninjurin-1 in the migration of myeloid cells to central nervous system inflammatory lesions. Ann Neurol *70*, 751-763.

Janeway, C.A., and Medzhitov, R. (2002). Innate immune recognition. Annu Rev Immunol *20*, 197-216.

Jang, Y.S., Kang, J.H., Woo, J.K., Kim, H.M., Hwang, J.I., Lee, S.J., Lee, H.Y., and Oh, S.H. (2016). Ninjurin1 suppresses metastatic property of lung cancer cells through inhibition of interleukin 6 signaling pathway. Int J Cancer *139*, 383-395.

Jennewein, C., Sowa, R., Faber, A.C., Dildey, M., von Knethen, A., Meybohm, P., Scheller, B., Dröse, S., and Zacharowski, K. (2015). Contribution of Ninjurin1 to Toll-like receptor 4 signaling and systemic inflammation. Am J Respir Cell Mol Biol *53*, 656-663.

Jiang, D., Liang, J., Campanella, G.S., Guo, R., Yu, S., Xie, T., Liu, N., Jung, Y., Homer, R., Meltzer, E.B.*, et al.* (2010). Inhibition of pulmonary fibrosis in mice by CXCL10 requires glycosaminoglycan binding and syndecan-4. J Clin Invest *120*, 2049-2057.

Jung, Y.K., and Yim, H.J. (2017). Reversal of liver cirrhosis: current evidence and expectations. Korean J Intern Med *32*, 213-228.

King, T.E., Pardo, A., and Selman, M. (2011). Idiopathic pulmonary fibrosis. Lancet *378*, 1949-1961.

Kolilekas, L., Papiris, S., and Bouros, D. (2019). Existing and emerging treatments for idiopathic pulmonary fibrosis. Expert Rev Respir Med *13*, 229-239.

Kong, P., Christia, P., and Frangogiannis, N.G. (2014). The pathogenesis of cardiac fibrosis. Cell Mol Life Sci *71*, 549-574.

Lasithiotaki, I., Giannarakis, I., Tsitoura, E., Samara, K.D., Margaritopoulos, G.A., Choulaki, C., Vasarmidi, E., Tzanakis, N., Voloudaki, A., Sidiropoulos, P.*, et al.* (2016). NLRP3 inflammasome expression in idiopathic pulmonary

fibrosis and rheumatoid lung. Eur Respir J *47*, 910-918.

Lebrun, A., Lo Re, S., Chantry, M., Izquierdo Carerra, X., Uwambayinema, F., Ricci, D., Devosse, R., Ibouraadaten, S., Brombin, L., Palmai-Pallag, M.*, et al.* (2017). CCR2+ monocytic myeloid-derived suppressor cells (M-MDSCs) inhibit collagen degradation and promote lung fibrosis by producing transforming growth factor-β1. J Pathol *243*, 320-330.

Lee, H.J., Ahn, B.J., Shin, M.W., Choi, J.H., and Kim, K.W. (2010). Ninjurin1: a potential adhesion molecule and its role in inflammation and tissue remodeling. Mol Cells *29*, 223-227.

Lee, H.K., Lee, H., Luo, L., and Lee, J.K. (2016). Induction of Nerve Injury-Induced Protein 1 (Ninjurin 1) in Myeloid Cells in Rat Brain after Transient Focal Cerebral Ischemia. Exp Neurobiol *25*, 64-74.

Leng, D., Huan, C., Xie, T., Liang, J., Wang, J., Dai, H., Wang, C., and Jiang, D. (2013). Meta-analysis of genetic programs between idiopathic pulmonary fibrosis and sarcoidosis. PLoS One *8*, e71059.

Li, M., and Ransohoff, R.M. (2009). The roles of chemokine CXCL12 in embryonic and brain tumor angiogenesis. Semin Cancer Biol *19*, 111-115.

Livak, K.J., and Schmittgen, T.D. (2001). Analysis of relative gene expression data using real-time quantitative PCR and the 2(-Delta Delta C(T)) Method. Methods *25*, 402-408.

Manicone, A.M. (2009). Role of the pulmonary epithelium and inflammatory signals in acute lung injury. Expert Rev Clin Immunol *5*, 63-75.

Manzer, R., Dinarello, C.A., McConville, G., and Mason, R.J. (2008). Ozone

exposure of macrophages induces an alveolar epithelial chemokine response through IL-1alpha. Am J Respir Cell Mol Biol *38*, 318-323.

Martinez, F.O., and Gordon, S. (2014). The M1 and M2 paradigm of macrophage activation: time for reassessment. F1000Prime Rep *6*, 13.

Martinez, F.O., Helming, L., and Gordon, S. (2009). Alternative activation of macrophages: an immunologic functional perspective. Annu Rev Immunol *27*, 451-483.

Misharin, A.V., Morales-Nebreda, L., Reyfman, P.A., Cuda, C.M., Walter, J.M., McQuattie-Pimentel, A.C., Chen, C.I., Anekalla, K.R., Joshi, N., Williams, K.J.N.*, et al.* (2017). Monocyte-derived alveolar macrophages drive lung fibrosis and persist in the lung over the life span. J Exp Med *214*, 2387-2404.

Moeller, A., Ask, K., Warburton, D., Gauldie, J., and Kolb, M. (2008). The bleomycin animal model: a useful tool to investigate treatment options for idiopathic pulmonary fibrosis? Int J Biochem Cell Biol *40*, 362-382.

Moore, B.B., Kolodsick, J.E., Thannickal, V.J., Cooke, K., Moore, T.A., Hogaboam, C., Wilke, C.A., and Toews, G.B. (2005). CCR2-mediated recruitment of fibrocytes to the alveolar space after fibrotic injury. Am J Pathol *166*, 675-684.

Murray, L.A., Chen, Q., Kramer, M.S., Hesson, D.P., Argentieri, R.L., Peng, X., Gulati, M., Homer, R.J., Russell, T., van Rooijen, N.*, et al.* (2011). TGF-beta driven lung fibrosis is macrophage dependent and blocked by Serum amyloid P. Int J Biochem Cell Biol *43*, 154-162.

Nash, J.R., McLaughlin, P.J., Butcher, D., and Corrin, B. (1993). Expression of tumour necrosis factor-alpha in cryptogenic fibrosing alveolitis.

Histopathology *22*, 343-347.

Piguet, P.F., Ribaux, C., Karpuz, V., Grau, G.E., and Kapanci, Y. (1993). Expression and localization of tumor necrosis factor-alpha and its mRNA in idiopathic pulmonary fibrosis. Am J Pathol *143*, 651-655.

Raghu, G., Collard, H.R., Egan, J.J., Martinez, F.J., Behr, J., Brown, K.K., Colby, T.V., Cordier, J.F., Flaherty, K.R., Lasky, J.A.*, et al.* (2011). An official ATS/ERS/JRS/ALAT statement: idiopathic pulmonary fibrosis: evidence-based guidelines for diagnosis and management. Am J Respir Crit Care Med *183*, 788-824.

Reynolds, H.Y. (2005). Lung inflammation and fibrosis: an alveolar macrophage-centered perspective from the 1970s to 1980s. Am J Respir Crit Care Med *171*, 98-102.

Ritchie, M.E., Phipson, B., Wu, D., Hu, Y., Law, C.W., Shi, W., and Smyth, G.K. (2015). limma powers differential expression analyses for RNA-sequencing and microarray studies. Nucleic Acids Res *43*, e47.

Sawant, K.V., Poluri, K.M., Dutta, A.K., Sepuru, K.M., Troshkina, A., Garofalo, R.P., and Rajarathnam, K. (2016). Chemokine CXCL1 mediated neutrophil recruitment: Role of glycosaminoglycan interactions. Sci Rep *6*, 33123.

Seibold, M.A., Wise, A.L., Speer, M.C., Steele, M.P., Brown, K.K., Loyd, J.E., Fingerlin, T.E., Zhang, W., Gudmundsson, G., Groshong, S.D.*, et al.* (2011). A common MUC5B promoter polymorphism and pulmonary fibrosis. N Engl J Med *364*, 1503-1512.

Selman, M., King, T.E., Pardo, A., Society, A.T., Society, E.R., and Physicians, A.C.o.C. (2001). Idiopathic pulmonary fibrosis: prevailing and evolving

hypotheses about its pathogenesis and implications for therapy. Ann Intern Med *134*, 136-151.

Selman, M., and Pardo, A. (2006). Role of epithelial cells in idiopathic pulmonary fibrosis: from innocent targets to serial killers. Proc Am Thorac Soc *3*, 364-372.

Sharma, A.K., Mulloy, D.P., Le, L.T., and Laubach, V.E. (2014). NADPH oxidase mediates synergistic effects of IL-17 and TNF-α on CXCL1 expression by epithelial cells after lung ischemia-reperfusion. Am J Physiol Lung Cell Mol Physiol *306*, L69-79.

Shin, M.W., Bae, S.J., Wee, H.J., Lee, H.J., Ahn, B.J., Le, H., Lee, E.J., Kim, R.H., Lee, H.S., Seo, J.H., *et al.* (2016). Ninjurin1 regulates lipopolysaccharide-induced inflammation through direct binding. Int J Oncol *48*, 821-828.

Strock, S.B., Alder, J.K., and Kass, D.J. (2017). From bad to worse: when lung cancer complicates idiopathic pulmonary fibrosis. J Pathol.

Tajouri, L., Fernandez, F., and Griffiths, L.R. (2007). Gene expression studies in multiple sclerosis. Curr Genomics *8*, 181-189.

Tao, B., Jin, W., Xu, J., Liang, Z., Yao, J., Zhang, Y., Wang, K., Cheng, H., Zhang, X., and Ke, Y. (2014). Myeloid-specific disruption of tyrosine phosphatase Shp2 promotes alternative activation of macrophages and predisposes mice to pulmonary fibrosis. J Immunol *193*, 2801-2811.

Tao, F., and Kobzik, L. (2002). Lung macrophage-epithelial cell interactions amplify particle-mediated cytokine release. Am J Respir Cell Mol Biol *26*, 499-505.

Tatler, A.L., and Jenkins, G. (2012). TGF-β activation and lung fibrosis. Proc Am Thorac Soc *9*, 130-136.

Wilson, M.S., Madala, S.K., Ramalingam, T.R., Gochuico, B.R., Rosas, I.O., Cheever, A.W., and Wynn, T.A. (2010). Bleomycin and IL-1beta-mediated pulmonary fibrosis is IL-17A dependent. J Exp Med *207*, 535-552.

Wilson, M.S., and Wynn, T.A. (2009). Pulmonary fibrosis: pathogenesis, etiology and regulation. Mucosal Immunol *2*, 103-121.

Woo, J.K., Jang, J.E., Kang, J.H., Seong, J.K., Yoon, Y.S., Kim, H.C., Lee, S.J., and Oh, S.H. (2017). Lectin, Galactoside-Binding Soluble 3 Binding Protein Promotes 17-N-Allylamino-17-demethoxygeldanamycin Resistance through PI3K/Akt Pathway in Lung Cancer Cell Line. Mol Cancer Ther *16*, 1355-1365.

Wuyts, W.A., Agostini, C., Antoniou, K.M., Bouros, D., Chambers, R.C., Cottin, V., Egan, J.J., Lambrecht, B.N., Lories, R., Parfrey, H.*, et al.* (2013). The pathogenesis of pulmonary fibrosis: a moving target. Eur Respir J *41*, 1207-1218.

Wynn, T.A. (2008). Cellular and molecular mechanisms of fibrosis. J Pathol *214*, 199-210.

Wynn, T.A. (2011). Integrating mechanisms of pulmonary fibrosis. J Exp Med *208*, 1339-1350.

Wynn, T.A., and Barron, L. (2010). Macrophages: master regulators of inflammation and fibrosis. Semin Liver Dis *30*, 245-257.

Wynn, T.A., and Ramalingam, T.R. (2012). Mechanisms of fibrosis: therapeutic translation for fibrotic disease. Nat Med *18*, 1028-1040.

Wynn, T.A., and Vannella, K.M. (2016). Macrophages in Tissue Repair, Regeneration, and Fibrosis. Immunity *44*, 450-462.

Yang, J., Wheeler, S.E., Velikoff, M., Kleaveland, K.R., LaFemina, M.J., Frank, J.A., Chapman, H.A., Christensen, P.J., and Kim, K.K. (2013). Activated alveolar epithelial cells initiate fibrosis through secretion of mesenchymal proteins. Am J Pathol *183*, 1559-1570.

Yin, G.N., Choi, M.J., Kim, W.J., Kwon, M.H., Song, K.M., Park, J.M., Das, N.D., Kwon, K.D., Batbold, D., Oh, G.T.*, et al.* (2014). Inhibition of Ninjurin 1 restores erectile function through dual angiogenic and neurotrophic effects in the diabetic mouse. Proc Natl Acad Sci U S A *111*, E2731-2740.

Young, L.R., Gulleman, P.M., Short, C.W., Tanjore, H., Sherrill, T., Qi, A., McBride, A.P., Zaynagetdinov, R., Benjamin, J.T., Lawson, W.E.*, et al.* (2016). Epithelial-macrophage interactions determine pulmonary fibrosis susceptibility in Hermansky-Pudlak syndrome. JCI Insight *1*, e88947.

Zeki, A.A., Schivo, M., Chan, A.L., Hardin, K.A., Kenyon, N.J., Albertson, T.E., Rosenquist, G.L., and Louie, S. (2010). Geoepidemiology of COPD and idiopathic pulmonary fibrosis. J Autoimmun *34*, J327-338.

Zhang, Q., Raoof, M., Chen, Y., Sumi, Y., Sursal, T., Junger, W., Brohi, K., Itagaki, K., and Hauser, C.J. (2010). Circulating mitochondrial DAMPs cause inflammatory responses to injury. Nature *464*, 104-107.

Zhang, X., Goncalves, R., and Mosser, D.M. (2008). The isolation and characterization of murine macrophages. Curr Protoc Immunol *Chapter 14*, Unit 14.11.

Zhang, X.Y., Shimura, S., Masuda, T., Saitoh, H., and Shirato, K. (2000).

Antisense oligonucleotides to NF-kappaB improve survival in bleomycin-induced pneumopathy of the mouse. Am J Respir Crit Care Med *162*, 1561-1568.

Ziegler, D.M., and Kehrer, J.P. (1990). Oxygen radicals and drugs: in vitro measurements. Methods Enzymol *186*, 621-626.

Zoz, D.F., Lawson, W.E., and Blackwell, T.S. (2011). Idiopathic pulmonary fibrosis: a disorder of epithelial cell dysfunction. Am J Med Sci *341*, 435-438.

국문 초록

폐섬유화증 발생 과정에서 Ninjurin1 의 역할에 대한 연구

서울대학교 대학원

수의학과 수의생명과학 전공

최 승 호

(지도교수: 윤 여 성)

특발성 폐섬유화증은 만성 염증성 질환으로서 허파조직 내에 흉터조직이 발생하는 질병으로서 발병의 원인이 뚜렷하지 않고 증상이 비특이적이기 때문에 진단과 치료제의 개발이 어려운 질병이다. 현재까지의 연구 결과에 따르면 오염된 공기 및 방사선에 노출되거나 블레오마이신(bleomycin)과 같은 약물의 부작용 등에 의해 폐섬유화증이 발병할 수 있다. 이러한 원인들에 의해 지속적인 허파상피세포의 손상이 발생하면 만성 염증을 유발하고 결국 폐섬유화증으로 발전한다. 폐섬유화증 발병 과정에서 큰포식세포는 염증 인자 및 섬유화증 유발 인자들을 생산하는 주요 세포 종으로 알려져 있으며 염증 유발 인자인 IL-1β 및 TNFα와 섬유모세포를 활성화시켜 섬유화증을 유발하는 인자인 TGF-β1를 생산하는 것으로 알려져 있다.

세포막 단백질의 일종인 Nerve injury-induced protein 1(Ninjurin1 or Ninj1)은 다발성 경화증과 자가면역 뇌질환과 같은 염증성 질병 유발에서 중요한 역할을 한다. Ninj1은 대부분의 조직에서 발현 하는 것으로 알려져 있으며 특히 염증세포에서 Ninj1의 발현이 높다. Ninj1은 단핵 백혈구, 큰포식세포, 미세아교세포와 같은 면역세포의 이동성을 증가시키며 큰포식세포의 염증반응 유발을 촉진하여 다발성 염증성 질환을

유발하는데 중요한 역할을 한다. 따라서 Ninj1이 만성 염증성 질환인 섬유화증 발생에서도 중요한 역할을 할 것이라는 가설을 설정하여 하여 폐섬유화증 발생 과정에서 Ninj1의 새로운 기능을 밝히는 것을 본 연구의 목표로 하고 있다.

특발성 폐섬유화증 환자의 샘플을 이용한 통계학적 분석을 통해 Ninj1의 발현이 정상인들에 비해 높은 것을 확인하였다. 또한 블레오마이신에 의한 폐섬유화증이 유도된 쥐의 허파조직에서도 대조군 쥐에 비해 Ninj1의 발현이 현저히 증가한 것을 관찰하였으며 특히 큰포식세포와 허파상피세포에서 블레오마이신 처리에 의해 Ninj1의 발현이 증가하는 것을 허파조직과 세포주에서 확인하였다. 따라서 본 연구에서는 폐섬유화증 발생의 염증 변화과정에서 Ninj1이 중요한 역할을 할 것이란 가설을 세워 연구를 진행하였다.

가설 증명을 위해 먼저 야생형(WT) 쥐와 Ninj1의 발현을 억제한(Ninj1 KO) 쥐에 블레오마이신을 투여하여 Ninj1 발현 감소에 따른 폐섬유화증의 발생 변화를 분석하였다. 동물 실험 결과 WT 쥐에 비해 Ninj1 KO 쥐에서 폐섬유화증의 발병도가 현저히 낮은 것을 확인하였다. 또한 허파조직 내에 섬유모세포 및

근육섬유모세포의 수가 WT 쥐에 비해 Ninj1 KO 쥐에서 현저히 감소하였다.

폐섬유화증 발생 과정에서 WT 쥐와 Ninj1 KO 쥐 사이 염증 유발 차이를 확인하기 위해 먼저 WT 쥐와 Ninj1 KO 쥐에 BLM을 투여하여 침윤된 염증세포 수와 분포 차이를 확인하였다. WT 쥐에 비해 Ninj1 KO 쥐에서 폐섬유화증 발병도가 낮음에도 불구하고 허파에 침윤된 염증세포의 수와 분포의 차이는 없었다. 그러나 염증 및 섬유화증 유발 인자들인 IL-1β, TNFα, TGF-β1의 발현 정도를 확인해본 결과 WT 쥐에 비해 Ninj1 KO 쥐의 허파에서 각 인자들의 발현이 감소되어 있었다. 따라서 BLM 처리에 의한 폐섬유화증 발생에서 Ninj1은 면역세포의 분포변화가 아닌 염증신호 변화를 유도할 것으로 예상하였다.

폐섬유화증 유발에서 중요한 역할을 하는 세포 종은 섬유모세포, 큰포식세포, 허파상피세포이므로 각각의 세포에서 Ninj1 유전자의 기능을 확인하였다. Ninj1 기능 연구를 위해 WT 쥐와 Ninj1 KO 쥐의 허파를 적출하여 섬유모세포를 분리하였으며 각 쥐의 복강에서 큰포식세포를 분리하여 사용하였다. 또한 CRISPR Cas9을 이용하여 Ninj1의 발현을 억제한 큰포식세포주와 허파상피세포주를

제작하여 다음 실험을 진행하였다. 먼저 WT과 Ninj1 KO 허파섬유모세포에 각각 TGF-β1 처리하여 활성화 차이를 분석한 결과 Ninj1 유전자가 억제되어도 TGF-β1에 의해 유도되는 아교질의 발현량에는 변화가 없었다. 다음으로 WT 및 Ninj1 KO 복강큰포식세포 또는 큰포식세포주에 블레오마이신 처리 후 염증 및 섬유화 유발 인자들의 발현 차이를 확인해 본 결과 Ninj1 발현 억제에 따른 차이는 없는 것을 확인하였다. WT 및 Ninj1 KO 허파상피세포에 블레오마이신을 처리하여 염증 유발 인자들의 발현 차이를 확인해 본 결과 마찬가지로 Ninj1 발현 유무에 따른 차이는 없었다. 종합적으로 섬유모세포의 활성과 블레오마이신에 의한 큰포식세포 및 허파상피세포의 염증반응은 Ninj1 발현 유무에 따른 차이가 없는 것을 알 수 있었다.

큰포식세포와 허파상피세포와의 상호작용은 폐섬유화증 발생 과정에서 염증반응 유도에 중요한 역할을 하는 것으로 알려져 있으므로, 세포간 물리적 접촉을 유도하는 단백질인 Ninj1 발현이 두 세포 간 상호작용에 변화를 유발하는지 확인하였다. 큰포식세포와 허파상피세포는 각각 Ninj1 발현이 억제되어도 두 세포 간 접착 정도는 차이가 없음을 유세포 분석을 통해 확인하였다. 다음으로 두 세포간 접착에 의한 큰포식세포의 활성이

Ninj1 발현 유무에 따라 차이가 있는지 확인하였다. 큰포식세포와 허파상피세포를 공생교배 시 물리적 접촉에 의해 큰포식세포가 활성화되어 염증 인자들의 발현이 증가하였다. 또한 블레오마이신에 의해 허파상피세포의 Ninj1 발현이 증가하였고 이에 따라 큰포식세포의 활성이 더욱 증가하였다. 반면 WT 큰포식세포와 Ninj1 KO 허파상피세포와 공생교배 시에도 두 세포간 접촉에 의한 큰포식세포의 활성이 관찰되나 블레오마이신을 처리한 Ninj1 KO 허파상피세포와 접촉 시 큰포식세포의 활성이 증가하지 않은 것을 관찰하였다. 허파상피세포에 블레오마이신 처리 시 Ninj1의 발현이 증가하므로 Ninj1은 큰포식세포를 직접 활성화시키는데 중요한 역할을 할 것이라 생각하였다.

Ninj1에 의해 큰포식세포가 활성화되는 지 확인하기 위해 Ninj1 재조합 단백질(rmNinj1$^{1-50}$)을 제작하여 Ninj1 발현 억제 큰포식세포에 처리하여 염증신호 및 염증 유발 인자들의 발현을 확인해보았다. 그 결과 정상 큰포식세포에 재조합 단백질을 처리 시 염증 인자들의 발현이 증가하는 것을 확인하였으나 Ninj1 KO 큰포식세포에 rmNinj1$^{1-50}$ 처리 시 염증신호 및 염증 유발 인자들의 발현 증가가 미미하였다.

위의 결과를 바탕으로 Ninj1은 손상된 허파상피세포와

큰포식세포의 접촉에 의한 상호작용을 매개하고 촉진 함으로써 큰포식세포 활성을 유도하여 염증 및 폐섬유화증 유발에 역할을 한다는 결론을 도출하였다.

주요어: Ninjurin1, 큰포식세포, 블레오마이신, 염증, 특발성 폐섬유화증

학 번: 2014-30543

감사의 글

늦은 나이에 박사학위과정을 시작하겠다는 어려운 결정을 하고 좋은 논문으로 단기간 안에 학위를 마치겠다 굳센 다짐을 하며 시작한 학위과정이 어느덧 5년 반이란 시간이 흘렀습니다. 인생에서 5년은 짧다면 짧고 길다면 긴 시간일 것입니다. 저의 박사학위 과정은 다른 많은 분들과 마찬가지로 결코 순탄치 만은 않았습니다. 무수히 많은 실패를 거듭하며 좌절하고 하루에도 몇 번씩 포기하고 싶다는 생각도 많이 하였습니다. 하지만 주위 많은 분들께서 응원해 주시고 힘을 실어주셨기에 이렇게 학위과정을 무사히 마치게 되었습니다.

먼저 결혼 직후 박사과정을 시작하기로 결심 하고 학위과정 동안 옆에서 묵묵히 기다려주고 응원해 준 아내에게 깊은 감사의 마음을 전하고 싶습니다. 그리고 힘들 때마다 저를 지탱해준 저의 딸 민경이와 동생 승훈이에게 감사합니다. 특히 10년전 아버지께서 돌아가시고 홀로 저희 두 형제를 아껴주시고 응원해주신 저의 어머님께 가슴 깊이 죄송하고 감사의 인사를 올립니다.

저의 지도교수님이신 윤여성교수님, 학위과정을 무사히 마칠 수 있도록 조언해주시고 항상 신경을 써주셔서 감사합니다. 저의 부족한 부분을 항상 챙겨주시고 연구의 방향을 냉철히 지도해 주신 오승현 교수님께 감사의 인사 올립니다. 그리고 부족한 저의

학위심사위원을 맡아 주시고 조언해 주신 성제경 교수님, 황인구 교수님, 이순신 교수님께 감사의 인사 올립니다.

학위과정동안 옆에서 같이 고생하며 응원해주고 저의 부족한 부분을 채워주며 도와준 정은이, 장영수 박사, 현진이, 강주희 박사, 민우에게 미안하고 감사합니다. 많은 시간을 함께 하진 못했지만 저에게 많은 도움을 주었던 김종휘 박사와 규리에게 감사의 인사를 올립니다. 저의 학위과정에서 연구란 무엇인지, 박사란 무엇인지 알려주신 우종규 박사님, 제가 박사학위를 무사히 끝마칠 수 있도록 큰 도움을 주셔서 정말 감사합니다. 일일이 열거 할 수는 없지만 저를 응원해 주신 주변 모든 분들께 감사의 인사 올립니다. 저의 주변 분들이 없었다면 결코 박사학위를 무사히 마칠 수 없었을 것입니다.

끝으로 박사학위를 마치게 되었지만 아직 부족한 부분이 많습니다. 박사학위는 앞으로 더욱 열심히 공부하고 연구하여 발전하라는 채찍과 같다고 생각합니다. 이제 시작이라는 마음으로 더욱 정진하여 발전된 모습을 보여드릴 수 있도록 열심히 살겠다고 모든 분들께 다짐합니다.